

**BAG3 induction is required to mitigate proteotoxicity
via selective autophagy following inhibition of
constitutive protein degradation pathways**

Dissertation
For attaining the PhD degree
of Natural Science

submitted to the Faculty
of the Johann Wolfgang Goethe University
in Frankfurt am Main

by
Francesca Rapino
from Rome, Italy

Frankfurt am Main, 2013

(D 30)

accepted by the Faculty 14 of the Johann Wolfgang Goethe University as a Dissertation.

Dean: Prof. Dr. Thomas Prisner

First Supervisor: Prof. Dr. Rolf Marschalek

Second Supervisor: Prof. Dr. Simone Fulda

Date of the disputation: 31st October 2013

List of contents

List of Figures	I
List of Abbreviations	III
Abstract	VI
1. Introduction.....	1
1.1. The Protein Quality Control Systems.	1
1.1.1. The UPS.....	2
1.1.1.1. Protein ubiquitylation.	2
1.1.1.2. The Proteasome.....	3
1.1.2. The Autophagy-Lysosome System.....	4
1.1.2.1. Selective autophagy of protein aggregates and aggresomes.....	6
1.1.2.2. HDAC6: a key player of selective autophagy of protein aggregates.....	9
1.1.3. The on demand PQC system: the role of BAG3 mediated autophagy.	12
1.1.4. Crosstalk between PQC systems.	13
1.2. Cancer.	15
1.2.1. Rhabdomyosarcoma.	16
1.3. PQC in cancer.	18
2. Aim of the Study.....	20
3. Materials and Methods.....	21
3.1. Materials.....	21
3.1.1. Cell lines.....	21
3.1.1.1. Rhabdomyosarcoma and fibroblast cell lines	21
3.1.1.2. Virus packaging cell lines.....	21
3.1.2. Cell culture reagent.....	21
3.1.3. Apoptosis inducing agents, inhibitors	22

3.1.4. Protein electrophoresis and western blot reagents.....	22
3.1.5. Antibodies.....	23
3.1.5.1. Primary western blot antibodies	23
3.1.5.2. Secondary western blot antibodies	23
3.1.6. Plasmids.....	24
3.1.7. shRNA plasmids	24
3.1.8. Cloning related material	24
3.1.9. Oligonucleotides for qRT-PCR	25
3.1.10. Kits	25
3.1.11. General chemicals	25
3.1.12. Plastic material	26
3.1.13. Equipment.....	27
3.2. Methods.....	28
3.2.1. Cell culture	28
3.2.2. Generation of stable genetic modified cell lines	28
3.2.2.1. Retroviral transduction	28
3.2.2.2. Lentiviral transduction (shRNA)	28
3.2.3. Fluorescence-activated cell-sorting (FACS) analysis	29
3.2.3.1. Determination of apoptosis.....	29
3.2.3.2. Determination of lysosomal acidification.....	29
3.2.4. Determination of cell viability and colony formation	30
3.2.5. Molecular biology methods.....	30
3.2.5.1. Protein extraction and quantification.....	30
3.2.5.2. Western blot analysis.....	30
3.2.5.3. Detection of protein aggregates: Triton-X fractionation	31
3.2.5.4. Detection of protein aggregates: Filter Trap assay	31

3.2.6. Generation of pTRIPZ-shRNA plasmids.	32
3.2.7. Quantitative Reverse Transcription PCR (qRT-PCR).....	32
3.2.8. Statistical analysis	32
4. Results.....	33
4.1. A subpopulation of RMS cells is able to survive and recover upon ST80/ Bortezomib co-treatment.....	33
4.2. ST80/Bortezomib surviving cells accumulate protein aggregates upon co- treatment.....	35
4.3. ST80/Bortezomib surviving cells up-regulate co-chaperone BAG3 in a NFκB- dependent manner.	38
4.4. BAG3 mediates protein aggregates clearance during cell recovery.	42
4.5. BAG3 is necessary for cell regrowth after ST80/Bortezomib co-treatment.	46
4.6. Impairment of autophagosome formation leads to loss of cell recovery and protein aggregates accumulation upon ST80/Bortezomib removal.	48
4.7. Impairment of lysosome acidification leads to loss of cell proliferation and protein aggregates accumulation upon ST80/Bortezomib removal.	52
5. Discussion.....	54
Summary (Deutsche Zusammenfassung).	61
References.....	i
Acknowledgments	xii
Curriculum Vitae	xiii
E R K L Ä R U N G.....	xvii

List of Figures

Figure 1: The PQC systems [12].	2
Figure 2: The autophagy-lysosome system.	5
Figure 3: Selective autophagy adaptors for degradation of protein aggregates [42].	8
Figure 4: HDAC6 is a key player of protein aggregates selective autophagy.	11
Figure 5: PQC systems interplay.	13
Figure 6: The canonical NF- κ B pathway.	16
Figure 7: ST80 synergistically co-operates with Bortezomib to induce cell death in RMS.	33
Figure 8: Experimental design for recovery studies.	34
Figure 9: ST80/Bortezomib surviving cells are able to regrowth upon drug removal.	35
Figure 10: ST80/Bortezomib surviving cells show accumulation of protein aggregates.	36
Figure 11: ST80/Bortezomib surviving cells undergo bulk autophagy.	37
Figure 12: RMS ST80/Bortezomib surviving cells up-regulate co-chaperone BAG3.	39
Figure 13: ST80/Bortezomib surviving cells show slow kinetic of BAG3 up-regulation.	40
Figure 14: BAG3 up-regulation is a specific feature of ST80/Bortezomib treatment.	40
Figure 15: I κ B α -SR cells are insensitive to TNF α stimulation.	41
Figure 16: NF- κ B mediates BAG3 up-regulation in ST80/Bortezomib surviving cells.	42
Figure 17: shBAG3 cells are unable to up-regulate BAG3 after ST80/Bortezomib treatment.	43
Figure 18: BAG3 is not involved in ST80/Bortezomib induced cell death.	44
Figure 19: BAG3 mediates clearance of protein aggregates during cell recovery.	45
Figure 20: BAG3 plays a key role in protein aggregates clearance upon ST80/Bortezomib removal.	45

Figure 21: BAG3 up-regulation is necessary for cell regrowth in ST80/Bortezomib surviving cells.	46
Figure 22: Loss of BAG3 up-regulation triggers cell death during cell recovery.	47
Figure 23: BAG3 is necessary for long term and clonogenic survival after ST80/Bortezomib removal.....	48
Figure 24: Inducible knock down of ATG7 does not interfere with ST80/Bortezomib-induced cell death.	49
Figure 25: Impairment of autophagosome formation leads to accumulation of protein aggregates during recovery.	50
Figure 26: RD shATG7 cells show loss of cell proliferation and increase apoptosis during recovery.	51
Figure 27: Autophagy impairment leads to decrease in cell proliferation in untreated conditions.....	51
Figure 28: Impairment of the autophagic cargo degradation leads to protein aggregates accumulation during recovery.	52
Figure 29: Impairment of lysosomal degradation results in loss of cell viability and increased cell death upon ST80/Bortezomib removal.	53
Figure 30: Scheme of proposed mechanism.	55

List of Abbreviations

Abbreviation	Extended form
μM	Micro molar
3-MA	3-Methyladenine
ALFY	Autophagy-linked FYVE protein
ALFY	Autophagy-linked FYVE protein
ALS	Amyotrophic lateral sclerosis
ARMS	Alveolar Rhabdomyosarcoma
ATG	Autophagy related genes
BafA1	Bafilomycin A1
BAG	BCL2-associated athanogene
BCL2	B-cell lymphoma 2
BCL-X _L	B-cell lymphoma-extra large
BH3	Bcl2 homology domain 3
BS	Bortezomib/ST80
BUZ	Binder of ubiquitin zinc finger
Caspase	Cystein-dependent aspartate-specific protease
CCT	Chaperonin containing TCP-1
CP	Core proteasomal particle
Cvt	Cytosol to Vacuole transport
DNA	Deoxyribonucleic acid
EGF	Epidermal growth factor
EGFR	Epidermal growth factor receptor
EMT	Epithelial-mesenchymal transition
ER	Endoplasmatic reticulum
ERMS	Embrional Rhambomyosarcoma
EV	Empty vector
FACS	Fluorescence-activated cell-sorting
FDA	Food and Drug Administration
FOXO1A	Forkhead box protein O1
GAPDH	Glycerinaldehyd-3-phosphate

	dehydrogenase
GLI	Glioma-associated oncogene family zinc finger
HDACs	Histone deacetylases
HSF	Heat shock factor
HSP	Heat shock protein
HSPB8	Heat shock protein beta-8
IKK	Inhibitor of NF- κ B kinase
I κ B	Inhibitor of NF- κ B
I κ B α -SR	I κ B α Super Repressor
Keap1	Kelch-like ECH-associated protein 1
LC3	Microtubule-associated protein 1A/1B-light chain 3
LIR	LC3 interacting region
LTR	Lysotracker Red
Lys	Lysine (amino acid)
MCL-1	Modified central lead 1
MDM2	Mouse double minute 2 homolog
MPP(+)	1-methyl-4-phenylpyridinium
MTOC	Microtubule organizing center
mTOR	Mammalian target of rapamycin
MYCN	v-myc myelocytomatosis viral related oncogene, neuroblastoma derived
MyoD	Myogenic regulatory factor D
NBR1	Neighbor of BRCA1 gene 1 protein
NDP52	Nuclear dot protein 52 kDa
NF- κ B	nuclear factor kappa-light-chain-enhancer of activated B cells
Nix	BCL2/adenovirus E1B 19 kDa protein-interacting protein 3-like
nM	Nano molar
Nrf1	Erythroid-derived 2-related factor 1
PAX	Paired box protein

PB1	Phox and Bem 1
PI3K III	class III phosphatidylinositol 3-kinase complex
PKC	Protein kinase C
PQC	Protein quality control
qRT-PCR	Quantitative reverse transcription PCR
RAS	Rat sarcoma associated protein
RelA	Transcription factor p65
RMS	Rhabdomyosarcoma
RNAi	Ribonucleic acid interference
ROS	Reactive oxygen species
RP	Regulator proteasomal particules
Ser	Serine (amino acid)
shRNA	Short harpin RNA
SOD1	Superoxide dismutase 1
TNF α	Tumor necrosis factor
TRAIL	TNF-related apoptosis inducing ligand
UBA	Ubiquitin-binding domain
ULK1	Unc-51 like autophagy activating kinase 1
UPR	Unfolded protein response
UPS	Ubiquitin proteasome system
VCP/p97	97-kDa valosin-containing protein
WW domain	Protein interaction domain with two conserved tryptophans

Abstract

Protein quality control systems (PQC), i.e. UPS and aggresome-autophagy pathway, have been suggested to be a promising target in cancer therapy. Simultaneous pharmacological inhibition of both pathways have shown increase efficacy in various tumors, such as ovarian and colon carcinoma. Here, we investigate the effect of concomitant inhibition of 26S proteasome by FDA-approved inhibitor Bortezomib, and HDAC6, as key mediator of the aggresome-autophagy system, by the highly specific inhibitor ST80 in rhabdomyosarcoma (RMS) cell lines. We demonstrated that simultaneous inhibition of 26S proteasome and selective aggresome-autophagy pathway significantly increases apoptosis in all tested RMS cell lines. Interestingly, we observed that a subpopulation of RMS cells was able to survive the co-treatment and, upon drug removal, to recover similarly to untreated cells. In this study, we identified co-chaperone BAG3 as the key mediator of this recovery: BAG3 is transcriptionally up-regulated specifically in the ST80/Bortezomib surviving cells and mediates clearance of cytotoxic protein aggregates by selective autophagy. Impairment of the autophagic pathway during the recovery phase, both by conditional knock-down of ATG7 or by inhibition of lysosomal degradation by BafylomicinA1, triggers accumulation of insoluble protein aggregates, loss of cell recovery and cell death similarly to stable short harpin RNA (shRNA) BAG3 knock-down.

Our results are the first demonstration that BAG3 mediated selective autophagy is engaged to cope with proteotoxicity induced by simultaneous inhibition of constitutive PQC systems in cancer cell lines during cell recovery. Moreover, our data give new insights in the regulation of constitutive and on demand PQC mechanisms pointing to BAG3 as a promising target in RMS therapy.

1. Introduction

1.1. The Protein Quality Control Systems.

Cellular homeostasis is achieved by a complex and tightly regulated series of constitutive and inducible pathways which control the correct execution of cell cycling by mitigating potentially toxic events, such as DNA and organelle damaging and protein misfolding [1-3]. In order to maintain cellular homeostasis, the correct translation, folding and degradation of proteins is crucial (Figure 1): to this end, eukaryotic cells have developed a network of constitutive and inducible pathways which are in charge to control protein homeostasis in order to avoid proteotoxic stress which can eventually trigger apoptosis and/or insurgence of disease [4]. The ER (Endoplasmatic Reticulum) is the main sensor of protein misfolding in eukaryotic cells [5]. Linear newly translated proteins are folded in the ER by chaperones and co-chaperones complexes in order to decrease the exposure of hydrophobic residues. Hydrophobic residues are prone to unspecific binding towards proteins leading to the impairment of their correct functions. When accumulation of misfolded proteins occurs, sensors present in the ER, such as Grp78, recognize and bind the exposed hydrophobic residues and induce a pro-survival response known as unfolded protein response (UPR) [5]. UPR mediates the decrease of CAP-dependent mRNA translation and the induction of chaperones and co-chaperones in order to increase the correct protein folding. Moreover, UPR increases protein degradation *via* proteasome and autophagy by the induction of key components of those degradative processes [6]. When misfolded proteins accumulation is prolonged or acute, the UPR response switches from a pro-survival to a pro-death pathway, mainly by the induction of apoptosis [7, 8]. In this scenario, the degradation of unfolded and misfolded proteins plays a key role in protein quality control (PQC) in order to avoid induction of cell death.

Constitutive PQC is mainly taken on by two systems: the ubiquitin proteasome system (UPS) and the autophagy-lysosomal pathway [9]. Linearized misfolded proteins are generally degraded by the UPS; larger structures, such as aggresomes, protein aggregates or p62-bodies, are cleared *via* the selective autophagic machinery. The interplay between these two systems enables cells to adapt to acute and chronic proteotoxicity by increasing the activity of one or both pathways: this crosstalk plays a crucial role not

only in the maintenance of healthy cells and tissues, but also it increases tumor cell survival and drug-induced resistance [10, 11].

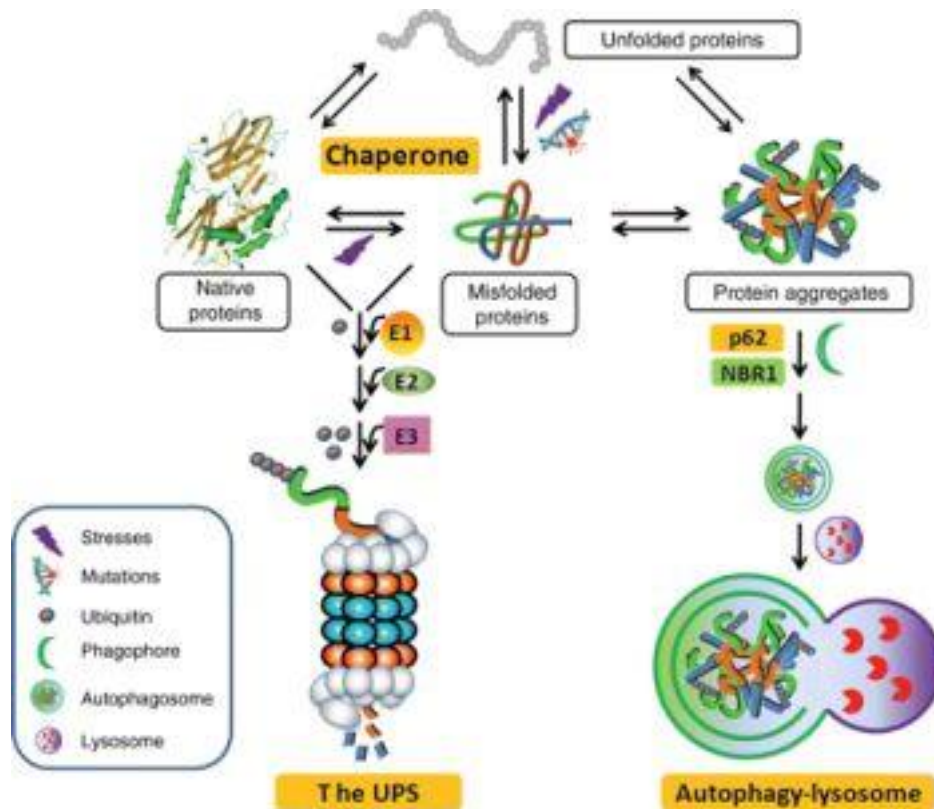


Figure 1: The PQC systems [12].

Unfolded proteins are recognized by chaperones which mediate the correct folding process; when folding is incorrect, misfolded proteins can either be linearized, ubiquitin-tagged and degraded by the UPS, or form larger structures (protein aggregates) which are cleared by the autophagy-lysosome system

1.1.1. The UPS.

In eukaryotic cells, the UPS is in charge of the ubiquitylation, degradation and turnover of many regulatory and structural proteins. UPS is divided in two major steps: 1) protein ubiquitylation which target the tagged protein to degradation, compartmentalization or signaling; and 2) protein degradation mediated by the proteasome [13].

1.1.1.1. Protein ubiquitylation.

In order to target unfolded, regulatory or damaged proteins towards degradation and signaling, a tightly regulated ATP-dependent series of events need to be performed: final goal of these events is to tag the protein of interest with mono- or poly-ubiquitin chains which will serve as a regulatory signal for proteins fate [14]. The identification of ubiquitin as the covalently attached degradation signal of proteins was delineated in the early 1990s; in the last twenty years a great amount of work has been done to

understand in detail the regulation and biological relevance of this process with particular emphasis on its implication on pathology [15]. In a simplified model, ubiquitin needs to be activated by a two-step ATP-dependent reaction mediated by a family of enzymes known as E1 ubiquitin-activating enzymes. The final product of the reaction is a thioester linkage between the ubiquitin and the E1 enzyme [16]. Second, ubiquitin is transferred to the active cysteine site of an ubiquitin-conjugating enzyme E2: a single E1 can selectively transfer ubiquitin to dozens of E2s, amplifying, in this way, the reaction. The specificity of the substrate which has to be ubiquitinated is mediated by the third step of the protein ubiquitylation pathway: one of the hundreds of E3 ubiquitin-protein ligases encoded in the human genome will act as a substrate-recognition enzyme leading to the formation of a covalent bond between a lysine residue of the target protein and the C-terminal glycine of the ubiquitin [16]. Recently, a fourth class of ubiquitin ligases has been discovered: the E4-ligase family seems to be responsible for the elongation of the ubiquitin chains while, the E3-ligase family mainly mediates mono- or multi-ubiquitylation of the substrate [17]. A growing amount of evidence [14] demonstrates that protein fate depends on the lysine residue involved in ubiquitylation and on the presence of a polyubiquitin chain versus multiple monoubiquitin chains. As a general concept, polyubiquitination on Lys11, Lys29, and Lys48 residues is considered to target substrate to degradation, while monoubiquitylation on Lys63 generally leads the tagged protein towards the lysosomal pathway [18].

1.1.1.2. The Proteasome.

When proteins are specifically ubiquitin-tagged to degradation, the cytosolic multisubunit complex, known as proteasome, is engaged to mediate proteolysis of the substrate in an ATP-dependent manner. The proteasome is composed of three main subunits: a catalytic core particle (CP) and two regulatory particles (RPs) [19]. The CP, also known as 20S proteasome, is a barrel made of two outer α -rings and two inner β -rings: the inner β -rings contain the catalytically active threonine residues which are associated to caspase-like, trypsin-like and chymotrypsin-like activity and are therefore responsible for protein proteolysis [19]. Crystallographic structural studies of the CP demonstrate that the active cavity of the 20S proteasome is generally closed in cells, in order to prevent unregulated degradation of proteins: the RPs, which assemble

symmetrically on the two ends of the CP, are necessary for selective protein degradation by recognition of the ubiquitin chains attached to the substrate. Moreover, RPs promote substrate unfolding and translocation into the CP [20]. The assembly of the active proteasome complex, composed by one CP with two RPs and also known as 26S proteasome, is of crucial importance for the maintenance of protein homeostasis: it has been reported that 0.5% of all genes on the human genome codify for proteasome-interacting proteins (PIPs) needed for the correct regulation and assembly of the 26S proteasome [19]. Although the synthesis of proteasome components is constitutively ongoing, induction of proteotoxicity, by pro-oxidant stress or pharmaceutical proteasomal inhibition, leads to induction of proteasomal genes transcription [21]. Nrf1 (Erythroid-derived 2-related factor 1) has been proposed as the key mediator of this induced transcription: upon normal condition Nrf1 is target towards the ER preventing its nuclear translocation; when proteotoxicity is enhanced, Nrf1 is post-translational modified and translocate to the nucleus where it stimulates proteasomal gene transcription, increasing protein degradation in order to cope with the induced proteotoxicity [21].

1.1.2. The Autophagy-Lysosome System.

The autophagy-lysosome system is an evolutionary conserved catabolic pathway constitutively active in cells: its dynamic characteristics and its tight regulation makes this system an extremely adaptable mechanism of degradation of large protein aggregates, organelles and virus upon normal and stress conditions [22]. The autophagy-lysosome system is divided into three different sub-types which share the dependency on lysosomes for the final degradation of the substrate: microautophagy, where cytoplasmic material is directly engulfed by lysosomes [23]; chaperone-mediated autophagy, which is a very selective process where proteins are recognized by chaperone HSP70 (Heat shock protein 70) and delivered to lysosomes [24] and macroautophagy. Here, we will specifically talk of macroautophagy (from now on called autophagy) as the main type of autophagic-lysosomal system involved in PQC.

Autophagy is a flux, dynamic process which can be divided in three steps: initiation; elongation and maturation; and fusion (Figure 2). All three steps of the autophagy pathway are tightly regulated by a class of genes known as AuTophagy-related genes (ATGs) which have been primarily discovered in yeast and are conserved in mammals with high sequences homology [25]. In normal conditions, autophagy is maintained at

basal level by the key metabolic and growth sensor mTOR (mammalian target of rapamycin) [26]. mTOR stimulates cell proliferation and inhibits autophagy in presence of nutrients; upon stress conditions, such as starvation, mTOR is inhibited enabling the autophagy initiator ULK1(Unc-51 like autophagy activating kinase 1)-complex to trigger autophagy induction to finally degrade cellular macromolecules into their basal components, such as amino acids and lipids, and cope with stress. Furthermore, depletion of nutrients activates the PI3K III (Class III phosphatidylinositol 3-kinase)-complex which is needed to increase the amount of phosphatidylinositol-3-phosphate inducing membrane nucleation and thereby induction of autophagy [27] (Figure 2).

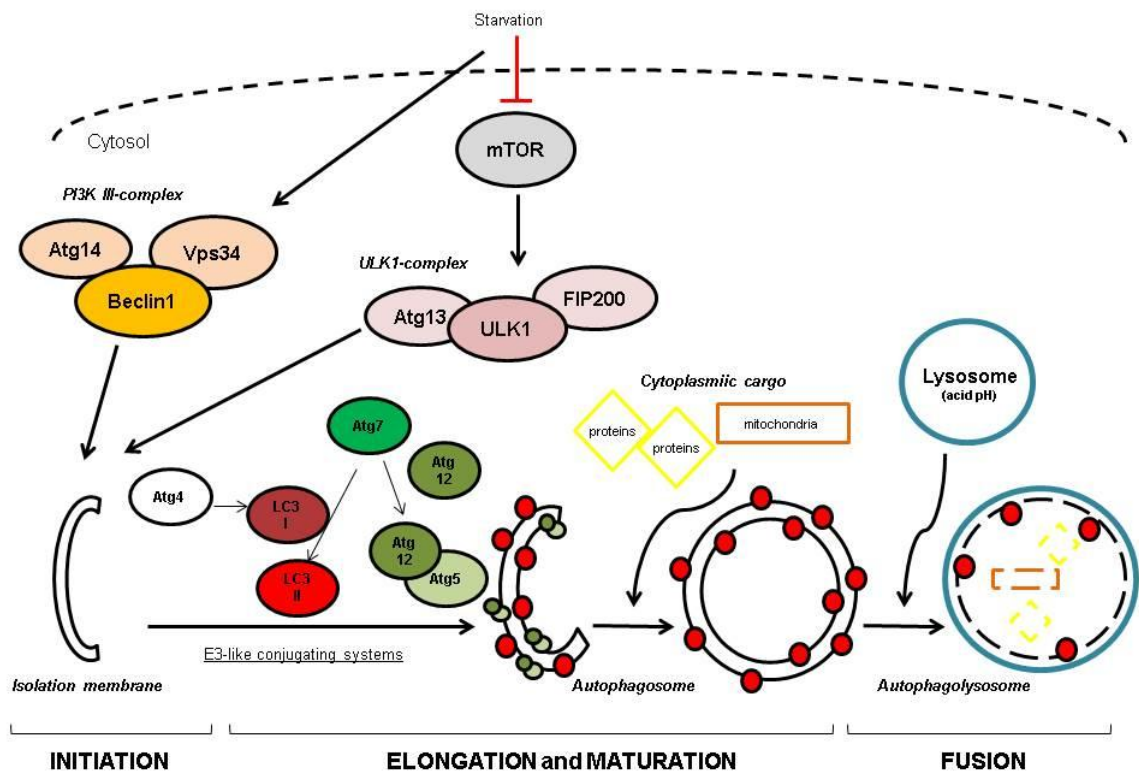


Figure 2: The autophagy-lysosome system.

Nutrient deprivation and/or other cellular stress inhibit the negative regulator of autophagy mTOR triggering ULK1 and PI3K III complexes activity and induction of the isolation membrane nucleation. The E3-like conjugating systems enrich the isolation membrane with specific autophagy related proteins (e.g. LC3-II) and trigger membrane elongation and closure after the engulfment of the cytoplasmic cargo forming the autophagosome. Finally, autophagosomes fuse with lysosomes leading to autophagolysosome formation and digestion of the cargo. (See text for details).

The origin of nucleation of the forming double membrane vesicle, known as isolation membrane or phagofore, is still matter of debate: some evidences support the ER or the mitochondria as the primary site of phagofore nucleation, other support the *de novo* synthesis of the membrane as the main mechanism engaged for phagofore formation [28]. When formed, the isolation membrane is then enriched with specific autophagic

markers derived from protein post-translational maturation mediated by two ubiquitin-like conjugating systems: the ATG12 and the LC3 (microtubule-associated protein 1A/1B-light chain 3) systems [29]. ATG7 plays a major role in both ubiquitin-like conjugation systems: in the ATG12 system, ATG7 conjugates and activates ATG12 in an ATP-dependent manner; then ATG7 mediates, through an ATG10 intermediate, the formation of a stable isopeptide bond between ATG12-ATG5 which will integrate in the phagofore membranes. In the LC3 system, ATG4 cuts and activates LC3 (LC3 I isoform); then, ATG7 recognizes LC3 I and mediates its lipidation with phosphatidylethanolamine (LC3 II) through an ATG3 intermediate passage [30]. LC3 II integrates in the inner and outer membrane of the phagofore, remaining stably attached to the membrane until the complete degradation of the cargo: for this reason LC3 I/II conversion is nowadays the most important and used marker for detection of autophagy [31]. Moreover, LC3 plays a crucial role in the selection of the cytoplasmic material which is brought to degradation [32].

During membrane enrichment, the phagofore elongates, engulf the cytoplasmic cargo and close forming a mature double membrane vesicle known as autophagosome (Figure 2). Finally, the autophagosome eventually fuses with lysosomes, forming the degradative compartment known as autophagolysosome, in which the engulfed cargo will be digested [25]. Little is known on the exact mechanism of autophagosome-lysosome fusion: among others, the monomeric G proteins Rab7 and Rab11 have been reported to be necessary for autophagolysosome formation [33, 34]. Acidification of lysosomes is of crucial importance for the correct degradation of cytoplasmic material: lysosomal enzymes need an acidic environment in order to be activated and degrade the cargo in the autophagolysosome, permitting the maintenance of the autophagic flux. For this reason, inhibitors of lysosomal acidification, such as BafilomycinA1, induce accumulation of autophagosomes and inhibition of the autophagic pathway due to impaired cargo digestion and consequent flux engulfment [35].

1.1.2.1. Selective autophagy of protein aggregates and aggresomes.

Autophagy have been described as a bulk catabolic process for many years due to its massive induction during starvation and consequent role in supporting cell metabolic stress by macromolecules recycling [36]. In the last years, a mounting amount of evidences suggested that autophagy can be an extremely selective pathway [37]: autophagy selectivity is present also in yeast where the selective delivery of hydrolase

aminopeptidase I from the cytoplasm to the vacuole (Cvt) has served as a model to study the much more complex selectivity of autophagy in mammals [38]. A big step towards the understanding of selective autophagy mechanisms has been the discovery and characterization of protein adaptors necessary for the specific recognition of the cytosolic cargo and its targeting towards the autophagosomes [39]. Several autophagic receptors have been described: for example, Parkin1 and Nix (BCL2/adenovirus E1B 19 kDa protein-interacting protein 3-like) have been reported to be specific adaptors for selective degradation of mitochondria [40] and NDP52 (nuclear dot protein 52 kDa) is necessary for the selective autophagic degradation of bacteria [41].

In order to selectively degrade protein aggregates, a selective autophagy adaptor protein must fulfil three important functions: i) a direct or indirect interaction with the autophagosomal protein marker LC3; ii) the capability of polymerize or aggregate and iii) the ability to recognize the substrates [39]. To mediate these functions, proteins present specific domains of interaction: based on the presence or absence of one or more protein-interaction domains, protein aggregate selective adaptors have been divided in four groups (Figure 3).

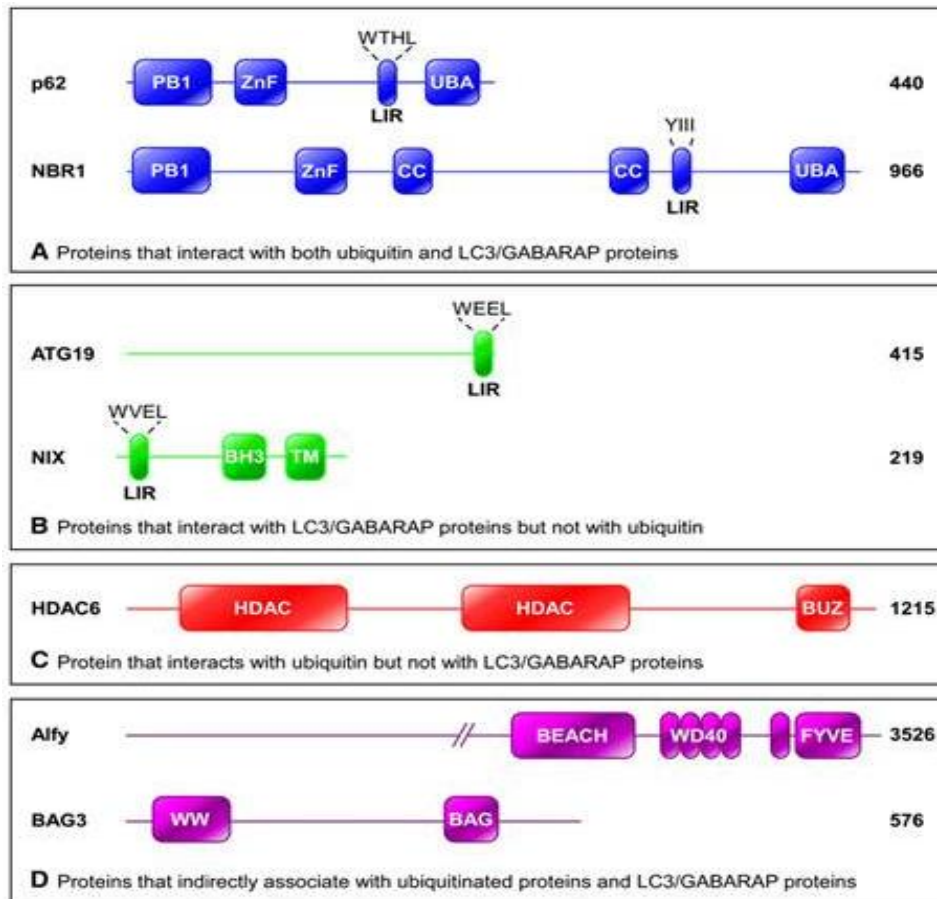


Figure 3: Selective autophagy adaptors for degradation of protein aggregates [42].

Selective autophagic adaptors for protein aggregates are classified by the presence or absence of the LC3-interacting domain (LIR) and the ubiquitin-recognizing domains (UBA and/or BUZ).

p62 is the most studied selective autophagic adaptor for protein aggregates selective autophagy. p62 plays a crucial role in selective degradation of ubiquitin-positive protein aggregates although a role of p62 in ubiquitin-independent degradation of mutant SOD1 (superoxide dismutase 1) in an ALS (amyotrophic lateral sclerosis) model has been reported [43]. The human p62 is a 440 amino acid protein with several structural domains: among these domains, the UBA (ubiquitin-interacting) domain, the PB1 (Phox and Bem 1) domain and the LIR (LC3-interacting region) domain play an important role in autophagy [44]. The LIR domain is a conserved 11 amino acid sequence which allows p62, and other receptors such as NBR1 (Neighbor of BRCA1 gene 1 protein), to directly interact with LC3 II on the nascent and maturing autophagosome membrane. Through the LIR domain, p62 is constantly degraded by the autophagic pathway, becoming one of autophagy's main substrates: when autophagy is impaired, p62 protein levels rapidly accumulate and generally associate with undigested autophagosomes and/or ubiquitin-positive protein aggregates [45]. Concerning selective

degradation of aggregates, p62 plays a double role: first, thanks to its UBA domain, p62 recognizes ubiquitin-tagged proteins and triggers protein aggregation *via* self oligomerization through its PB1 domain; second, p62 targets protein aggregates towards the autophagosome [46]. Protein ubiquitylation has been shown to be the recognition signal for autophagic degradation of protein aggregates: although protein aggregation *per se* is sufficient to trigger autophagy [47], protein ubiquitylation enhances aggregates formation and cargo recognition [48]. p62 preferentially binds to Lys63 mono-ubiquitinated chains *in vitro*, concordantly with proteasome preference towards Lys48 poly-ubiquitinated proteins [49, 50]. Phosphorylation of p62 on Ser403 has been demonstrated to increase p62 selectivity toward ubiquitinated proteins, in order to clear them through autophagy [51]. This evidence points to an important role of p62 post-translational modifications in the aggresome-autophagy pathway in order to increase substrate recognition. Moreover, p62 levels are also regulated at a transcriptional level upon proteotoxic stress [52]. Proteasome inhibition triggers p62 transcriptional induction by Nrf1: p62 binds Nrf1 inhibitor Keap1 (kelch-like ECH-associated protein 1) possibly mediating its degradation through autophagy and stimulating a positive feedback loop by freeing Nrf1 which translocates to the nucleus and increases the transcription of its target genes such as p62 [53]. p62 up-regulation is needed by cells to stimulate protein aggregation and autophagy induction in order to cope with the increased proteotoxicity.

Together with p62 and Nbr1, other protein adaptors are needed to carry out protein aggregates autophagic degradation (Figure 3): for example, ALFY (autophagy-linked FYVE protein), does not possess any ubiquitin recognition domain or LIR domain but can interact with p62 and mediate protein aggregates selective targeting to autophagosomes by stimulating protein aggregation as a scaffold protein [54]. Importantly, ALFY deficient *Drosophila*'s showed diminished life span, ubiquitin protein aggregates accumulation and neurodegeneration, pointing to a crucial role of ALFY in PQC maintenance through autophagy [55].

1.1.2.2. HDAC6: a key player of selective autophagy of protein aggregates.

Histone deacetylases (HDACs) are an important class of enzymes which regulate the level of protein acetylation in cells: mainly these enzymes target histones in the nucleus modulating chromatin structure and gene transcription [56]. Also, some HDACs are able to modulate acetylation of non-histone proteins in the cytosol: acetylation,

together with other post-translational modifications such as phosphorylation or ubiquitylation, cooperates to precisely regulate proteins functions and fate in order to maintain cellular homeostasis [57]. HDACs are divided in three classes based on their sequence homology with *Saccaromyces cerevisiae*: HDACs class I, II and IV [58]; a fourth class, Sirtuins, is present only in mammals (class III) but their sequence and catalytic functions differ from the other HDACs classes [59]. HDACs class I, II and IV share the same conserved catalytic domain which consists of a 390 amino acid tube-like structure with two adjacent histidine residues, two aspartic residues and one threonine residue needed to remove an acetylic group from the specific protein substrate [60]. Moreover, all three HDACs classes need Zn^{2+} as cofactor. The main difference among HDACs classes is their cellular localization and tissue-related expression: class I HDACs (HDAC1, HDAC2, HDAC3, and HDAC8) are ubiquitously expressed and prevalently present in the nucleus, their main function is to regulate transcription acting as repressors [61]. Class II HDACs are tissue-specific and are divided in two subgroups: class IIa (HDAC4, HDAC5, and HDAC7) has both nuclear and cytosolic localization; moreover, the HDACs of this class share a conserved N-terminal domain which regulates DNA-binding and nuclear-cytoplasmic shuttling through 14-3-3 protein binding and phosphorylation [62]. Class IIb (HDAC6 and HDAC10) are cytosolic proteins: they possess two functional catalytic domains and are involved in deacetylation of cytosolic proteins regulating a huge range of cellular processes such as migration, cell proliferation and apoptosis [63]. Class IV HDACs (HDAC11) is located in the cytoplasm and is the less studied HDAC's class: recent reports suggest its involvement in the regulation of the immune system [64].

HDAC6 is a unique HDAC protein due to the presence of an ubiquitin-binding domain (BUZ) in its sequence (Figure 3) which plays a crucial role in PQC. In contrast with p62 UBA domain, the BUZ domain needs Zn^{2+} as cofactor: both, UBA and BUZ domains, are able to bind to mono-ubiquitin as well as poly-ubiquitin chains *in vitro*, although specific ubiquitin recognition and interaction are different between the two domains [65]. HDAC6 is a key regulator of several cellular processes [63]; in PQC, HDAC6 is involved in two crucial steps of the selective degradation of protein aggregates and aggresomes by autophagy (Figure 4).

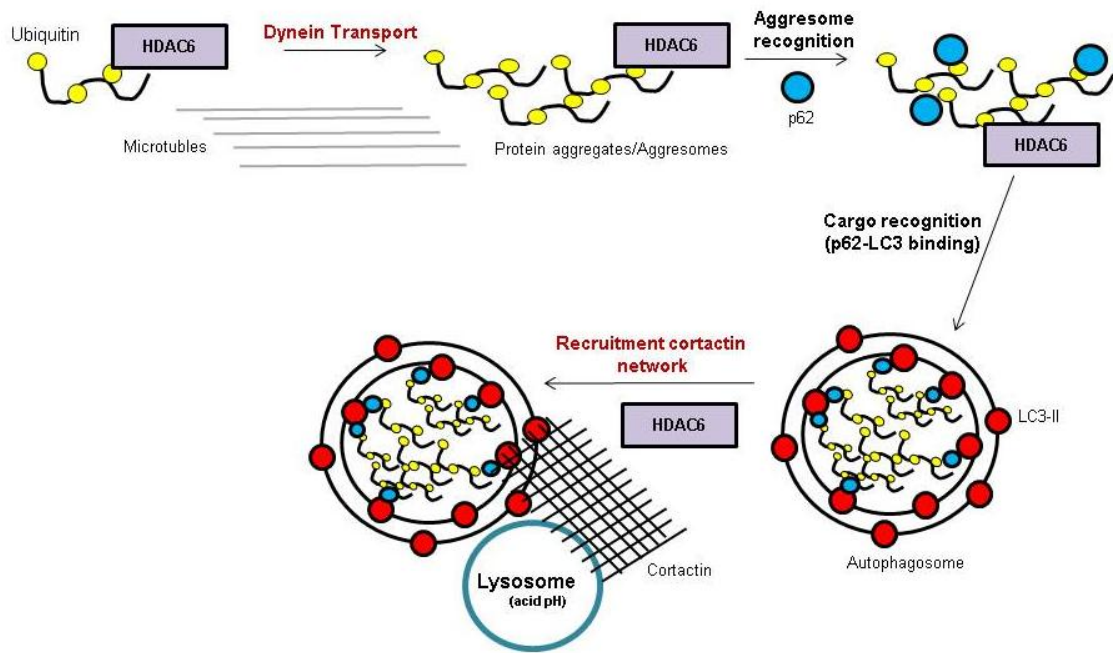


Figure 4: HDAC6 is a key player of protein aggregates selective autophagy.

HDAC6 is needed in the aggresome-autophagy system in two different steps: 1) HDAC6 mediates aggresome formation by dynein transport on microtubules; 2) HDAC6 recruits a cortactin network to mediate autophagosome-lysosome fusion.

HDAC6 is able to recognize misfolded and unfolded ubiquitin tagged proteins through its BUZ domain; then, HDAC6 triggers proteins agglomeration and dynein transport along the microtubules towards the MTOC (microtubule organizing center) by deacetylation of α -tubulin in order to form aggresomes [66]. Upon proteotoxic stress, protein aggregate formation is stimulated in cells as a cytoprotective mechanism [66]: protein aggregates are less reactive compared to unfolded and misfolded proteins towards unspecific binding to other proteins and are more prone towards degradation by autophagy. In fact, protein aggregation stimulates autophagy *per se*: p62 interacts with protein aggregates and aggresomes leading to specific cargo recognition by the autophagosome [44, 51]. Moreover, protein aggregates and aggresomes are restrict in proximity of the MTOC, near the nuclear membrane, in order to decrease casual protein-protein interaction and, by this, toxicity. HDAC6 deficiency triggers increase formation of non-perinuclear protein aggregates and increase cell death upon proteotoxic stimuli, such as MPP(+) (1-methyl-4-phenylpyridinium), compared to control cells due to HDAC6-deficient cells incapability in forming complete cytoprotective aggresomes [67, 68]. Also, HDAC6 is needed to mediate lysosome-autophagosome fusion by recruitment of a cortactin network which is specifically needed for selective degradation of protein aggregates by autophagy but dispensable for

bulk autophagy triggered by starvation [69]. The catalytic activity of HDAC6 is needed for both autophagy-related functions: protein aggregates/aggresomes formation and autophagosome-lysosome fusion.

In conclusion, HDAC6 plays a crucial role in the aggresome-autophagy system by supporting the formation of the specific autophagic cargo – protein aggregates, aggresomes- and by mediating autophagosome-lysosome fusion and cargo degradation *via* remodeling of the cytoskeleton – through the recruitment of the cortactin network.

1.1.3. The on demand PQC system: the role of BAG3 mediated autophagy.

Basal protein degradation homeostasis is controlled by the constitutive PQC systems, UPS and HDAC6 mediated selective aggresome-autophagy system; upon increase proteotoxicity, such as pharmaceuticals inhibition of proteasome or aging, on demand PQC pathways are activated in order to guarantee an adequate level of protein aggregates clearance in order to decrease cytotoxicity [70]. Co-chaperone BAG3 plays a key role in mediating the induction and accomplishment of on demand selective autophagy of protein aggregates upon acute and chronic proteotoxic conditions [71]. BAG3 is part of the BCL2-associated athanogene (BAG) protein family (BAG1-6) which share the conserved 110-124 amino acid BAG domain responsible for the ATP-dependent interaction of these proteins with HSP70 [72]. In addition to the BAG domain, BAG3 possess a WW domain and a proline-rich domain (Figure 3) which mediate the interaction with other proteins, apart from HSP70 [73]. As a selective adaptor for the aggresome-autophagic pathway, BAG3 doesn't possess neither a LIR nor a ubiquitin-interacting domain: BAG3 mediates selective autophagy by forming a complex with the molecular chaperone HSPB8 (heat shock protein beta-8) which is essential for autophagy induction upon proteotoxic stress [74, 75]. Moreover, BAG3 stimulates substrate transfer from HSP70 to the dynein motor complex, acting as a nucleotide-exchange factor, thereby facilitating the dynein-mediated retrograde transport of misfolded proteins towards the MTOC to form aggresomes [76]. Finally, BAG3 is able to interact with p62: through this interaction, BAG3 controls the sequestration of aggresomes and protein aggregates into the forming autophagosome [77]. Recently, BAG3 has been found to control protein folding by interaction with the cytosolic chaperonin CCT (chaperonin containing TCP-1) [78] underlining the importance of BAG3 in PQC from the folding step to the degradation step of misfolded and unfolded proteins.

BAG3 is poorly express in the majority of healthy young tissues [77], upon stress such as oxidants, serum deprivation or proteasome inhibition, BAG3 is transcriptionally up-regulated through HSF1(heat shock transcription factor 1) [79]. Apart from its key role in selective degradation of protein aggregates through autophagy, BAG3 is engaged to regulate several others cellular process such as the development of the central nervous system [80], cell migration [81] and apoptosis [82].

1.1.4. Crosstalk between PQC systems.

PQC systems interplay is a key regulatory mechanism necessary for the correct protein degradation and homeostasis. Several transcription factors are responsible for the induction of the key mediators of the UPS and of the aggresome-autophagy system in order to increase their activity upon proteotoxic stress (Figure 5).

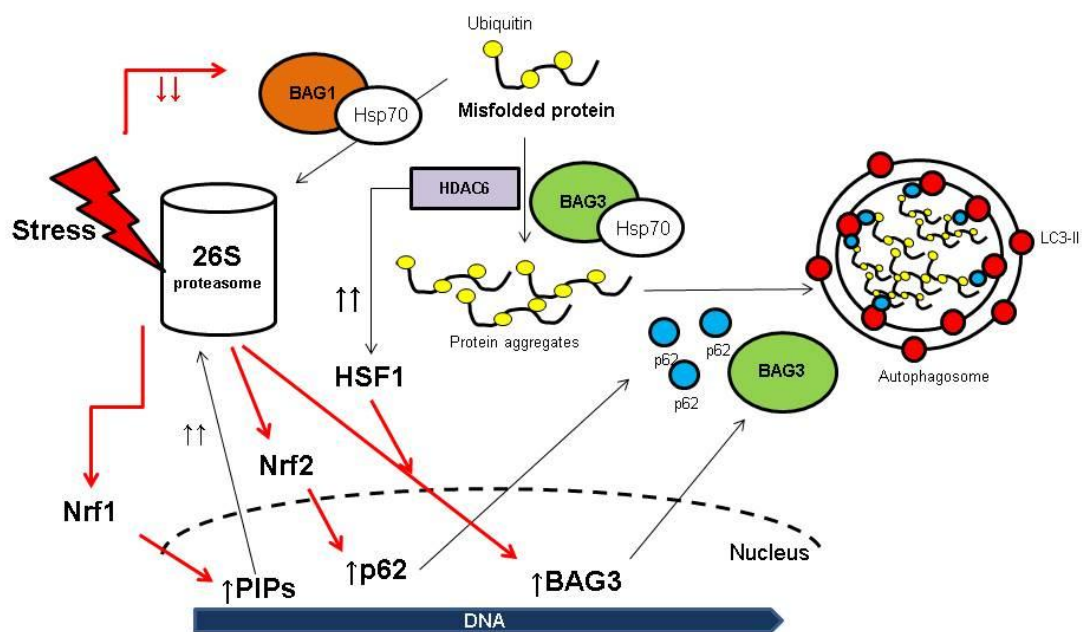


Figure 5: PQC systems interplay.

Misfolded proteins are direct to proteasomal degradation by BAG1/HSP70 complex and to the autophagy system by HDAC6. When proteotoxic stress occurs, the induction of several transcription factors and genes (red arrows) leads to increase activity of constitutive and on demand PQC systems. (See text for details).

Upon normal condition, the proteasome is able to functionally degrade misfolded proteins; when proteotoxic stress occurs, as consequence of stimuli such as xenobiotics or pro-oxidant compounds, the level of misfolded proteins rapidly increases leading to proteasome overloading [83]. To prevent the accumulation of toxic misfolded and unfolded proteins, the transcription factor Nrf1 is target from the ER to the nucleus in

order to induce the transcription of the PIP genes which mediate the increase assembly of new functional proteasomes [21]. Proteasome inhibition has been largely described to induce the up-regulation of the autophagic pathway: proteasome inhibitors, such as Bortezomib or MG132, have been shown to increase the autophagic pathways in several tumor cell lines [10]. On demand PQC systems are mainly engaged during chronic and acute proteotoxic stress: it is not surprising that the key mediator of the on demand selective aggresome-autophagy pathway, BAG3, is transcriptionally induced upon proteasome inhibition [84]. Gamerding and colleagues have elegantly showed in a model of aged cell line (I90) that BAG3 induction is tightly related to the decrease of another BAG family member, BAG1, which is mainly engaged in delivering misfolded proteins towards proteasomal degradation [77]. In young cells, BAG1 mediates protein degradation through its binding to HSP70; when cells are aging, proteasome activity decreases triggering transcriptional inhibition of BAG1 and increase transcription of BAG3 (mechanism known as: BAG1/BAG3 switch) leading to increase protein degradation through selective autophagy [77]. Accumulation of misfolded proteins triggers BAG3 up-regulation also *via* HDAC6 [85]: in non-stress conditions, HDAC6 is sequestered by the ER ATPase VCP/p97 (97-kDa valosin-containing protein) to form a complex with HSP90 and HSF1 preventing the latter to translocate to the nucleus and induce the transcription of its target genes, for example BAG3. When misfolded proteins are accumulated, HDAC6 binds them and dissociates from the complex, freeing HSF1 and consequentially leading to BAG3 induction (Figure 5).

Another important sensor and modulator of UPS and selective autophagy interplay is p62 [86]. p62 gene transcription is mediated by the transcriptional factor Nrf2: upon proteasomal inhibition Nrf2 translocation to the nucleus is enhanced, promoting p62 transcription and translation. As a consequence, p62 accumulates in the cytosol mediating protein aggregation and recognition by the autophagic pathway [87]. On the contrary, upon autophagy inhibition, cytosolic p62 protein levels increase as a consequence of its impaired degradation: elevated cytosolic p62 protein levels lead to proteasomal inhibition and trigger the induction of PQC systems by enhancing the transcription of proteasomal genes, such as PIPs, and regulators of selective and bulk autophagy [53, 86].

1.2. Cancer.

Cancer, also known as tumor or malignant neoplasm, is one of the first cause of death worldwide: in 2008, 12.7 millions of people were diagnosed with cancer and, of these, more than 50% died [88]. Cancer is a wide and very different set of diseases which can potentially occur in every cell type of an organism; this wide heterogeneity makes this malignancy very difficult to diagnose and treat. In general, cancer can be described as a deregulated growth of single or multiple cells which acquire specific characteristics, such as motility or angiogenesis, which lead to impairment of the normal homeostasis of the tissue, eventually causing death of the organism. It is largely accepted that all tumor types develop as consequence of mutations in the DNA. Two different kinds of mutations can occur in the genes: i) the “*gain of function*” mutations, where the lesion in the gene hyper-activates the transcription or the activity of the related protein [89]; and ii) “*loss of function*” mutations, where the gene involved is silenced, or the protein encoded by the specific gene is not anymore functional [89]. Genes involved in cell cycling regulation, DNA damage and in the induction of apoptosis are generally targets of “*loss of function*” mutations: as an example, p53, one of the key sensors of DNA damage, is found mutated in 50% of diagnosed cancers [90]. Mutated p53 is unable to inhibit cell proliferation upon DNA damage and, in case the damage is too pronounced, to induce cell death. In neuroblastoma cell lines, “*loss of function*” mutations of the effectors of apoptosis, the caspase family, have been reported [91].

“*Gain of function*” mutations occur in genes which regulate the response to cell growth stimuli: growth factors receptors, such as EGF (epidermal growth factor) receptors, have been reported to be mutated in lung cancer, promoting cell proliferation [92]. The tyrosine-kinase RAS (Rat sarcoma associated protein), which plays a key role in modulating cell growth, has been reported mutated in different tumors, such as melanoma, triggering enhanced survival and resistance toward treatments [93].

Due to their intense proliferation and high mutation rates, cancer cells are generally more inclined to accumulate mutated and truncated proteins as a result of enhanced uncontrolled DNA synthesis, nutrient starvation or oxidative stress which generate increased levels of unfolded and misfolded proteins in the cytosol, triggering constitutive activation of the UPR [94]. Enhancement of pro-survival pathways is a key feature of many tumor types: among others, the NF- κ B (nuclear factor kappa-light-chain-enhancer of activated B cells) pathway plays a master role in cell proliferation and survival of

many tumors [95]. Briefly, the NF- κ B pathway is activated in response to exogenous stimuli, e.g. TNF α (tumor necrosis factor α), or endogenous cellular stress, i.e. ROS (reactive oxygen species). The canonical activation of the pathway (Figure 6) involves the phosphorylation of I κ B α (inhibitor of NF- κ B), an inhibitor subunit which prevents the nuclear translocation of the transcriptional factors RelA (transcription factor p65) and p50 and consequent I κ B α proteasomal degradation. After I κ B α degradation, RelA and p50 can translocate to the nucleus, bind the DNA and enhance transcription of several pro-survival genes which sustain tumor growth [96].

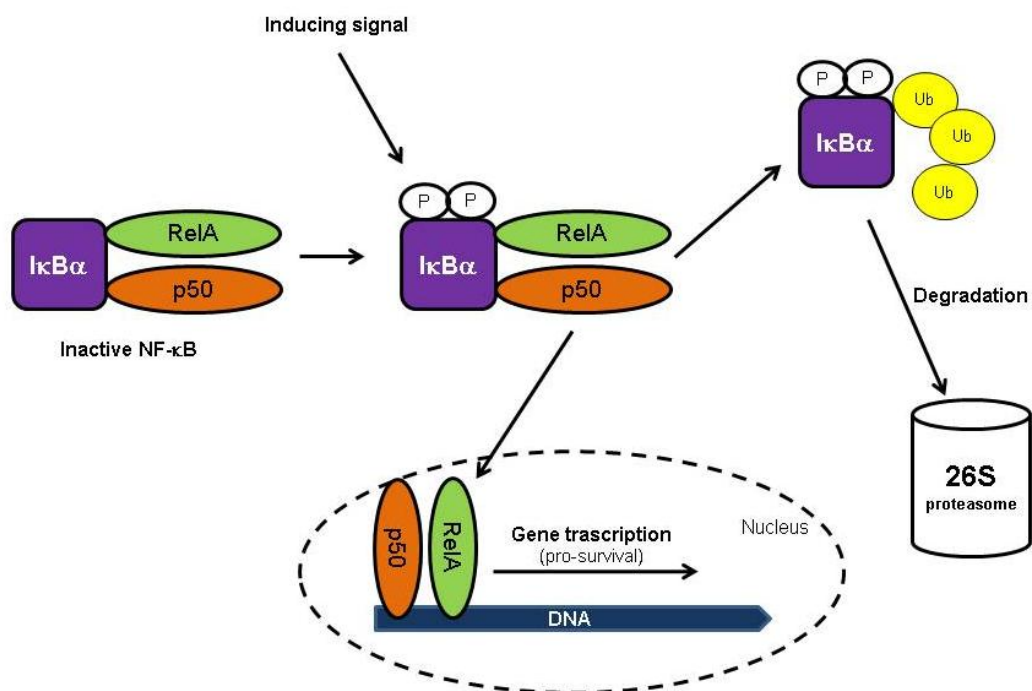


Figure 6: The canonical NF- κ B pathway.

Inactive I κ B α -p50-RelA cytosolic complex is activated by phosphorylation of I κ B α and its further ubiquitylation and proteasomal degradation. RelA and p50 are able to translocate to the nucleus and induce NF- κ B target genes.

Although, NF- κ B pathway is mostly involved in tumor survival, some recent reports suggest that the activation of NF- κ B is enhancing cell death in glioblastoma cell lines upon TRAIL treatment [97]

1.2.1. Rhabdomyosarcoma.

Rhabdomyosarcoma (RMS) is the most common soft tissue sarcoma in children. This tumor likely originates from an imbalanced differentiation process of the precursor cells of the skeletal muscle [98]: RMS cells are unable to reach terminal differentiation

exhibiting sustained proliferation, and muscle-specific markers of fetal muscle development such as MyoD (Myogenic regulatory factor D) and Vimentin [99].

RMS tumors are divided in three histological subgroups: the embryonal subgroup (ERMS), which is the most common kind of pediatric RMS; the alveolar subgroup (ARMS), which is more aggressive and less common than the ERMS subgroup; and the rare adult variant of RMS known as pleomorphic variant rhabdomyosarcoma (PRMS) [100]. Little is known of the genetic aberrations which drive the insurgences of the different pediatric RMS: ERMS has no specific gain or loss function mutations associated with the insurgence of the tumor; in contrast, 85% of ARMS diagnosed tumors are associated with the translocation of genes encoding the transcriptional factor FOXO1A (forkhead box protein O1) with PAX-3 or PAX-7 (paired box proteins -3 and -7) resulting in FOXO1A uncontrolled transcriptional activity with consequent induction of proliferating genes such as MDM2 (Mouse double minute 2 homolog), MYCN (v-myc myelocytomatosis viral related oncogene, neuroblastoma derived) and GLI (Glioma-associated oncogene family zinc finger) [101]. Moreover RMS is associated with mutation of growth pathways, such as RAS (mainly NRAS or KRAS mutations), which in the last years have been associated with increased basal autophagy in different tumor types [102]. Immortal RMS cell lines differing for chromosomal background and histological subgroups are now available: for example, the RMS RD embryonal cell line possess a NRAS mutation [103], while the alveolar RMS RMS13 cell line is wild type for RAS but shows FOXO1-PAX3 fusion gene overexpression [104]

Currently, the therapy used for RMS patients involves surgery, and usually radiotherapy followed by chemotherapy- commonly a combinatory treatment of vincristine and dactinomycin together with alkylating agents, either cyclophosphamide or ifosfamide [105]. Despite the therapeutic efforts, RMS prognosis remains poor: for this reason, the study of novel targets and therapeutic agents which can improve RMS patients' outcome is of crucial importance. In the last years, the development of animal models for RMS has improved research on this topic [106]. Recently, inhibitors of the Hedgeog pathway have been described to sensitize RMS cell lines toward cell death [107]; moreover, co-treatment with PI3K/Akt/mTOR inhibitors and RAS/MEK/ERK inhibitors have been reported to increase cell death in different RMS cell lines [108].

1.3. PQC in cancer.

PQC systems have been proposed to be an interesting target in cancer therapy [109]. Drugs which selectively target 26S proteasome or key components of the aggresome-autophagy system, such as HDAC6, have been tested *in vitro* and *in vivo* and showed encouraging results in different types of tumors [110, 111]. Bortezomib is the first selective 26S proteasomal inhibitor which has been approved for clinical use by the FDA (Food and Drug Administration) for multiple myeloma treatment. Bortezomib is a N-protected dipeptide (Pyz-Phe-boroLeu) with a boron atom at the C-terminus [112]: boron interacts specifically with the catalytic subunit of the 26S proteasome and reversibly inhibits it triggering accumulation of short living proteins, pro-apoptotic regulators and misfolded and unfolded proteins [112]. Single treatment with Bortezomib triggers apoptosis in many cancer models; nevertheless, inhibition of proteasome causes induction of the autophagic branch of PQC leading to the selection of tumor cells which are resistant towards Bortezomib treatment [113].

HDACs have been reported to play a key role in cancer promotion and maintenance [114]: particular interest has been given to the synthesis of selective HDAC6 inhibitors due to its key role in modulation of many cellular pathways, mostly the aggresome-autophagy system. Several kind of specific HDAC6 inhibitors have been synthesized [115] and tested, showing induction of apoptosis in different cancer models, such as ovarian carcinoma [116]. ST80 is a newly synthesized HDAC6 inhibitor: this hydroxamate shows 31-fold more selectivity towards HDAC6 inhibition compared to HDAC1 inhibition [117].

As a consequence of the strong interplay between PQC systems (Figure 5), single treatment towards one of the constitutive PQC pathways determines a poor tumor apoptosis outcome due to increase activation of the other PQC system and consequent induced-resistance towards the treatment [10]. To overcome this acquired resistance, co-treatment strategies have been proposed: apoptosis induction by Bortezomib is significantly enhanced when the drug is used concomitantly with autophagic interfering drugs, such as chloroquine [118], or HDACs inhibitors [119]. Also, co-treatment strategies allow to decrease the concentration of drugs used, possibly diminishing off-target effects on healthy cells, and toxic side effects of the therapy on patients.

Little is known on the role of on demand BAG3 mediated autophagy in response to treatments in tumors. BAG3 protein expression has been found enhanced in different tumors, such as leukemia [120] and glioblastoma [121] and BAG3 knock-down has

been reported to increase cell death upon drug treatment [122]. It is still not clear if co-treatments which affect the constitutive PQC systems can induce resistance mechanisms based on BAG3 similarly to single treatments which increase the efficiency of proteasome or autophagy when the other PQC system is impaired.

Rhabdomyosarcoma has been found to be sensitive towards Bortezomib single agent treatment [112]: Bortezomib triggers apoptosis and induces accumulation of misfolded ubiquitin tagged proteins in the cytosol. According to these data, rhabdomyosarcoma cell lines are a suitable model to study the effects of simultaneous inhibition of proteasome and HDAC6-mediated aggresome-autophagy system.

2. Aim of the Study

Increasing the efficiency of cancer treatments is one of the primary goals of translational cancer research. On one hand, efforts have been made in order to find a set of specific druggable targets which can be selectively exploited to kill tumor cells; on the other hand, the high rate of mutations occurring in tumors leads to high level of acquired resistance towards drugs. Constitutive protein quality control systems (PQC), i.e. proteasome and the selective aggresome-autophagy pathway, have recently been described as interesting targets to selectively induce apoptosis in various tumor entities [111]: for example, inhibitors of proteasome, such as Bortezomib, showed encouraging results in trial studies of myeloma patients [123]; and inhibitors of HDAC6, a key component of the aggresome-autophagy system, show toxicity toward tumors in preclinical studies [124]. Single agent treatment against one of the two main branches of PQC often triggers the compensatory induction of the other PQC branch, leading to acquired tumor resistance toward the treatment [10]. Combinatory treatment strategies have been proposed to overcome this resistance, showing synergism in a various number of tumor types [125, 126].

Here we aimed to investigate the effect on cell death of concomitant pharmacological inhibition of constitutive PQC (proteasome and aggresome-autophagy system) by Bortezomib and HDAC6 catalytic inhibitor ST80 in rhabdomyosarcoma cell lines. Moreover, we focused our attention on the insurgence of inducible resistance mechanisms triggered by the co-treatment which would allow ST80/Bortezomib surviving cells to overcome the induced proteotoxicity and recover upon drug removal.

3. Materials and Methods

3.1. Materials

3.1.1. Cell lines

3.1.1.1. Rhabdomyosarcoma and fibroblast cell lines

<i>Cell line</i>	<i>Provider</i>
BJ	American Type Culture Collection
RD	American Type Culture Collection
RMS13	American Type Culture Collection
TE671	American Type Culture Collection

3.1.1.2. Virus packaging cell lines

<i>Cell line</i>	<i>Provider</i>
HEK293T	American Type Culture Collection
RetroPack™ PT67 Cell line	Clontech Laboratories/ BD Biosciences

3.1.2. Cell culture reagent

<i>Reagent</i>	<i>Provider</i>
Doxycyclin	Santa Cruz Biotechnology
Dulbecco's modified eagle medium (DMEM)	Gibco
Fetal Calf Serum (FCS)	Invitrogen
HEPES	Gibco
MEM α , GlutaMAX™, no Nucleosides	Invitrogen
PBS (Dulbecco's phosphate buffered saline) (1x)	PAA Laboratories
Penicillin/ Streptomycin (100x)	PAA Laboratories
Puromycin	PAA Laboratories
RPMI Medium 1640(1x) - GlutaMAX™-I	Invitrogen
Sodium pyruvate (100x)	Gibco

Trypan blue	Invitrogen
Trypsin/EDTA solution	Gibco
Zeocin	InvivoGen

3.1.3. Apoptosis inducing agents, inhibitors

<i>Reagent</i>	<i>Provider</i>
ABT-737	Kindly provided by Abbott Laboratories
Bafilomycin A1	Sigma
Bortezomib	Purchased by Jansen-Cilag
Lexatumumab	Kindly provided by R. Humphreys
ST80	Kindly provided by M. Jung
TNF α	Biochrom

3.1.4. Protein electrophoresis and western blot reagents

<i>Reagent</i>	<i>Provider</i>
Albumin fraction V (BSA)	Carl Roth
Ammonium persulfate	Carl Roth
Dithiothreitol (DTT)	Calbiochem
Gel blot paper	Carl Roth
Hybond ECL 0.45 μ m	Amersham Bioscience
Hyperfilm ECL	Amersham Bioscience
Milk powder	Carl Roth
N,N,N',N'-Tetramethyl-ethylenediamine (TEMED)	Carl Roth
Nitrocellulose Membrane	Amersham Bioscience
PageRuler Plus Prestained Protein Ladder	Fermentas
Pierce® ECL Western Blotting Detection Reagents	Thermo Scientific
Protease inhibitor cocktail	Carl Roth
PVDF Membrane	Millipore
Roentoroll HC x-ray developer	TETENAL
Rotiphorese® Gel 30	Carl Roth

Sodium Dodecyl sulfate (SDS)	Carl Roth
Starter for x-ray developer	TETENAL
Superfix MRP x-ray fixing solution	TETENAL
Triton X-100	Carl Roth
Tween® 20	Carl Roth

3.1.5. Antibodies

3.1.5.1. Primary western blot antibodies

(diluted in 2% BSA/PBS, 0.02% sodium azide)

<u>Antibody</u>	<u>Dilution</u>	<u>Provider</u>
mouse anti-GAPDH	1:5000	HyTest
mouse anti-polyubiquitin	1:1000	Millipore
mouse anti- α -tubulin (DM1A)	1:3000	Calbiochem
mouse anti- β -actin	1:10000	Sigma
rabbit anti-ATG7	1:500	AbCam
rabbit anti-BAG3	1:1000	AbCam
rabbit anti-Histone 3	1:1000	AbCam
rabbit anti-I κ B α	1:500	Cell Signaling
rabbit anti-LC3	1:2000	Thermo Scientific
rabbit anti-p62/SQSTM1	1:1000	MBL

3.1.5.2. Secondary western blot antibodies

(diluted in 5% milk/PBS-T)

<u>Antibody</u>	<u>Dilution</u>	<u>Provider</u>
anti-mouse infrared dye-labeled green	1:10000	Li-COR Bioscience
anti-mouse infrared dye-labeled red	1:20000	Li-COR Bioscience
anti-rabbit infrared dye-labeled green	1:10000	Li-COR Bioscience
anti-rabbit infrared dye-labeled red	1:20000	Li-COR Bioscience

goat anti-mouse IgG conjugated to HRP	1:5000	Santa Cruz
goat anti-rabbit IgG conjugated to HRP	1:5000	Santa Cruz

3.1.6. Plasmids

<u>Plasmid</u>	<u>Provider</u>
pCFG5-IEGZ	kindly provided by B.Baumann
pCFG5-IEGZ I κ B α -S(32,36)A	kindly provided by B.Baumann
pCMV-dR8.91	Thermo Fisher Scientific
pGIPZ-shRNAmir	Thermo Fisher Scientific
pMD2.G	Thermo Fisher Scientific
pTRIPZ-shRNAmir	Thermo Fisher Scientific

3.1.7. shRNA plasmids

(provided by Thermo Fisher Scientific)

<u>Gene</u>	<u>Library reference number</u>
ATG7	RHS4430
BAG3 (#1)	RHS4430
BAG3 (#3)	RHS4430
BAG3 (#4)	RHS4430
Control (Ctrl)	RHS4346

3.1.8. Cloning related material

<u>Reagent</u>	<u>Provider</u>
Agarose	Invitrogen
Generuler TM 1 kb DNA ladder	Fermentas
MluI enzyme	Fermentas
One Shot Top 10 E.coli competent cells	Invitrogen
Restriction enzyme buffer R	Fermentas
T4 DNA Buffer Ligase	Fermentas
T4 DNA ligase	Fermentas
XhoI enzyme	Fermentas

3.1.9. Oligonucleotides for qRT-PCR

<u>Name</u>	<u>Sequence</u>
18S forward (for)	CGCAAATTACCCACTCCCG
18S reverse (rew)	TTCCAATTACAGGGCCTCGAA
BAG1 forward (for)	TCACCCACAGCAATGAGAAG
BAG1 reverse (rew)	ATTAACATGACCCGGCAACC
BAG3 forward (for)	CTCCATTCCGGTGATACACGA
BAG3 reverse (rew)	TGGTGGGTCTGGTACTCCC
TNF α forward (for)	ACAACCCTCAGACGCCACAT
TNF α reverse (rew)	TCCTTCCAGGGGAGAGAGG

3.1.10. Kits

<u>Kit</u>	<u>Provider</u>
7900HT fast real-time PCR system	Applied Biosystems
GeneJET™ Gel extraction Kit	Fermentas
peqGOLD Total RNA kit	Peqlab Biotechnologie GmbH
Pierce® BCA Protein Assay Kit	Thermo Scientific
Pure Link HiPure Plasmid Filter	Invitrogen
Maxiprep Kit	
RevertAid H Minus First Strand cDNA	MBI Fermentas GmbH
Synthesis Kit	

3.1.11. General chemicals

<u>Reagent</u>	<u>Provider</u>
Bromphenolblue	Carl Roth
Crystal violet	Carl Roth
Dimethyl sulfoxide (DMSO)	Sigma
di-Natriumhydrogenphosphat-Dihydrat (Na ₂ HPO ₄)	Carl Roth
Ethanol	Carl Roth
Glycerol	Carl Roth
Glycin	Carl Roth

Kaliumdihydrogenphosphat (KH ₂ PO ₄)	Carl Roth
Lipofectamine 2000	Invitrogen
LysoTracker® Red CMXRos	Molecular Probes
Methanol	Carl Roth
Phenylmethylsulfonyl fluoride (PMSF)	Carl Roth
Polybrene (Hexadimethrine bromide)	Sigma
Potassium Chloride (KCl)	Riedel-de Haen
Propidium iodide	Sigma
Sodium chloride	Carl Roth
Tris	Carl Roth
β-Mercaptoethanol	Merck

3.1.12. Plastic material

<i>Material</i>	<i>Provider</i>
Cell culture flasks (25 cm ² , 75 cm ² , 175 cm ²)	Greiner Bio-One
Collagen type 1 coated plates (24, 96-well)	Greiner Bio-One
Combitips (0.5 ml, 1 ml, 2.5 ml, 5 ml, 10 ml)	Eppendorf
Conical polystyrene tubes (15 ml, 50 ml)	Greiner Bio-One
Cryotubes	Starlab
Micro Amp TM optical 96-well reaction plate	Applied Biosystems
Pasteur pipettes	Carl Roth
Pipette tips (10 µl, 200 µl, 1000 µl)	Starlab
Reaction tubes (0.5 ml, 1.5 ml, 2 ml)	Starlab
Round bottom tubes (FACS tubes)	BD Biosciences
Sterile pipettes (2 ml, 5 ml, 10 ml, 25 ml)	Greiner Bio-One
Syringe	B.Braun
Tissue culture dishes (6, 10 cm)	Greiner Bio-One
Tissue culture plates (24-well)	Starlab
Tissue culture plates (6-, 12-, 96-well)	Greiner Bio-One

3.1.13. Equipment

<u>Equipment</u>	<u>Provider</u>
7900HT fast real-time PCR system	Applied Biosystems
Analytical balance 770	KERN
Autoclave Systec V150	Systec
Balance 440-47N	KERN
Blotting chamber	BioRad
Cell culture incubator, MCO-20AIC	Sanyo
Centrifuge 50RS	Hettich
Centrifuge Avanti J26-XP	Beckman Coulter
Centrifuge Micro 200R	Hettich
Counting chamber (Neubauer)	Marienfeld GmbH
DNA-electrophoresis system	BioRad
Electrophoresis power supply	BioRad
FACSCanto II with FACSDIVA Software	BD Biosciences
Gel dryer (model 583)	BioRad
Heating block	Eppendorf
Infinite®M200	TECAN
Infrared Odyssey® imaging system	Li-COR
Microscope IX71 (light)	Olympus
Multipette® plus	Eppendorf
Nanodrop 1000 spectrometer	Peqlab
PCR Thermocycler	Eppendorf
Pipetboy acu	Eppendorf
Pipettes	Eppendorf
Rocking shaker	CAT
Roller mixer	Ratek
Rotator	Stuart
Sonicator H2070	Bandelin Sonplus
Table centrifuge	Carl Roth
Thermo mixer comfort	Eppendorf
Vortex mixer	Velp Scientifica

Water bath	Medingen
WTW-pH-meter	Norfab

3.2. Methods

3.2.1. Cell culture

Rhabdomyosarcoma cell lines and human fibroblast cell line (BJ) were kept in culture in RPMI 1640 (RMS13, TE671) or DMEM medium (RD, BJ) supplemented with 10 % fetal calf serum (FCS), 1 mM glutamine, 1 % penicillin/streptomycin and 25 mM HEPES.

3.2.2. Generation of stable genetic modified cell lines

3.2.2.1. Retroviral transduction

Production of RMS NF κ B super-repressor cell lines (I κ B α -SR) were obtained by transfecting pCFG5-IEGZ vector or pCFG5-IEGZ vector containing I κ B α -S(32, 36)A into PT67 gamma-retroviral producer cells as previously described [127]. PT67 were seeded in 6-well plates (2×10^5 cells/cm²) in penicillin/streptomycin free medium to then be transfected with a solution of 4 μ l Lipofectamine 2000 and 4 μ g plasmid DNA for each well. After 6 hours incubation, medium was changed and cells were grown in DMEM complete medium for 48 hours. PT67 virus-containing supernatant was collected the day of infection. RMS cells were seeded in 6-well plates (0.15×10^5 cells/cm²) 24 hours previous infection and then spin-transduced with 3 ml supernatant containing 8 μ g/ml polybrene at 1300 rpm for 90 min at 25°C. After 6 hours incubation, virus containing medium was removed and cells were selected for 2 weeks with 1 μ g/ml zeomycin. Infection efficiency was determined by western blot analysis.

3.2.2.2. Lentiviral transduction (shRNA)

For stable or inducible gene knockdown, HEK293T producer cells were transfected with pGIPZ-shRNAmir or pTRIPZ-shRNAmir vector using calcium phosphate transfection as previously described [128]. Shortly, HEK293T cells were seeded in 10 cm dishes (5×10^6 cells/cm²) 24 hours prior transfection. DNA mix solution of 7.5 μ g

pGIPZ-shRNAmir or pTRIPZ-shRNAmir vector, 12.5µg pCMV-dR8.91 and 1µg pMD2.G in ddH₂O containing 50µl of 2M CaCl₂ was added to 2x HEPES buffered solution (HBS) for 20 minutes (transfection solution). Meanwhile, HEK293T DMEM-complete medium was changed with fresh media containing 25µM chloroquine. Transfection solution was drop wise added. Medium was exchanged after 10-12 hours and cells were grown in fresh medium for 48 hours. Virus containing supernatant was filtered using a 45µm filter and then added to target RMS cells together with 8 µg/ml polybrene. Spin-transduction of target cells was carried on at 1300 rpm for 90 min at 25°C. Cells were selected for 1 week with 1 ng/ml puromycin. Knock down efficiency was evaluated by qRT-PCR and/or western blot analysis.

3.2.3. Fluorescence-activated cell-sorting (FACS) analysis

3.2.3.1. Determination of apoptosis

Apoptosis was measured by fluorescence-activated cell-sorting (FACS) analysis of DNA fragmentation of propidium iodide-stained nuclei as previously described [129]. Cells were seeded in 24-well plates (0.15×10^5 cells/cm²) 24 hours previous treatment. At indicated time points, cells were trypsinized and washed in cold 1xPBS for 5 minutes at 1800rpm at 4°C. After supernatant was discharged, pellets were resuspended in a hypotonic fluorochrome solution containing 50 µg/ml propidium iodide, 0.1% sodium citrate and 0.4% Triton-X 100 for at least 1 hour at 4°C. The content of hypodiploid DNA (sub-G1 peak) was quantified by FACS as indicator of apoptotic cell death.

3.2.3.2. Determination of lysosomal acidification

Acidification of lysosome was measured by fluorescence-activated cell-sorting (FACS) analysis of LysoTracker Red stained lysosomes according to manufacture instructions. Cells were seeded in 24-well plates (0.15×10^5 cells/cm²) 24 hours previous treatment. At indicated time points 0.05 nM LysoTracker Red was added to the medium directly in the well for 10 minutes. Medium was then eliminated and cells were recovered by trypsinization and washed with 1xPBS for 5 minutes at 1800rpm at room temperature. Pellets were resuspended in 100 µl 1xPBS and fluorescence was directly measured by FACS.

3.2.4. Determination of cell viability and colony formation

Cell viability was assessed by crystal violet staining of living cells. RMS cell lines were seeded in 6-well plates (0.15×10^5 cells/cm²) and treated after 24 hours. At indicated time points, medium was discharged and cells were stained directly on plate with crystal violet solution containing 0.75 % crystal violet, 50 % ethanol, 0.25 % NaCl, 1.57 % formaldehyde for 10 minutes. Crystal violet solution was then removed and stained cells were resuspended in 1% SDS. Absorbance at 550nm was measured by microplate reader.

For colony formation assay, RMS treated cells were reseeded in 6-well plates as single cells (200 cells/well) and grown in drug free medium for 14 days. After removal of the medium, colonies were stained with crystal violet solution. The number of colonies was assessed by counting under the microscope.

3.2.5. Molecular biology methods

3.2.5.1. Protein extraction and quantification

Cells were lysate in lytic buffer (30 mM Tris HCl, 150 mM NaCl, 1% Triton-X 100, 10% Glycerol 0.5 mM, PMSF, 2mM DTT and protease inhibitor cocktail) supplemented with 100mM PMSF and phosphatase inhibitors (1 mM Sodium-orthovanadate, 1 mM β -glycerophosphate, 5mM Sodium Fluoride) for 30 minutes on ice. After hypercentrifugation (14000 rpm, 30 minutes, 4°C), supernatant was collected. Protein determination of the supernatant was assessed by Pierce® BCA Protein Assay Kit according to manufacture instructions.

3.2.5.2. Western blot analysis

Western blot analysis was performed as described previously [129]. Briefly, equal amounts of proteins were diluted in 1xSDS loading buffer (TrisBase (1M; pH 6.8), 5% Glycerol, 1% SDS, 2mM DTT; 0.01 mg/ml Bromphenolblue) and denatureted for 5 minutes at 96°C. Proteins were then loaded into home made polyacrylamide gels (resolving gel: 10% 12% 13.5% Acrylamide, 0.1% SDS, 250 mM Tris HCl pH 8.8, 0.1% APS, 0.04% TEMED; stacking gel: 5% Acrylamide, 0.1% SDS, 125 mM Tris HCl pH 6.8, 0.1% APS, 0.1% TEMED). Proteins were run on the gel at constant voltage (100-150 V) until they reached the end of the gel. Blotting on hybond

nitrocellulose or polyvinylidene difluoride (PVDF) membrane was performed by semidry blotting system. Gel paper, gel and membranes were equilibrated in blotting buffer (125 mM Tris Base, 1.25 mM Glycine, 0.1% SDS, 20% Methanol) and piled on the anode plate. Blotting was performed with constant ampere (1 mA/cm²) for 1 hour or 1 hour 40 minutes depending on the thickness of the gel. Membranes were then blocked in a 5% milk/PBS-T solution for 1 hour to prevent unspecific binding. Primary antibodies (see paragraph 3.1.5.1) were diluted in blocking solution or 2% BSA, 0.05% Sodium azide containing PBS-T solution and were incubated over night at 4°C. To avoid unspecific binding of secondary antibody, membranes were washed three times with 1XPBS-T and incubated 1 hour with alternatively secondary antibody conjugated to horseradish peroxidase (HRP) or infrared dye-labeled secondary antibodies diluted in 5% milk/PBS-T. Specific protein signal was detected after three wash in 1xPBS-T by enhanced chemiluminescence (ECL) or infrared Odyssey[®] imaging system, respectively. Representative images of at least two independent experiments are shown.

3.2.5.3. Detection of protein aggregates: Triton-X fractionation

Protein aggregates were detected by fractionation in Triton-X as previously described [130]. Cells were lysate in 2% Triton-X/1% PBS solution supplemented with proteases and phosphatases (100mM PMSF, 1 mM Sodium-orthovanadate, 1 mM β-glycerophosphate, 5mM Sodium Fluoride) for 30 minutes on ice. Lysate were centrifuged (13000 rpm, 30 minutes, 4 °C); supernatant was collected as soluble fraction. Pellets were resuspended in 1% SDS supplemented with proteases and phosphatases and sonicated for 20 second (45% intensity). Expression of ubiquitin-positive protein aggregates was determined by western blot analysis.

3.2.5.4. Detection of protein aggregates: Filter Trap assay

Determination of protein aggregates by filter trap assay was performed as previously described [131]. Shortly, cells were recovered by scraping in 1XPBS and centrifuge 1800 rpm 5 minutes at 4 °C. Pellets were resuspended in 1XPBS supplemented with proteases and phosphatases and sonicated twice for 20 seconds (45% intensity). After protein determination, equal amount of proteins were resuspended in 1% SDS and directly vacuum-blotted on a nitrocellulose membrane. Ubiquitin-positive aggregates were detected by western blot.

3.2.6. Generation of pTRIPZ-shRNA plasmids.

Sub-cloning of shRNA control sequence and shATG7 sequence (see paragraph 3.1.7) from the pGIPZ plasmid to the doxocyclin inducible pTRIPZ plasmid was obtained by digestion of 8 µg pGIPZ-shRNA containing plasmid and 5 µg pTRIPZ empty plasmid with 1 µl of XhoI and MluI restriction enzymes for 3 hours. Digestion products were respectively run in a homemade 0.8% and 1% agarose gel supplemented with ethidium bromide. Gel extraction of the correspondent DNA band from the agarose gel was performed with GeneJET™ GEL extraction Kit according to manufacture instructions. 250 ng of pTRIPZ and 7.5 ng of the insertion sequences were ligate with 0.5 µl of T4 ligase enzyme for 1 hour. One Shot Top 10 E.coli competent cells were transformed with the ligation solution according to manufacture instructions and grown overnight. Plasmid extraction was performed by Pure Link HiPure Plasmid Filter Maxiprep Kit according to manufacture instructions.

3.2.7. Quantitative Reverse Transcription PCR (qRT-PCR)

Total RNA was extracted using peqGOLD Total RNA kit according to the manufacture instructions. 3 µg of total RNA were used to synthesize the corresponding cDNA using RevertAid H Minus First Strand cDNA Synthesis Kit.

Quantitative evaluation of selected genes (see paragraph 3.1.9) was determined by SYBR-Green based qRT-PCR performed by using the 7900HT fast real-time PCR system. Briefly, 500 ng cDNA was loaded in each well (96-well plate) with 2XSYBR-Green solution and 10 pMol/µl of forward and reverse gene specific oligonucleotide primer and/or reference oligonucleotide primer 18S. qRT-PCR reaction was performed for 40 cycles (50 °C 2 min.; 95°C 10 min.; 95°C 15 sec.; 60°C 1 min.). Denaturation curves were plotted to verify the specificity of the amplified products. All determinations were performed in triplicate. The relative expression of the target gene transcript and reference gene transcript was calculated as $\Delta\Delta C_t$.

3.2.8. Statistical analysis

Statistical significance was assessed by Student's *t*-Test (two-tailed distribution, two-sample, unequal variance).

4. Results

4.1. A subpopulation of RMS cells is able to survive and recover upon ST80/Bortezomib co-treatment.

To investigate the potential role of concomitant inhibition of constitutive PQC systems, i.e. UPS and aggresome-autophagy system, we selected three different RMS cell lines (RD, TE671 and RMS13) and one non-transformed fibroblast cell line (BJ) and treated them with specific inhibitors of the two pathways. Bortezomib, commercially known as Valcade®, is an N-protected dipeptide which selectively and reversibly inhibits the 26S proteasome [132]. ST80 is a second generation inhibitor of the HDACs: this hydroxamate is designed in order to selectively inhibit the catalytic activity of HDAC6 with a specificity 31.4 fold higher toward HDAC6 compared to HDAC1 [117]. We subject RMS cell lines to 48 hours of single or double treatment of 50 μ M ST80 and/or three different concentration of Bortezomib; then, we measured apoptosis by quantification of DNA fragmentation (Figure 7). Importantly, addition of ST80 significantly increased Bortezomib induced apoptosis in both embryonal (RD and TE671) and alveolar (RMS13) cell lines but showed no additional effect in non-transformed fibroblast, pointing to some tumor selectivity.

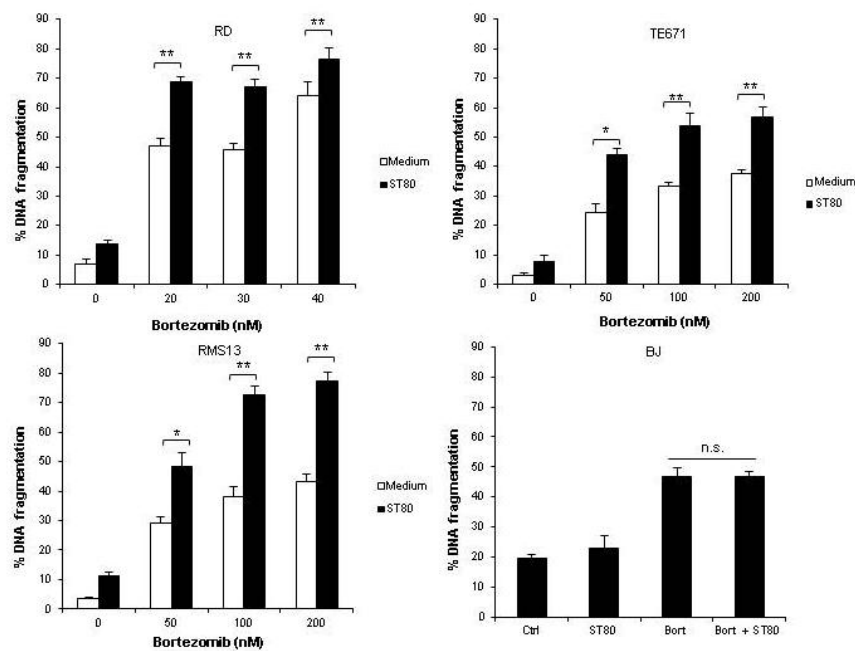


Figure 7: ST80 synergistically co-operates with Bortezomib to induce cell death in RMS.

Cells were treated for 48 hours with 50 μ M ST80 and/or Bortezomib as indicated. BJ cells were treated for 48 hours with 50 μ M ST80 and/or 20nM Bortezomib. Apoptosis was determined by FACS analysis of DNA fragmentation of propidium iodide stained nuclei. Three independent experiments in triplicate are shown. t-Student test was used to determine statistical significance: * $p < 0,05$; ** $p < 0,01$; n.s.: non significant.

Although we could increase cell death in RMS cell lines by ST80/Bortezomib co-treatment, we wondered if a subpopulation of cells was able to survive the treatment and, upon drug removal, was able to regrow at similar rates as the untreated or single treated surviving cells. To address this question we monitored cell recovery over time after drug removal (Figure 8).

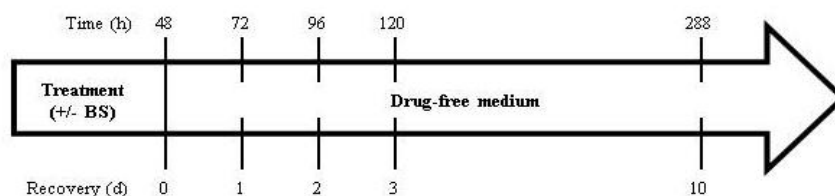


Figure 8: Experimental design for recovery studies.

Recovery experiments were done by treating the cells with single or double treatment (BS) for 48 hours before treatment was removed and cells were able to regrow in drug free medium up to 10 days

We selected two representative RMS cell lines, the embryonal RD cell line and the alveolar RMS13 cell line, as models for further studies. After 48 hours nearly one third of cells were able to survive ST80/Bortezomib co-treatment (Figure 9.a). Interestingly, upon drug removal, surviving ST80/Bortezomib cells were able to regrow at similar rates compare with ST80 and Bortezomib single treated surviving cells (Figure 9.b). This set of data suggests that ST80/Bortezomib surviving cells can activate a defense mechanism which can overcome the toxicity induced by the treatment and support cell recovery.

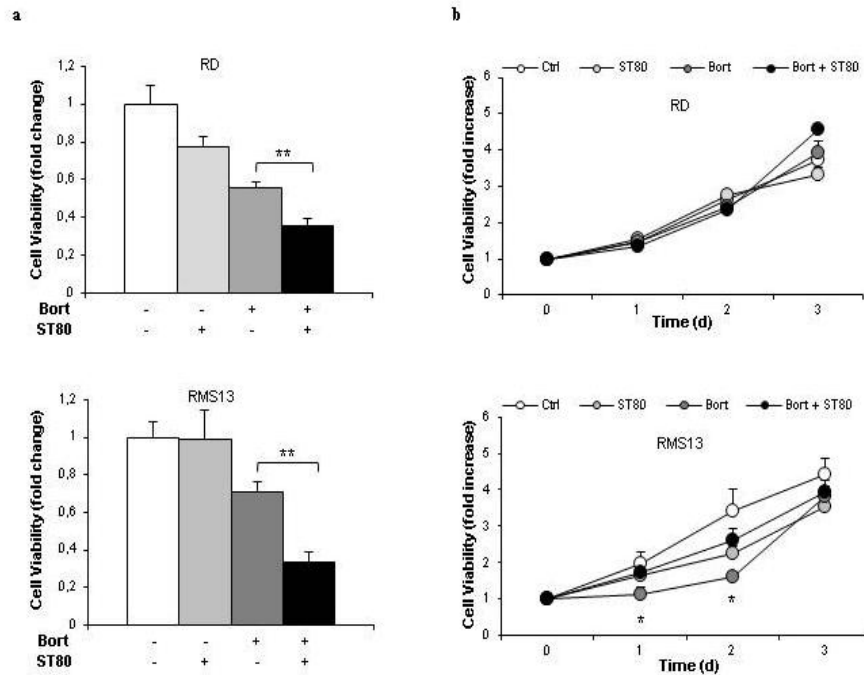


Figure 9: ST80/Bortezomib surviving cells are able to regrowth upon drug removal.

Cells were treated for 48 hours (day 0) with 20 nM (RD) or 50 nM (RMS13) Bortezomib +/- 50 μ M ST80. (a) Cell viability was measured by crystal violet assay after 48 hours. Data are expressed as fold change vs. untreated. (b) Cell regrowth was measured at indicated time points of the recovery period by crystal violet assay. Data are expressed as fold change vs. day 0. Mean of three independent experiments in triplicate is shown. t-Student test was used to determine statistical significance: * $p < 0.05$; ** $p < 0.01$.

4.2. ST80/Bortezomib surviving cells accumulate protein aggregates upon co-treatment.

To understand if ST80/Bortezomib surviving cells show a similar extent of proteotoxicity compared to single treated surviving cells, we determined the amount of protein aggregates after 48 hours treatment (Figure 10). Protein aggregates are insoluble in Triton-X and, due to proteasome inhibition mediated by Bortezomib, are mostly ubiquitin-tagged. Surprisingly, ST80/Bortezomib surviving cells show higher amount of ubiquitin positive aggregates after fractionation in 2% Triton-X buffer compared both with ST80 and Bortezomib single treated surviving cells. Moreover, increase levels of p62 are detectable in the insoluble fraction of ST80/Bortezomib surviving cells (Figure 10.a). p62 is a scaffold protein which posses a UBA and a LIR domain: these domains confer to the protein the capability to interact respectively with ubiquitin and LC3. Due to this, p62 acts as a “bridge” between aggregates and autophagosomes mediating recognition and clearance of cytotoxic aggregates through the aggresome-autophagy system.

To further confirm protein aggregates accumulation, filter trap assay showed increase ubiquitin staining in ST80/Bortezomib surviving cells (Figure 10.b). Aggregates can be detected by filter trap assay due to their high molecular weight: vacuum blotting of cell lysate performed in non-denaturant conditions will let small molecular weight protein pass through the membrane but not high weight multiprotein aggregates that can be then detected by western blot analysis (Figure 10.b). Taken together, these data point to increase accumulation of protein aggregates in ST80/Bortezomib surviving cells.

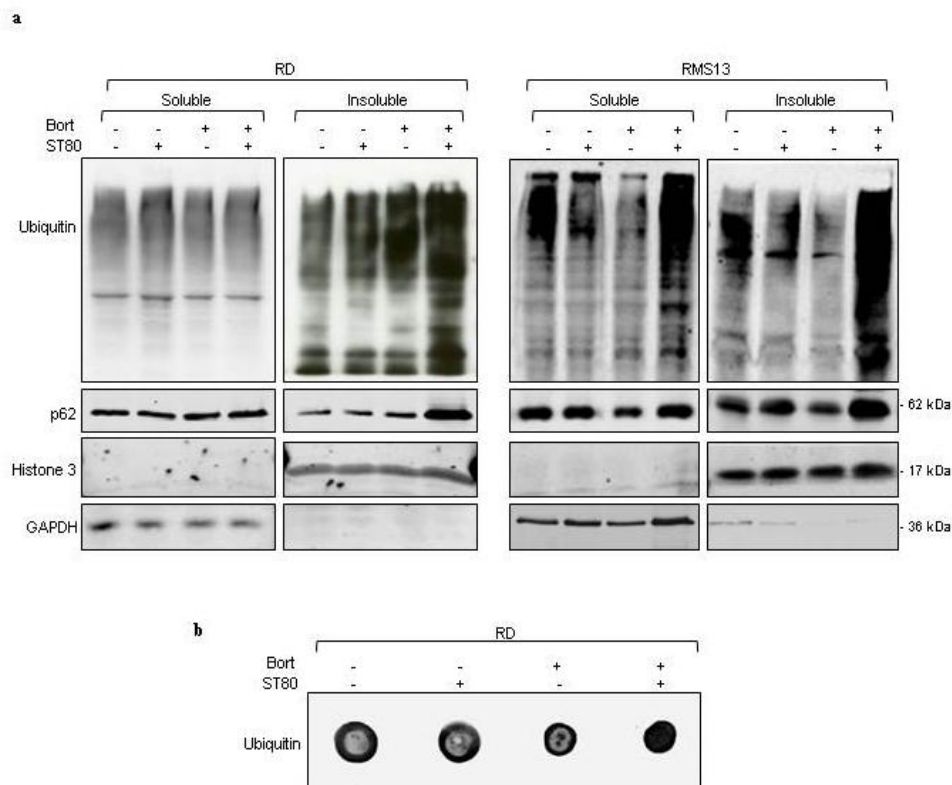


Figure 10: ST80/Bortezomib surviving cells show accumulation of protein aggregates.

Cells were treated for 48 hours with 20 nM (RD) or 50 nM (RMS13) Bortezomib +/- 50 μ M ST80. **(a)** Ubiquitin-positive protein aggregates were assessed by western blot analysis after fractionation of total viable cells in Triton-X. GAPDH and Histone 3 were used as loading and purity controls for soluble and insoluble fractions, respectively. **(b)** Ubiquitin positive aggregates were detected by filter trap assay of viable cells.

To exclude that protein aggregates accumulation was due to a general autophagy impairment mediated by the co-treatment; we measured LC3 conversion and lysosomal acidification in single and double treated surviving cells (Figure 11). During the autophagic flux, LC3 is processed into its lipid-conjugated isoform (LC3 II) which associates with autophagosome membranes: to monitor LC3 II accumulation by western blot analysis is, nowadays, the most used and described method in order to detect

autophagy *in vitro* [133]. As shown in Figure 11.a, ST80/Bortezomib surviving cells show similar or even more LC3 II compared with Bortezomib single treated cells, suggesting ongoing autophagy. Because accumulation of LC3 II can be caused both by induction of autophagy and by blockage of the autophagic flux, we quantified lysosome acidification by FACS measurement of LysoTracker Red (LTR) stained cells (Figure 11.b and c). Lysosomal acidification is a crucial step to finalize the digestion of the autophagosome cargo: loss of lysosome acidification results in blockade of the autophagy flux. Due to this, the measure of the acidity of the lysosomal compartment is an indirect method to quantify autophagy [133]. ST80/Bortezomib surviving cells show similar amount of acidic lysosome compared with Bortezomib treated cells during all 48 hours of drug treatment (Figure 11.c).

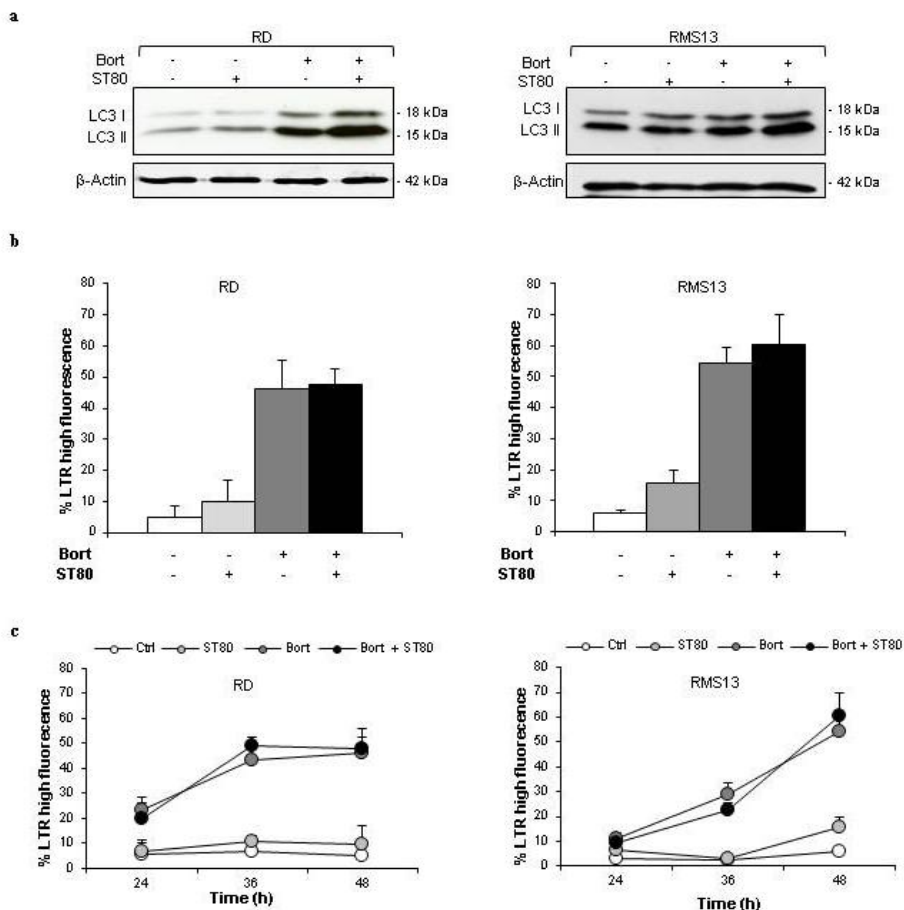


Figure 11: ST80/Bortezomib surviving cells undergo bulk autophagy.

Cells were treated with 20 nM (RD) or 50 nM (RMS13) Bortezomib +/- 50 μ M ST80. (a) LC3 I/LC3 II conversion was monitored by western blot analysis of viable cells after 48 hours treatment. β -Actin was used as loading control. (b-c) Lysosome acidification was measured by FACS analysis of LysoTracker Red staining of viable cells after 48 hours (in b) and over time (indicated time points, in c). Mean of three independent experiments in triplicate is shown.

Taken together, these data show that after 48 hours treatment ST80/Bortezomib surviving cells undergo high proteotoxic stress compared to Bortezomib treated cells due to the accumulation of ubiquitin-positive protein aggregates which can not be cleared by the ongoing bulk autophagy.

4.3. ST80/Bortezomib surviving cells up-regulate co-chaperone BAG3 in a NF κ B-dependent manner.

ST80/Bortezomib co-treatment inhibits simultaneously the two main branches of constitutive PQC, i.e. UPS and HDAC6 mediated aggresome-autophagy system. Since ST80/Bortezomib surviving cells show enhance accumulation of protein aggregates although they are still competent towards bulk autophagy (Figure 10 and 11), we hypothesized that an inducible rescue mechanism would be activated in those cells by the co-treatment in order to mitigate proteotoxicity. Co-chaperone BAG3 has been described to be induced upon proteasome inhibition, i.e. aging process [77]: BAG3 can theoretically compensate HDAC6 loss of activity and restore protein aggregates recognition by the autophagic machinery triggering their clearance [76]. In order to understand if BAG3 plays a role in ST80/Bortezomib surviving cells observed cell recovery (Figure 9), we quantified BAG3 mRNA and protein levels in the living RMS and BJ population after 48 hours of single or double treatment (Figure 12).

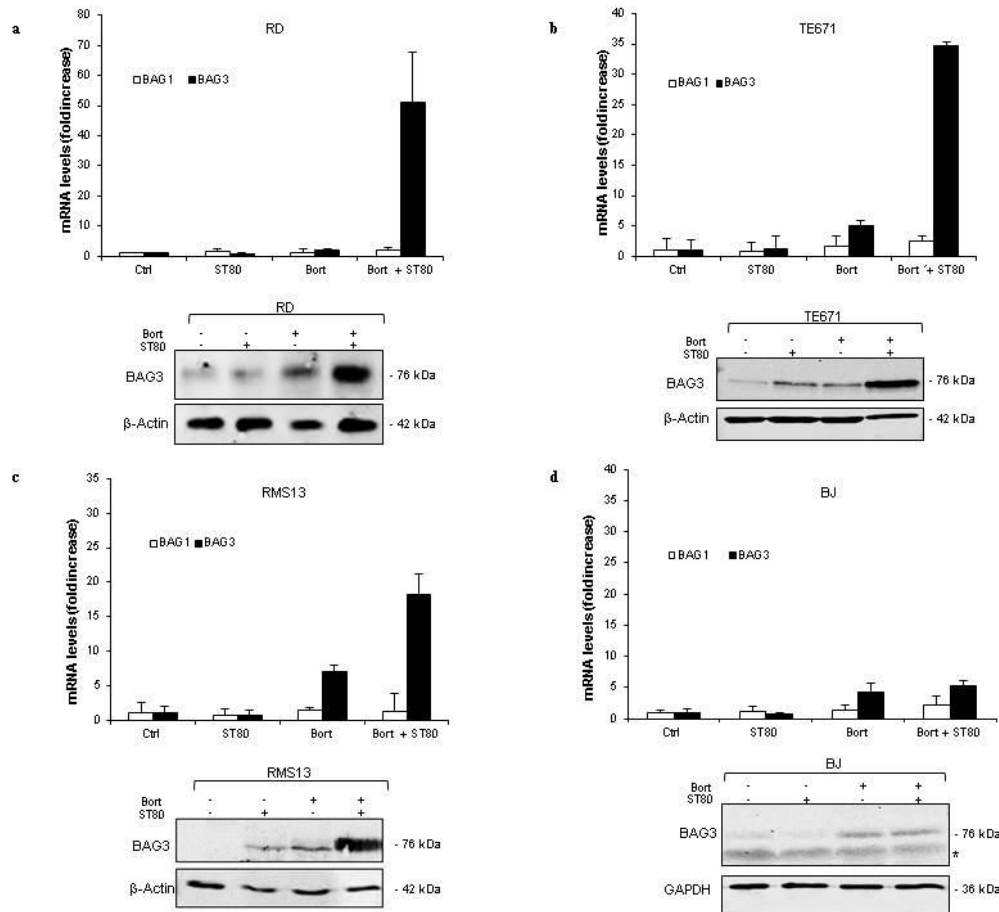


Figure 12: RMS ST80/Bortezomib surviving cells up-regulate co-chaperone BAG3.

Cells were treated with 20 nM (RD, BJ) or 50 nM (RMS13, TE671) +/- 50 μ M ST80 for 48 hours. mRNA levels were assessed by qRT-PCR. Mean of three independent experiments in triplicate is shown. Protein levels were assessed by western blot; β -Actin was used as loading control.

Interestingly, both BAG3 mRNA and protein levels are highly increased upon ST80/Bortezomib cotreatment in all RMS cell lines (Figure 12.a-c). Some increase in BAG3 mRNA and protein levels is also detectable upon Bortezomib single treatment, in line with previous publications [84]. Moreover, the BJ cell line, which shows no further sensitization toward ST80/Bortezomib co-treatment (Figure 7), have no transcriptional or translational induction of BAG3 in the ST80/Bortezomib surviving population (Figure 12.d). Previous data demonstrate that the co-chaperone BAG1 is implicated in proteasomal degradation of misfolded proteins [134]; to assure the specificity of BAG3 up-regulation we measured concomitantly BAG1 mRNA levels in the living population, showing no changes compared to untreated cells (Figure 12).

Kinetic analysis of BAG3 mRNA levels underlined a late up-regulation starting between 30-42 hours after ST80/Bortezomib co-treatment, in line with the hypothesis

that BAG3 plays a major role during the recovery phase and not in the initial phase of the treatment (Figure 13).

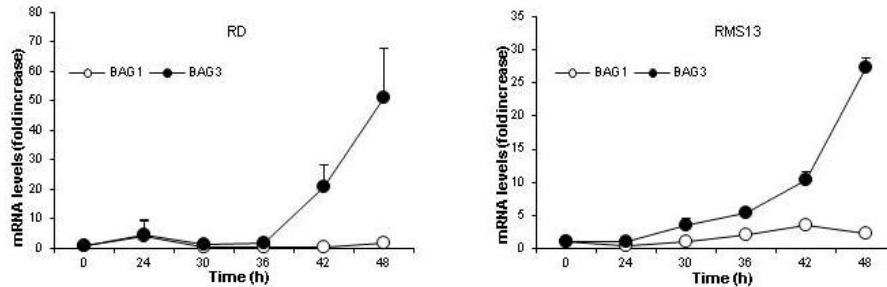


Figure 13: ST80/Bortezomib surviving cells show slow kinetic of BAG3 up-regulation.

Cells were treated with 20 nM (RD) or 50 nM (RMS13) and 50 μ M ST80 for indicated time points. mRNA levels were assessed by qRT-PCR. Mean of three independent experiments in triplicate is shown.

To exclude that BAG3 transcriptional up-regulation is simply an unspecific effect of massive cell death, we treated the RD cell line with two prototypic apoptotic stimuli and measured BAG3 mRNA levels in the surviving population (Figure 14). The TRAIL receptor 2 agonistic antibody, Lexatumumab, triggers apoptosis in RMS cell lines *via* death receptor (extrinsic pathway) [135]; the BH3 mimetic ABT-737 leads to cell death *via* the mitochondrial pathway, also known as intrinsic apoptotic pathway [136]. As shown in figure 14.a, induction of apoptosis by Lexatumumab and ABT-737 is comparable with ST80/Bortezomib co-treatment. Interestingly, no induction of BAG3 mRNA can be detected in Lexatumumab or ABT-737 surviving population, pointing to specificity of BAG3 transcriptional induction by ST80/Bortezomib co-treatment (Figure 14.b). No changes were detected in BAG1 mRNA levels (Figure 14.b)

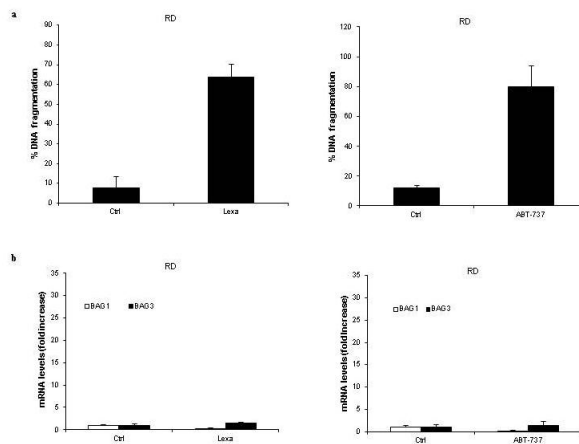


Figure 14: BAG3 up-regulation is a specific feature of ST80/Bortezomib treatment.

RD cell line was treated with 5 μ g/ml Lexatumumab or 5 μ M ABT-737 for 24 hours. (a) Apoptosis was determined by FACS analysis of DNA fragmentation of propidium iodide stained nuclei. (b) BAG1 and BAG3 mRNA levels were assessed with qRT-PCR. Mean of three independent experiments in triplicate is shown.

Recent evidences demonstrate that in a HeLA cell line heat shock model, BAG3 up-regulation was mediated by NF κ B [137]. To address the role of NF- κ B in our model, we create RMS cell lines with a phosphomutant I κ B α (I κ B α -SR) which can not be phosphorylated on Serine 32 and 36 and consecutively degraded (Figure 15.a). Impairing I κ B α degradation leads to incompetent NF κ B cell lines [138]; as shown in figure 15.b, TNF α mRNA induction is completely abolished in I κ B α -SR cells while is highly present in the empty vector (EV) cell line after TNF α stimulation.

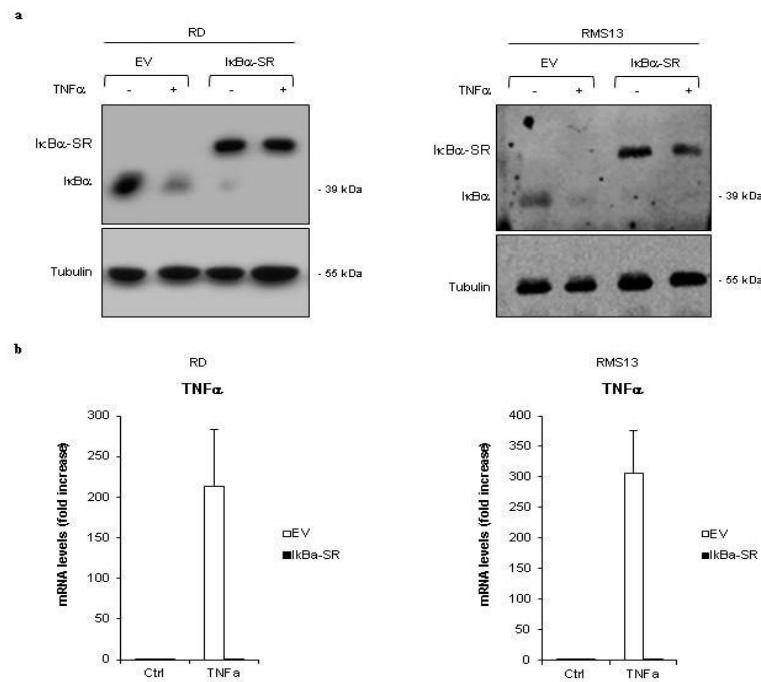


Figure 15: I κ B α -SR cells are insensitive to TNF α stimulation.

RMS cells stably expressing empty vector (EV) or I κ B α super repressor vector (I κ B α -SR) were treated with TNF α 20 ng/mL for 2h. (a) I κ B α protein levels were determined by western blot analysis. Tubulin was used as loading control. (b) TNF α mRNA levels were assessed by qRT-PCR. Mean of two different experiment performed in triplicate is shown.

Interestingly, induction of BAG3 mRNA and protein levels is completely abolished in the I κ B α -SR cells after ST80/Bortezomib co-treatment, while still present in the EV cell lines (Figure 16). Further studies need to be done to assess the exact role of NF- κ B in BAG3 up-regulation upon ST80/Bortezomib co-treatment.

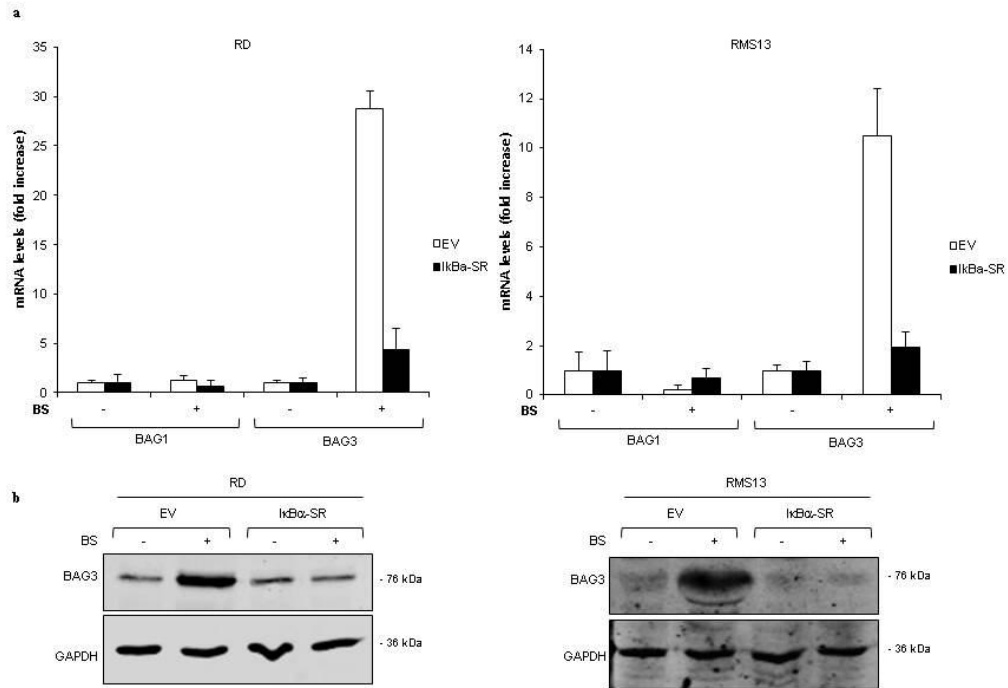


Figure 16: NF- κ B mediates BAG3 up-regulation in ST80/Bortezomib surviving cells.

Cells stably expressing empty vector (EV) or $\text{IkB}\alpha$ super repressor vector ($\text{IkB}\alpha$ -SR) were treated with 20 nM (RD) or 50 nM (RMS13) Bortezomib and 50 μ M ST80 (BS). (a) BAG1 and BAG3 mRNA levels were determined by qRT-PCR. Mean of two independent experiment performed in triplicate is shown. (b) Protein levels were determined by western blot analysis. GAPDH was used as loading control.

Taken together, these results demonstrate that ST80/Bortezomib surviving cells strongly and specifically induce BAG3 at transcriptional and translational level in a NF- κ B dependent manner.

4.4. BAG3 mediates protein aggregates clearance during cell recovery.

Since BAG3 has been previously reported to mediate protein aggregates clearance *via* selective autophagy [139], we created stable RMS BAG3 knock-down cells by short-hairpin RNA (shRNA) vectors in order to understand BAG3 role in modulating proteotoxicity upon ST80/Bortezomib treatment. As control we used a RNA sequence with no corresponding counterpart in the human genome (Figure 17). All three sequences against BAG3 mediate loss of basal and ST80/Bortezomib induced up-regulation of BAG3, both at protein and mRNA levels, while control cells (shCtrl) remain able to trigger BAG3 up-regulation up to day 3 of the recovery period (Figure 17.a and b). Constitutive BAG3 knock-down shows no effect on BAG1 mRNA level demonstrating no compensatory mechanism triggered by the loss of BAG3 in these cells (Figure 17.c).

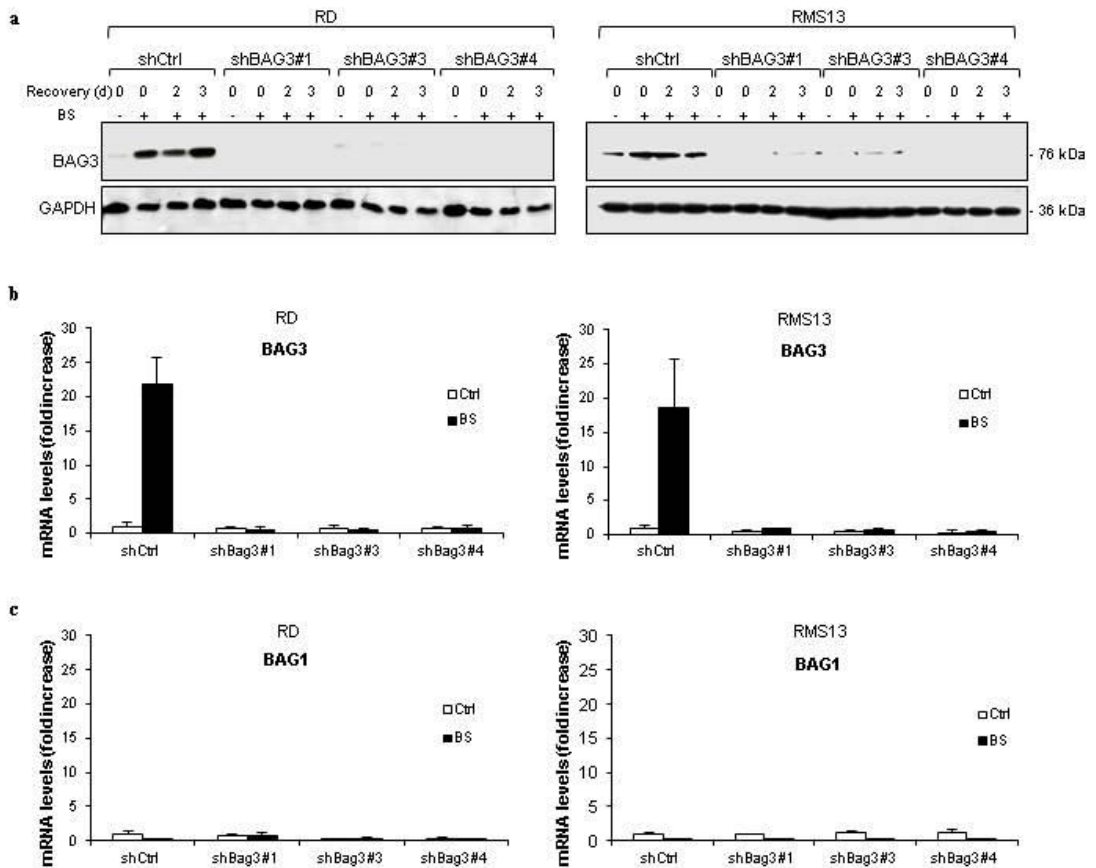


Figure 17: shBAG3 cells are unable to up-regulate BAG3 after ST80/Bortezomib treatment.

RD and RMS13 were stably transfected with three different sequences against BAG3 (shBAG3) and one control (shCtrl). (a) Cells were treated with 20 nM (RD) or 50 nM (RMS13) Bortezomib and 50 μ M ST80 (BS) for 48 hours (day 0) before treatment was removed and cells were grown in drug-free medium up to three days. BAG3 protein levels were assessed by western blot analysis at indicated time points. GAPDH was used as loading control. (b-c) Cells were treated with 20 nM (RD) or 50 nM (RMS13) Bortezomib and 50 μ M ST80 (BS) for 48 hours. BAG1 and BAG3 mRNA levels were assessed by qRT-PCR. Mean of three independent experiment performed in triplicate is shown.

In line with the late kinetic of BAG3 up-regulation (Figure 13), BAG3 knock down RMS cells show no difference in cell death compared with control vector supporting the hypothesis that BAG3 is mainly required during the recovery phase, upon drug removal, but is dispensable during the initial phase of ST80/Bortezomib treatment (Figure 18).

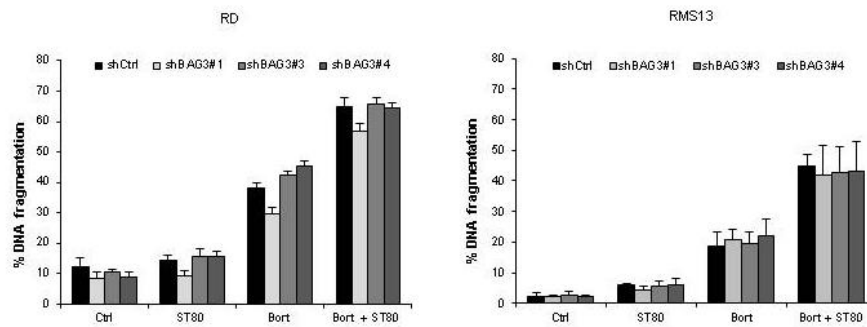


Figure 18: BAG3 is not involved in ST80/Bortezomib induced cell death.

RD and RMS13 were stably transfected with three different sequences against BAG3 (shBAG3) and one control (shCtrl). Cells were treated with 20 nM (RD) or 50 nM (RMS13) Bortezomib +/- 50 μ M ST80 for 48 hours. Apoptosis was determined by FACS analysis of DNA fragmentation of propidium iodide stained nuclei. Mean of three independent experiments in triplicate is shown.

In order to understand the impact of BAG3 on ubiquitin-positive protein aggregates accumulation, we measure Triton-X insoluble aggregates by fractionation of viable cells after 48 hours ST80/Bortezomib treatment (day 0; Figure 19.a), and at day 2 and day 3 of the recovery period (Figure 19.b). As expected, shBAG3 RMS cell lines show no differences compared with control cells in the amount of insoluble ubiquitin-positive aggregates and p62 protein levels after 48 hours of ST80/Bortezomib treatment (day 0 of recovery) in line with the dispensable role of BAG3 in the initial phase of treatment (Figure 19.a). By contrast, at day 2 and day 3 of recovery, loss of BAG3 up-regulation determines a striking accumulation of ubiquitin-positive aggregates and p62 protein levels in the insoluble fraction (Figure 19.b) compared with control cells. Moreover, control cells show decrease ubiquitin-positive aggregates at day 2 and day 3 of recovery period when compared to day 0, indicating that BAG3 plays a key role in mitigating proteotoxicity by clearing cytotoxic protein aggregates during the recovery phase. To further confirm this finding, we evaluate protein aggregates in BAG3 knock down cells by filter trap assay (Figure 20). Similarly to Triton-X fractionation, the filter trap assay shows increase accumulation of ubiquitin-positive protein aggregates at day 3 of the recovery period in shBAG3 cells while control cells show similar levels of protein aggregates as in the untreated condition (Figure 20).

Taken together, these results show that BAG3 up-regulation in ST80/Bortezomib surviving cells is necessary to decrease protein aggregates upon drug removal.

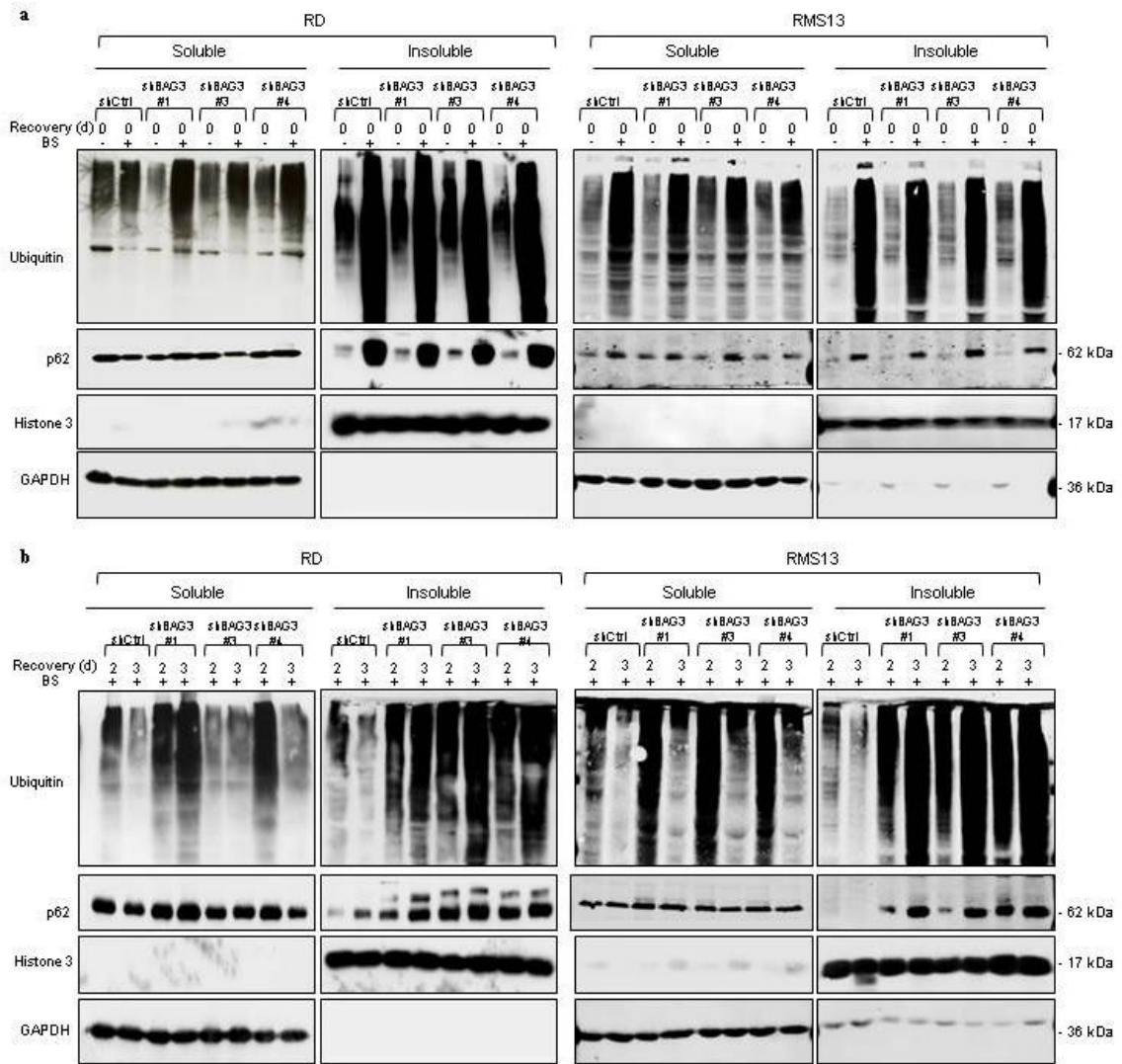


Figure 19: BAG3 mediates clearance of protein aggregates during cell recovery.

RD and RMS13 were stably transfected with three different sequences against BAG3 (shBAG3) and one control (shCtrl). Cells were treated with 20 nM (RD) or 50 nM (RMS13) Bortezomib and 50 μ M ST80 (BS) for 48 hours (day 0) before treatment was removed and cells were grown in drug-free medium up to three days. Ubiquitin-positive protein aggregates were assessed by western blot analysis after fractionation of total viable cells in Triton-X after 48 hours (a) and at day 2 and 3 of the recovery period (b). GAPDH and Histone 3 were used as loading and purity controls for soluble and insoluble fractions, respectively.

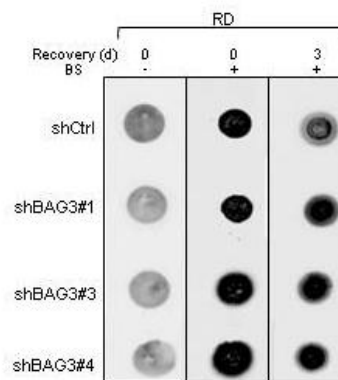


Figure 20: BAG3 plays a key role in protein aggregates clearance upon ST80/Bortezomib removal.

RD was stably transfected with three different sequences against BAG3 (shBAG3) and one control (shCtrl). Cells were treated with 20 nM Bortezomib and 50 μ M ST80 (BS) for 48 hours (day 0) before treatment was removed and cells were grown in drug-free medium up to three days. Ubiquitin positive aggregates were detected by filter trap assay of viable cells at indicated time points.

4.5. BAG3 is necessary for cell regrowth after ST80/Bortezomib co-treatment.

In order to investigate the importance of BAG3 up-regulation in mitigation of cytotoxicity during the recovery phase, we treated the shBAG3 and control cells for 48 hours with Bortezomib and/or ST80 (day 0). Then, we removed the treatment allowing cells to regrow in drug-free medium up to three days (Figure 21). Untreated and single treated surviving cells show comparable ratio of cell regrowth despite the presence or absence of BAG3 (Figure 21.a-c), in line with the absence of BAG3 up-regulation detected in these conditions (Figure 12.a and c). Contrarily, ST80/Bortezomib shBAG3 surviving cells completely lost the capability to regrow while shCtrl cells show cell regrowth up to three fold at day 3 of the recovery period (Figure 21.d). These data suggest that BAG3 up-regulation is necessary for ST80/Bortezomib surviving cells to cope with the elevated cytotoxicity induced by the treatment in order to recover upon drug removal.

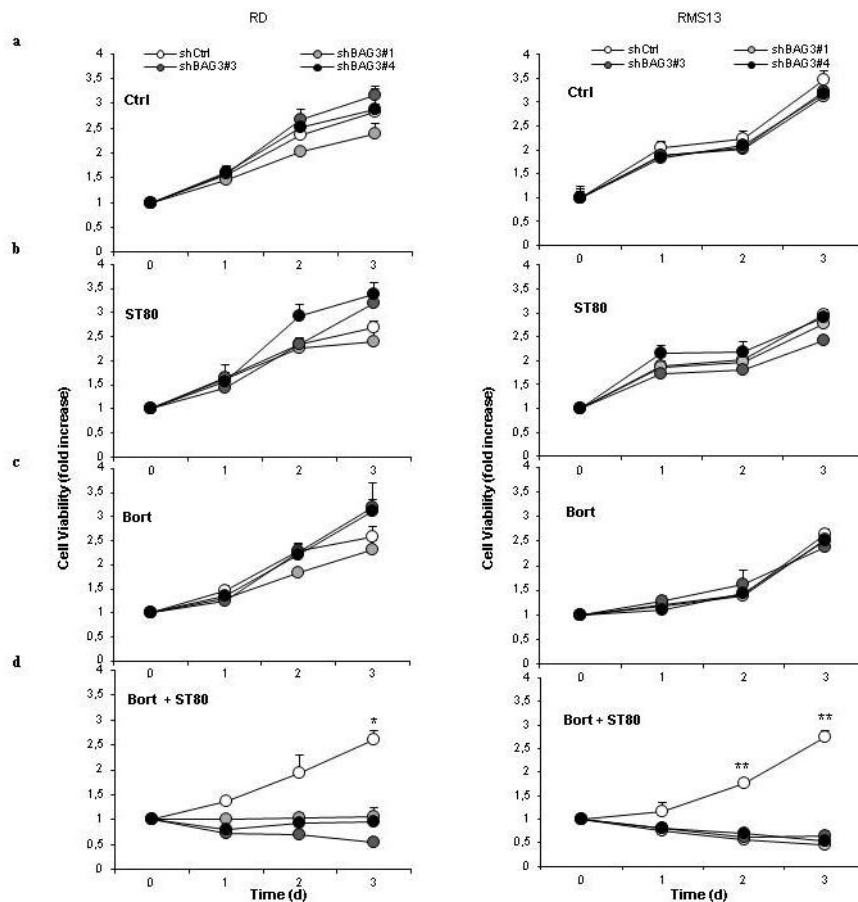


Figure 21: BAG3 up-regulation is necessary for cell regrowth in ST80/Bortezomib surviving cells.

RD and RMS13 were stably transfected with three different sequences against BAG3 (shBAG3) and one control (shCtrl). Cells were treated with 20 nM (RD) or 50 nM (RMS13) Bortezomib and/or 50 μ M ST80 for 48 hours (day 0) before treatment was removed and cells were grown in drug-free medium up to three days. Cell proliferation was measured by crystal violet staining at indicated time points. Data are expressed as fold change vs. day 0. Mean of three independent experiments in triplicate is shown. t-Student test was used to determine statistical significance between shBAG3 and control vector: * $p < 0,05$; ** $p < 0,01$.

In order to understand if the loss of viability of shBAG3 cells during the recovery period, is due to increase cell death, we measured apoptosis by FACS analysis of fragmented DNA after 48 hours of ST80/Bortezomib treatment (day 0 of recovery) and at day 3 of the recovery period (Figure 22). BAG3 knock down cells show enhanced cell death at day 3 of the recovery period compared with control vector, indicating actual cell death of the ST80/Bortezomib surviving cells which are unable to up-regulate BAG3.

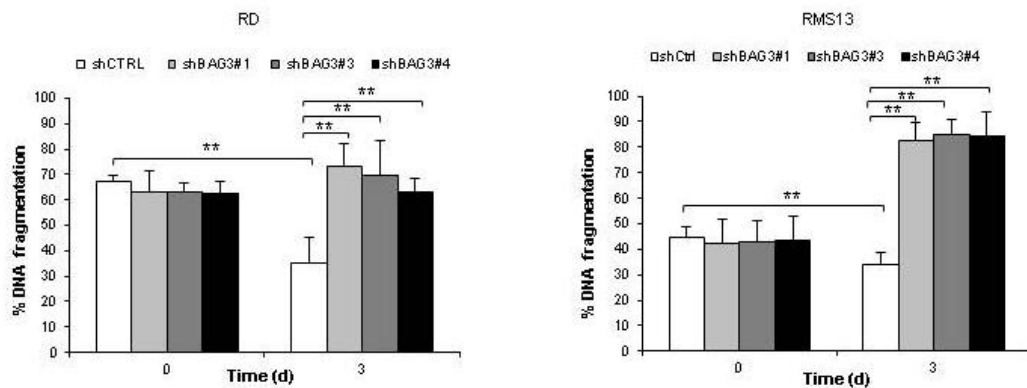


Figure 22: Loss of BAG3 up-regulation triggers cell death during cell recovery.

RD and RMS13 were stably transfected with three different sequences against BAG3 (shBAG3) and one control (shCtrl). Cells were treated with 20 nM (RD) or 50 nM (RMS13) Bortezomib and 50 μ M ST80 for 48 hours (day 0) before treatment was removed and cells were grown in drug-free medium up to three days. Apoptosis was determined by FACS analysis of DNA fragmentation of propidium iodide stained nuclei. Mean of three independent experiments in triplicate is shown. t-Student test was used to determine statistical significance between shBAG3 and control vector or between day 0 and day 3 of the recovery period: **p<0.01.

To understand the long term effects of BAG3 up-regulation, we followed BAG3 knock-down and control RMS cell lines up to ten days after drug removal (Figure 23.a). ST80/Bortezomib surviving cells which are still able to up-regulate BAG3 (shCtrl cell lines) show constant cell proliferation after drug removal; on the contrary, cells transfected with all three sequences against BAG3 are completely incapable of cell regrowth also in longer time periods (Figure 23.a). Then, we wanted to test the role of BAG3 in clonogenic survival. To this end, we seeded ST80/Bortezomib surviving cells as single cell in drug-free medium and counted the colony number after 14 days (Figure 23.b-c). Interestingly, BAG3 knock-down cells show significant decrease in colony formation compared to control vector although no difference in colony number among shBAG3 and control cells was detected for untreated cells, indicating that basal levels of BAG3 are dispensable for clonogenic survival in normal condition (Figure 23.b).

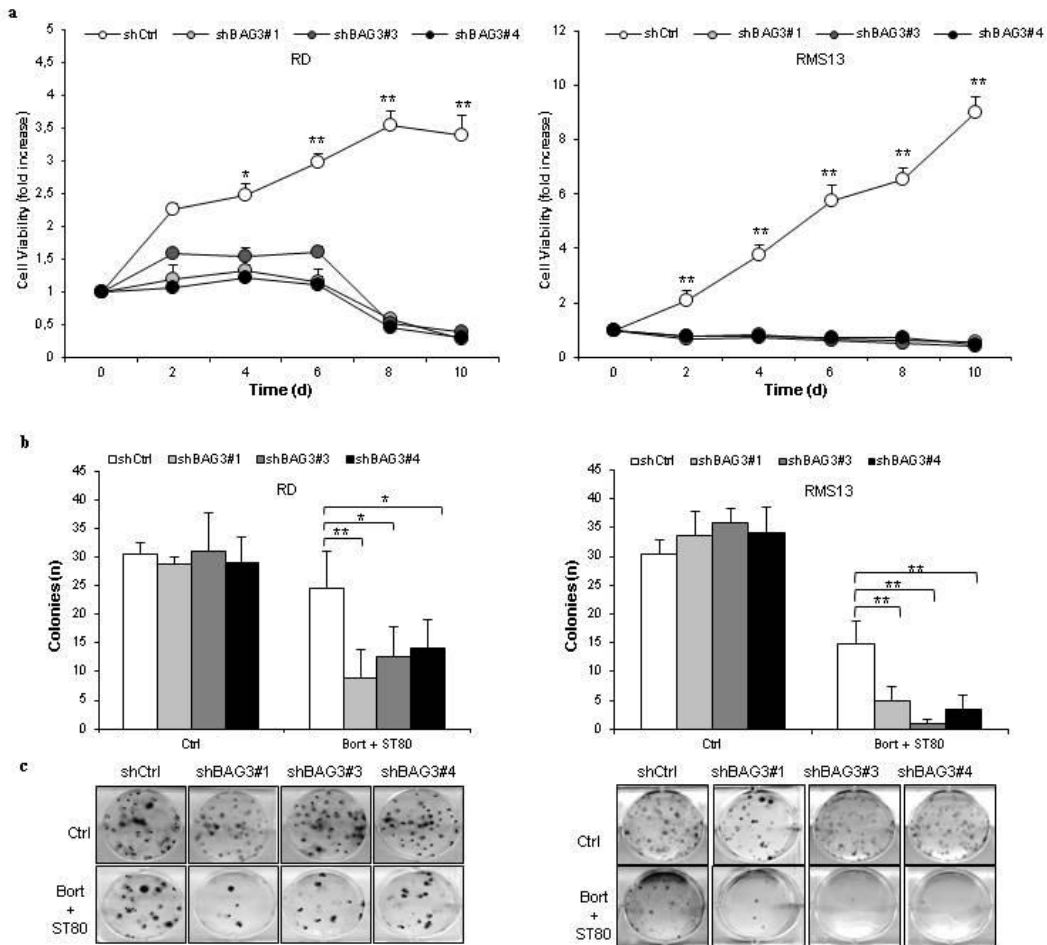


Figure 23: BAG3 is necessary for long term and clonogenic survival after ST80/Bortezomib removal.

RD and RMS13 were stably transfected with three different sequences against BAG3 (shBAG3) and one control (shCtrl). (a) Cells were treated with 20 nM (RD) or 50 nM (RMS13) Bortezomib and 50 μ M ST80 for 48 hours (day 0) before treatment was removed and cells were grown in drug-free medium up to ten days. Cell viability was measured at indicated time points by crystal violet staining. Data are expressed as fold change vs. day 0. (b-c) After 48 hours of ST80/Bortezomib treatment cells were seeded as single cell and grown in drug-free medium for 14 days. Colonies were visualized by crystal violet staining and counted under the microscope. Quantification of the number of colonies (b) and representative images (c) are shown. Mean of three (a) or two (b-c) independent experiments in triplicate is shown. t-Student test was used to determine statistical significance between shBAG3 and control vector: * $p < 0,05$; ** $p < 0,01$.

Taken together, this line of evidences supports the idea that BAG3 is necessary for cell regrowth and colony formation during the recovery phase, after ST80/Bortezomib removal.

4.6. Impairment of autophagosome formation leads to loss of cell recovery and protein aggregates accumulation upon ST80/Bortezomib removal.

Previous data associated BAG3 mediated clearance of protein aggregates with the selective autophagic pathway [71]. In order to understand if BAG3-dependent cell recovery upon ST80/Bortezomib removal is mediated by autophagy in our system, we created RD inducible ATG7 knock-down cell line (shATG7) (Figure 24.a). Starting 48

hours after treatment with doxycycline, ATG7 protein levels markedly decrease in shATG7 cells, while ATG7 is still present in the control vector (Figure 24.a). In order to exclude any interference of the inducible construct with the initial phase of ST80/Bortezomib treatment, we measured apoptosis and cell density after 48 hours of drug treatment (Figure 24.b-c). Importantly apoptotic levels and cell surviving ratios are comparable between shATG7 cells and control vector, in line with delayed down regulation of ATG7 starting 48 hours after doxycycline treatment (Figure 24.a).

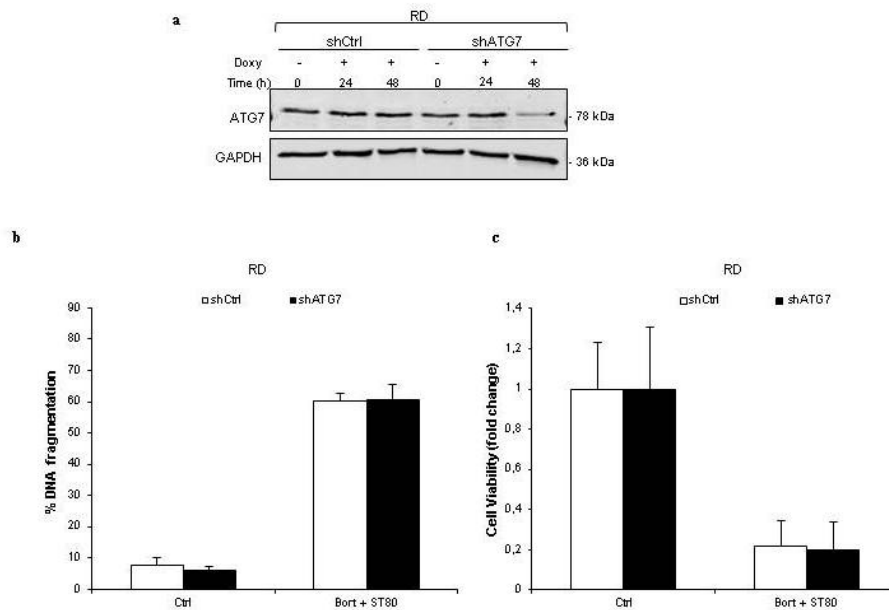


Figure 24: Inducible knock down of ATG7 does not interfere with ST80/Bortezomib-induced cell death. RD cell line was stably transfected with one sequences against ATG7 (shATG7) and one control (shCtrl). (a) Cells were treated with 1 ng/mL doxycyclin for indicated time points. ATG7 protein levels were assessed by western blot analysis. GAPDH was used as loading control. (b-c) Cells were treated for 48 hours with 20 nM Bortezomib and 50µM ST80. In (b), apoptosis was determined by FACS analysis of DNA fragmentation of propidium iodide stained nuclei. In (c), cell viability was measured by crystal violet assay. Data are expressed as fold change vs. untreated. Mean of three independent experiments in triplicate is shown.

Down regulation of ATG7 is maintained up to 120 hours (day 3 of recovery period) and leads to impairment of autophagosome formation as shown by the loss of LC3 I/II conversion, while control vector maintain ATG7 levels and LC3 I/II conversion ratio constant at the same time points (Figure 25.a). In order to understand if the impairment of the autophagic pathway, mediated by conditional ATG7 knock-down during the recovery phase, leads to accumulation of protein aggregates upon ST80/Bortezomib removal, we quantified ubiquitin-positive insoluble aggregates by fractionation of living cells in Triton-X (Figure 25.b). Interestingly, impairment of autophagosome formation leads to enhance accumulation of ubiquitin-positive aggregates and p62 protein levels in the insoluble fraction at day 2 and 3 after drug removal. Control vector cells show

decreasing amount of ubiquitin and p62 in the insoluble fraction at day 2 and 3 of the recovery period when compared to day 0, while shATG7 cells maintain similar level of ubiquitin and p62 protein levels over time, suggesting impairment in protein aggregates clearance (Figure 25.b). Moreover, untreated shATG7 cells show higher amount of insoluble ubiquitin-positive protein aggregates compared to control vector, underlining the importance of the aggresome-autophagy system to maintain protein homeostasis also in basal condition (Figure 25.b line 1 and 5 of insoluble fraction).

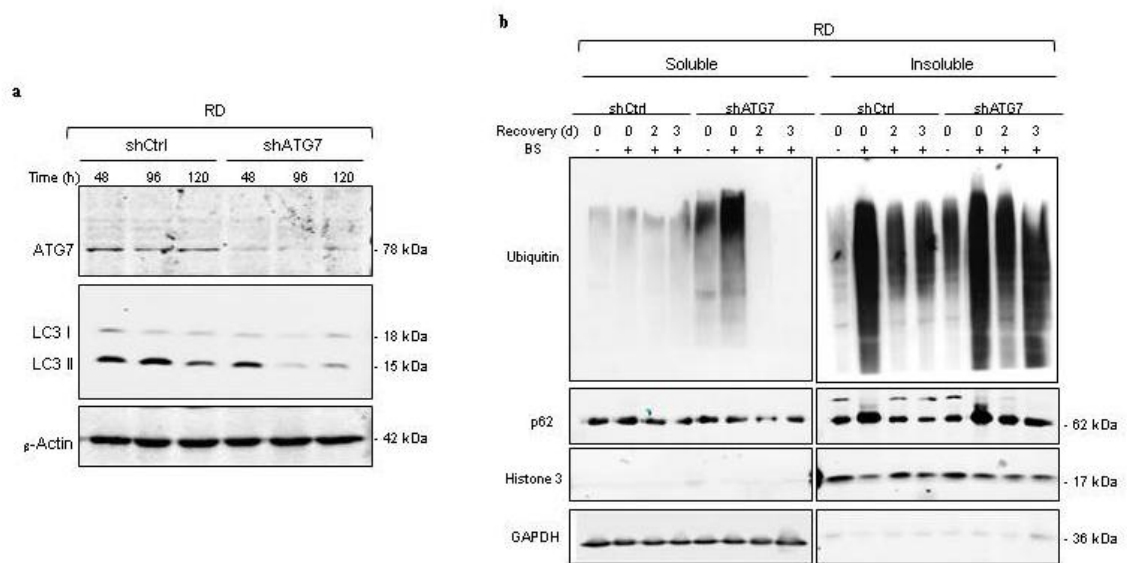


Figure 25: Impairment of autophagosome formation leads to accumulation of protein aggregates during recovery.

RD cell line was stably transfected with one sequences against ATG7 (shATG7) and one control (shCtrl). **(a)** Cells were treated with 1 ng/mL doxycycline for indicated time points. LC3 I/II and ATG7 protein levels were assessed by western blot analysis. β -Actin was used as loading control. **(b)** Cells were treated for 48 hours (day 0) with 20 nM Bortezomib and 50 μ M ST80 (BS) before treatment was removed and cell were grown in drug-free medium up to three days. Ubiquitin-positive protein aggregates and p62 protein levels were assessed by western blot analysis after fractionation of total viable cells in Triton-X at indicated time points. GAPDH and Histone 3 were used as loading and purity controls for soluble and insoluble fractions, respectively.

Accumulation of protein aggregates generally increases cytotoxicity leading to loss of cell recovery. To investigate if impairment of autophagosome formation, and consequent protein aggregates accumulation upon ST80/Bortezomib removal, leads to loss of cell viability, we followed cell proliferation of shATG7 and shCtrl ST80/Bortezomib surviving cells up to three days (Figure 26.a). As expected, control cells were able to grow in drug-free medium after ST80/Bortezomib removal while ATG7 knock down cells proliferation was completely lost. Moreover, shATG7 cells show significant increase of fragmented DNA compared to control vector at day 3 of the recovering period, indicating cell death during the recovery phase when the autophagic pathway is impaired (Figure 26.b).

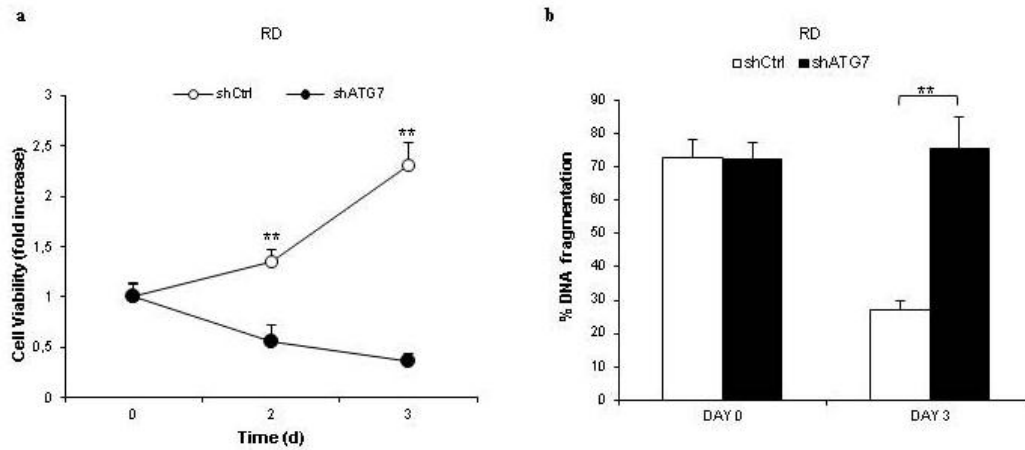


Figure 26: RD shATG7 cells show loss of cell proliferation and increase apoptosis during recovery.

RD cell line was stably transfected with one sequences against ATG7 (shATG7) and one control (shCtrl). Cells were treated for 48 hours (day 0) with 20 nM Bortezomib and 50 μ M ST80 before treatment was removed and cell were grown in drug-free medium up to three days. **(a)** Cell proliferation was measured by crystal violet staining at indicated time points. Data are expressed as fold change vs. day 0. **(b)** Apoptosis was determined by FACS analysis of DNA fragmentation of propidium iodide stained nuclei. Mean of three independent experiments in triplicate is shown. t-Student test was used to determine statistical significance between shATG7 and control vector: **p<0,01.

As a side note, we noticed that impairment of autophagosome formation by ATG7 knock down slightly but significantly decreased cell viability over time in untreated conditions compared to control vector (Figure 27). Although this basal loss of cell viability can not explain the great decrease in cell proliferation of shATG7 cells upon ST80/Bortezomib removal (Figure 26.a and 27), this observation points to a critical role of the autophagic pathway in RMS cells, in line with previous reports on the role of autophagy in tumor maintenance [102, 140].

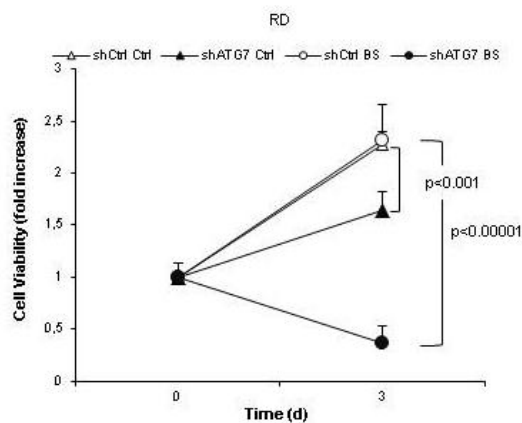


Figure 27: Autophagy impairment leads to decrease in cell proliferation in untreated conditions.

RD cell line was stably transfected with one sequences against ATG7 (shATG7) and one control (shCtrl). Cells were treated for 48 hours (day 0) with 20 nM Bortezomib and 50 μ M ST80 (BS) before treatment was removed and cell were grown in drug-free medium up to three days. Cell proliferation was measured by crystal violet staining at indicated time points. Data are expressed as fold change vs. day 0. Mean of three independent experiments in triplicate is shown. t-Student test was used to determine statistical significance between shATG7 and control vector.

Taken together, this set of evidences demonstrates that the impairment of autophagosome formation after ST80/Bortezomib removal, leads to protein aggregates accumulation, loss of cell proliferation and increase apoptosis during the recovery period similarly to shBAG3 cell lines.

4.7. Impairment of lysosome acidification leads to loss of cell proliferation and protein aggregates accumulation upon ST80/Bortezomib removal.

To further confirm that BAG3 clearance of protein aggregates after ST80/Bortezomib removal is mediated by the autophagic pathway, we interfered with the fusion between autophagosome and lysosome compartment by impairing lysosomal acidification with BafilomycinA1 (BafA1). BafA1 is an inhibitor of lysosomal V-ATPase which is responsible for the acidification of the lysosomal compartment: inhibition of acidification leads to inactivation of lysosomal enzymes with consequent inhibition of autophagosomal-cargo degradation and, finally, autophagy inhibition [133]. We treated ST80/Bortezomib surviving RMS cells with or without BafA1 at nanomolar concentration up to three days in order to determine protein aggregates by fractionation of viable cells in Triton-X (Figure 28). Importantly, BafA1 treated cells show, in the insoluble fraction, increase ubiquitin-positive protein aggregates and enhanced p62 protein levels at day 2 and 3 of the recovery period.

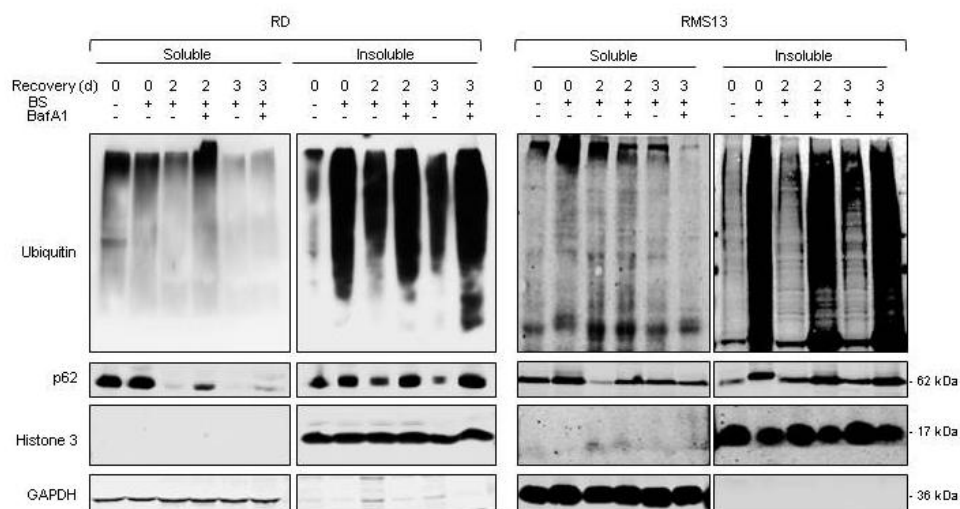


Figure 28: Impairment of the autophagic cargo degradation leads to protein aggregates accumulation during recovery. Cells were treated for 48 hours with 20 nM (RD) or 50 nM (RMS13) Bortezomib and 50 μM ST80 (BS) before treatment was removed and cells were grown up to three days in fresh medium with or without 5 nM of BafA1. Ubiquitin-positive protein aggregates and p62 protein levels were assessed by western blot analysis after fractionation of total viable cells in Triton-X at indicated time points. GAPDH and Histone 3 were used as loading and purity controls for soluble and insoluble fractions, respectively.

RMS cells supplied with BafA1 after ST80/Bortezomib removal show significantly reduced cell growth (Figure 29.a) accompanied by increase apoptosis (Figure 29.b) while cells grown in drug-free medium show sustained proliferation and decreased cell death.

Taken together, these results confirmed that inhibition of autophagy leads to accumulation of cytotoxic protein aggregates with consequent loss of cell growth and increased cell death upon ST80/Bortezomib removal, similarly to RMS cells which are not able to up-regulate BAG3 during recovery (Figure 19; 21 and 22).

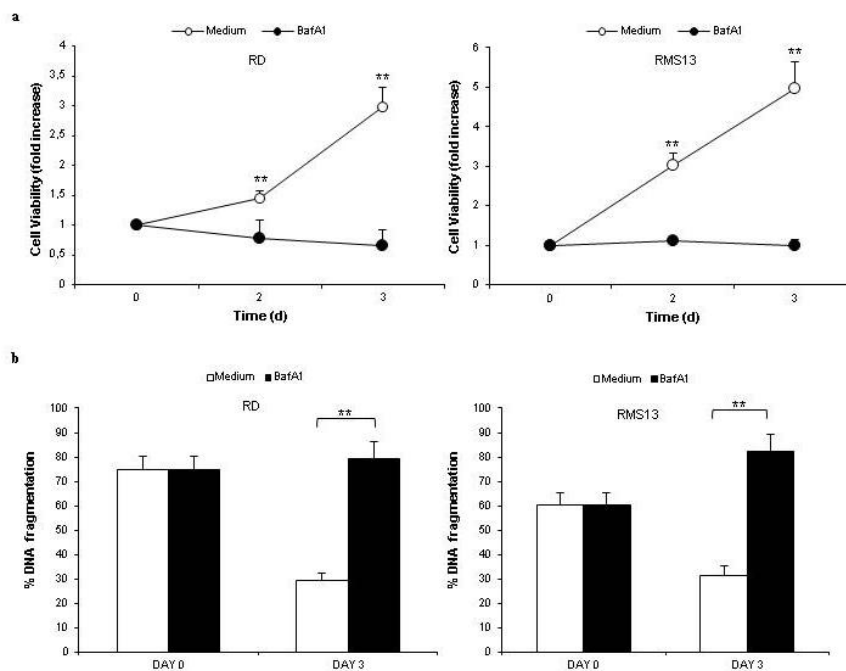


Figure 29: Impairment of lysosomal degradation results in loss of cell viability and increased cell death upon ST80/Bortezomib removal.

Cells were treated for 48 hours with 20 nM (RD) or 50 nM (RMS13) Bortezomib and 50 μ M ST80 before treatment was removed and cells were grown up to three days in fresh medium with or without 5 nM of BafA1. **(a)** Cell proliferation was measured by crystal violet staining at indicated time points. Data are expressed as fold change vs. day 0. **(b)** Apoptosis was determined by FACS analysis of DNA fragmentation of propidium iodide stained nuclei. Mean of three independent experiments in triplicate is shown. t-Student test was used to determine statistical significance between BafA1 treated and untreated cells: ** $p < 0,01$.

5. Discussion

Finding new strategies to enhance cell death in tumors is the main challenge of translational cancer research. Constitutive PQC systems – the UPS and the aggresome-autophagic system- have recently been suggested to be a promising target in cancer therapy [110, 111]. Single drug treatments against proteasome have been demonstrated to be just partially effective in tumors, due to compensatory induction of autophagy which enhances resistance against proteotoxicity and, in this way, limits cell death [10, 141, 142]. Thus, combinatory strategies have been proposed to overcome single proteasome agent induced resistance: addition of compounds which can inhibit bulk autophagy such as chloroquine or 3-MA (3-Methyladenine) have been widely tested in the last years in combination with proteasome inhibitors [143, 144].

HDAC6 has been recently shown to play a key role in the aggresome-autophagic system both by recruiting misfolded proteins towards the MTOC, and by mediating autophagosome-lysosome fusion *via* recruitment of a cortactin network [66, 69, 145]. Due to its key role in protein aggregates selective autophagy, HDAC6 inhibitors and proteasome inhibitors have been tested in combination in various tumor entities, such as ovarian, breast or colon carcinoma, showing synergism in cell killing [125, 141, 146].

Here, we combined a new specific catalytic inhibitor of HDAC6 -ST80- with the FDA-approved proteasome inhibitor Bortezomib in order to enhance proteotoxicity and trigger synergistic cell death in RMS cell lines. We indeed observed increased apoptosis upon combination treatment in all tested RMS cell lines but, interestingly, we always detected subpopulation of cells which survived ST80/Bortezomib co-treatment and was then able to recover, upon drug removal, at the same extent compared to untreated or single agent surviving cells. Therefore, we focused our attention on the induced compensatory mechanism up-regulated in this subpopulation of cells: we demonstrate, for the first time, that co-chaperone BAG3 plays a key role in tumor cell recovery, upon drug removal, specifically as a response to acute proteotoxicity triggered by concomitant inhibition of constitutive PQC systems. Moreover, we demonstrate that BAG3 mediates cell regrowth during cell recovery *via* selective clearance of cytotoxic protein aggregates by autophagy, thus mitigating proteotoxicity (Figure 30).

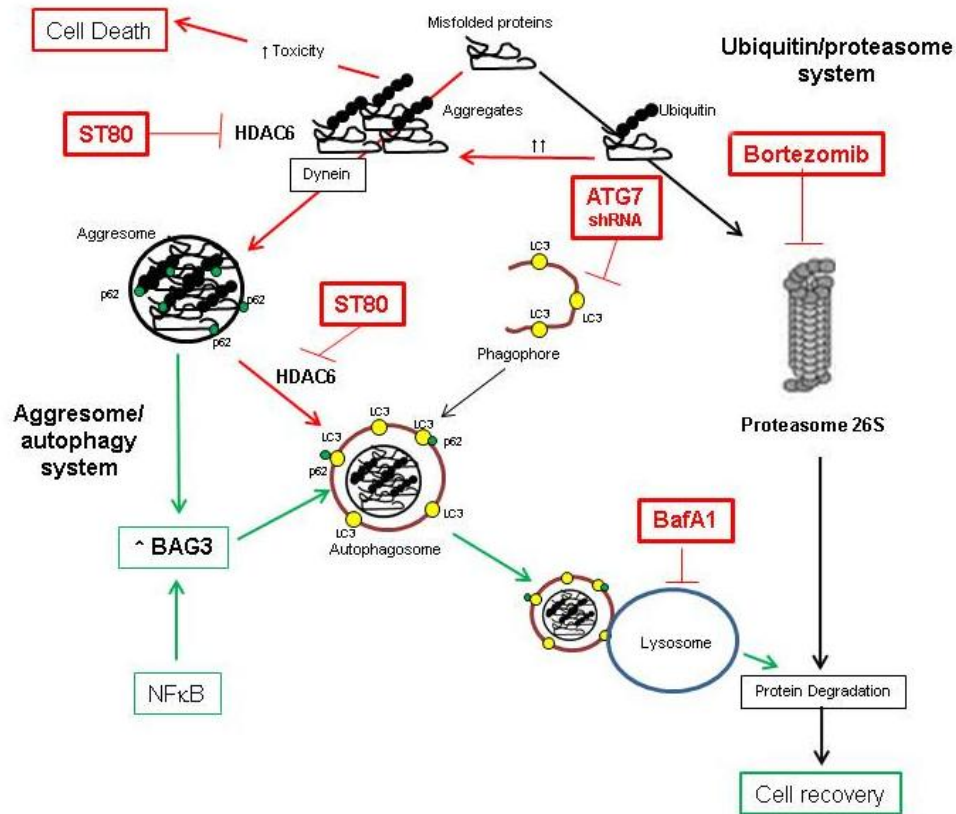


Figure 30: Scheme of proposed mechanism.

Inhibition of HDAC6 and proteasome triggers cell death and accumulation of insoluble protein aggregates (red). Surviving cells up-regulate BAG3 via NFκB in order to decrease proteotoxicity by autophagic clearance of protein aggregates therefore stimulating cell recovery (green). (See text for details).

Several lines of evidences support this conclusion: first, RMS ST80/Bortezomib surviving cells up-regulate massively BAG3 at transcriptional and protein levels while Bortezomib surviving cells or surviving cells of well established apoptotic inducers show no increase of BAG3 mRNA and/or protein levels (Figures 12 and 14). Similarly, non- transformed fibroblast cell line BJ show no increase in BAG3 mRNA and protein levels after ST80/Bortezomib treatment pointing to BAG3 up-regulation as a specific feature of RMS cells upon acute proteotoxicity. BAG3 up-regulation is mediated by NF-κB activation: in fact, impairment of NF-κB pathway by generation of phosphomutant IκBα RMS cell lines results in complete loss of BAG3 transcriptional and translational up-regulation in ST80/Bortezomib surviving cells. Second, BAG3 knock-down markedly impairs cell growth, clonogenic survival and clearance of cytotoxic protein aggregates leading to increased apoptosis upon ST80/Bortezomib removal (Figures 19-23). Finally, impairment of the aggresome-autophagy system during the recovery phase by inducible ATG7 knock-down or by BafA1 treatment,

leads to loss of cell proliferation, accumulation of insoluble protein aggregates and increase cell death, similarly to BAG3 knock down cells (Figures 25-26 and 28-29). These line of evidences strongly support a model in which BAG3 acts as an on demand PQC mechanism engaged by tumor cells upon simultaneous inhibition of constitutive PQC systems in order to selectively degrade accumulated protein aggregates and stimulate cell recovery upon drug removal.

Drug-induced resistance is one of the main limitations of efficacy in cancer therapy: simultaneous drug targeting of several cell pathways have increased efficacy in tumor cell killing, although drug induced resistance still plays a key role in tumor relapse and, finally, in the poor prognosis of many tumor types [147-149]. BAG3 has been previously described to play an important role in cancer survival by counteracting apoptosis. Due to its binding to HSP70, BAG3 is able to retain the pro-apoptotic protein BAX in the cytosol thereby preventing BAX translocation to the mitochondria and inhibiting cisplatin- or serum deprivation-induced apoptosis [121]. Moreover, BAG3 has been described to interfere with HSP70-mediated delivery to proteasome of several antiapoptotic proteins such as IKK γ , BCL2, BCL-X_L, mostly by competing with BAG1 for HSP70 binding [82, 150]. In neuroblastoma cell lines with a defined dependency for specific BCL2 family members, BAG3 expression was shown to correlate with MCL-1 dependency and ABT-737 resistance due to BAG3-mediated protection of MCL-1 proteasomal degradation in this model [151]. In our study, data suggest that BAG3 does not play a key role in preventing apoptosis triggered by ST80/Bortezomib co-treatment but acts mainly as a pro-survival mechanism during cell recovery phase through modulation of autophagy. We demonstrate a new important function of BAG3 as a pro-survival protein in cancer aside from its reported role related to modulation of pro- and anti-apoptotic proteins. In our model, BAG3 mediates cell recovery by directly decreasing the source of stress, i.e. protein aggregates, by selective degradation of cytotoxic protein aggregates *via* autophagy.

BAG3's role in selective autophagy has been intensively studied in healthy tissues [152]. As a co-chaperone, BAG3 is part of the HSPB8-HSP70-CHIP-BAG3 multichaperone complex in which it recognizes and binds misfolded proteins in order to enhance protein degradation [74, 153]. Also, BAG3 can compensate for HDAC6 functions in the aggresome-autophagy system by interacting with dynein motors promoting the retrograde transport of misfolded proteins along microtubules towards

the MTOC [76]. Moreover, BAG3 can interact with the selective autophagic receptor p62 linking, in this way, protein aggregates and aggresomes to the autophagic machinery *via* the p62-LC3 interaction on the autophagosomal membranes [77]. Here, we show that BAG3 acts as an on demand PQC mechanism engaged in RMS cell lines upon intense proteotoxic stress mainly to decrease toxicity during cell recovery through its key role in selective autophagy. Interestingly, our data clearly demonstrate that inhibition of proteasome by Bortezomib is not sufficient to trigger enhanced BAG3 transcriptional up-regulation: previous reports showed that inhibition of proteasome-mediated BAG3 mRNA up-regulation to some extent [154, 155]; however, concomitant inhibition of proteasome and of the catalytic activity of HDAC6 triggers, in RMS surviving population, a BAG3 mRNA increase of 40-80 fold (Figure 12) depending on the cell line, which is higher than the transcriptional up-regulation mediated by single Bortezomib treatment. We can speculate that BAG3 on demand activation is related to some kind of “proteotoxicity threshold”: the late kinetic of BAG3 up-regulation (30-42 hours after treatment) in our experiments and the massive increase of BAG3 mRNA in ST80/Bortezomib co-treated surviving cells compared to Bortezomib single treated cells support this hypothesis.

BAG3's engagement in decreasing acute and chronic proteotoxic stress due to accumulation of misfolded or damaged proteins has been described previously in different models: Nivon and colleagues reported that BAG3 was up-regulated in HeLa cells after heat shock and helped coping with the induced proteotoxicity by clearing protein aggregates *via* autophagy [137]. Furthermore, BAG3-mediated selective autophagy has been related to modulation of misfolded proteins in neurodegenerative disease [153]: HSPB8-BAG3 complex was found up-regulated in astrocytes taken from post mortem brains of Alzheimer's, Parkinson's and Huntington's diseases patients, pointing to a role of the complex in clearing protein aggregates released from neurons and cellular debris. In healthy condition, chronic proteotoxic stress occurs during aging [77]: a BAG1/BAG3 switch has been described to occur in an aging cell line model correlating with decreased activity of BAG1-mediated proteasome degradation and enhanced dependency of PQC on the BAG3-mediated aggresome-autophagy system. Moreover, a recent study on the apoptotic transcriptome of mature MII oocyte of aged women compared to young women showed that BAG3 is up-regulated in the first group underlining the importance of this co-chaperone as a stress response element activated during prolonged proteotoxic stress occurring during aging [156]. Those data suggest

that the engagement of BAG3, mediated by its transcriptional induction, is needed when the level of misfolded or damaged proteins are abruptly increased or constantly elevated. Our work adds insights to this general concept: we discovered that pharmacological inhibition of PQC systems triggers proteotoxic stress which leads to BAG3 induction. In this context, BAG3 plays a key role in mediating tumor cell growth and clonogenic survival which can enhance the risk of tumor relapse. The present study strengthens the idea of a general context where BAG3 is an on demand mechanism engaged by cells when the “proteotoxicity threshold” is exceeded expanding the concept from a disease-related condition to a new side effect of proteotoxic cancer therapy. In line with our data, BAG3 up-regulation has been linked with NF- κ B activation [137, 157]: the implications of this finding must be further analyzed in order to understand which role NF- κ B precisely plays in the regulation of the on demand response towards proteotoxic stress in cancer.

Enhanced expression of BAG3 has been reported in several tumors such as leukemia [120], neuroblastoma [158], pancreatic carcinoma [159], colon carcinoma [160] and melanoma [161]. Mainly, increased expression of BAG3 is correlated with poor prognosis due to enhanced resistances toward apoptosis: for example, a study on 346 patients affected by pancreatic adenocarcinoma showed that tumors with enhanced BAG3 expression had significant higher aggressiveness compared to tumors that express lower levels of BAG3, resulting in poorer prognosis of the patients [162]. Moreover, the same study showed that BAG3 mediates decreases sensitivity towards gemcitabine treatment in vitro [162]. In addition, BAG3 has been described to play a crucial role in cell adhesion and motility pointing to a role in metastasis [163]. PKC δ specific phosphorylation on Ser187 of BAG3 has been described to mediate epithelial-mesenchymal transition (EMT) in a thyroid carcinoma cell line [81]. EMT is a crucial process needed by cancer cells to gain invasiveness and form metastasis: BAG3's role in EMT suggests its involvement in promoting metastatic behavior thereby enhancing tumor invasiveness. In this context, our data on the role of BAG3 in clonogenic growth of ST80/Bortezomib surviving RMS cell lines gain new importance: our findings highlight that therapeutic strategies which enhance proteotoxicity as the main stress for apoptosis induction, trigger high BAG3 protein levels in the surviving population which might play a crucial role not only in cell regrowth but also in tumor invasiveness through BAG3 involvement in EMT promotion. More studies need to be done in order

to understand if cells which survive ST80/Bortezomib co-treatment are indeed able to migrate and/or invade more than untreated cells.

Importantly, BAG3 has been reported to be expressed at low levels in young healthy cells and to increase during aging in normal conditions [71]. RMS is mainly a childhood disease with peak between one and five years [164]: we can speculate that BAG3 protein levels in RMS patients are relatively low in healthy cells enhancing the possibility of creating effective selective inhibitors towards BAG3 with low side effects on non-tumor tissues.

Interestingly, we demonstrate that BAG3 up-regulation is mediated by NF- κ B activation: this finding opens new interesting question on the regulation of the NF- κ B pathway when proteasome is inhibited. Also, NF- κ B regulation of BAG3 highlights a new pro-survival role of this transcriptional factor in tumors: not only NF- κ B mediates tumor maintenance in stress condition [165] but plays an important role in recovery of surviving cells upon drug removal by the induction of pro-survival genes, such as BAG3, during the recovery phase. Our data suggest that NF- κ B plays a role in tumor recovery after drug treatment against constitutive PQC systems, but more detailed studies must be done to elucidate the detailed contribution of this transcription factor in this context.

Finally, BAG3 has been reported to be present in the hematopoietic stem cell vascular niche: silencing of BAG3 in this compartment results in loss of the hematopoietic stem cells [166]. This finding suggests that BAG3 might play some role in the maintenance of the microenvironment needed for cancer stem cell survival enhancing the importance of this protein in cancer survival and propagation. The possibility that BAG3 up-regulation in ST80/Bortezomib surviving cells could mediate an increase in cancer stem like population is intriguing: more studies need to be done to validate this possibility.

In conclusion, our study provides solid data on a novel role of BAG3 as the key mediator of an on demand PQC mechanism which is activated in surviving RMS cells upon ST80/Bortezomib co-treatment: BAG3 decreases cytotoxic aggregates by selective degradation *via* the aggresome-autophagy system thereby increasing cell proliferation and clonogenic survival. Moreover, we showed that BAG3 can overcome the loss of HDAC6 activity in ST80/Bortezomib surviving cells by taking over HDAC6's role in the aggresome-autophagy pathway. The present study also points out that combination strategies which simultaneously target the two main branches of

constitutive PQC, although enhancing induction of apoptosis, trigger an inducible rescue mechanism that, if not impaired, enable surviving cell to proliferate and possibly cause relapse. In this context, the evidences here reported suggest that more studies need to be done *in vitro* and *in vivo* in order to understand the inducible resistance mechanisms triggered by co-treatment approaches, specifically related to combination of drugs which intensively enhance proteotoxicity. Through the identification of the BAG3-mediated selective autophagy pathway as a novel mechanism of acquired resistance to compensate concomitant inhibition of the constitutive PQC systems, we add a new important piece of evidence on the biological compensatory regulation of PQC systems in cancer. We propose that the impairment of this inducible escape mechanism may potentiate the efficacy of co-treatment of inhibitors which target the protein degradations pathways: to this end, inhibition of both inducible and constitutive PQC pathways may open new perspectives for therapeutic exploitation in cancers.

Summary (Deutsche Zusammenfassung).

BAG3 Induktion wird benötigt um proteotoxischen Stress nach der Inhibition von konstitutiver Proteindegradation durch selektive Autophagie zu vermindern.

Proteinqualitätskontrollsysteme (PQK) sind ein interessanter Ansatzpunkt für die Weiterentwicklung von Krebstherapien [9]. In eukaryotischen Zellen sind zwei konstitutive Hauptkontrollsysteme bekannt, das unfolded protein response system (UPS) und das Aggresome/Autophagie System. Das UPS vermittelt die Ubiquitinierung und Degradierung linearer falsch-gefalteter Proteine durch das 26S Proteasom [132]. Das Aggresome/Autophagie System ist ein selektiver Autophagieprozess in welchem unlösliche und potentiell toxische Proteinaggregate degradiert werden. Hier wird die Autophagiemaschinerie zusammen mit spezifischen Proteinadaptoren, welche die Erkennung und die spezifische lysosomale Degradierung der Zielpoteine vermitteln, verwendet [70].

Autophagie ist ein dynamischer katabolischer Prozess. Durch Bildung eines Doppelmembran ummantelten Vesikels, des Phagophores, welches mit spezifischen Autophagiemarkern angereichert ist, hier ist vor allem LC3 zu nennen, wird zytosolisches Cargo umschlossen und es bildet sich das Autophagosom. Letztendlich fusioniert das Autophagosom mit sauren Lysosomen, das Autophagolysosom, in welchem das Cargo in seine basalen Komponenten verdaut wird, welche, z.B. unter Stressbedingungen als Nährstoffquelle verwendet werden können [25]. Obwohl Autophagie initial als unspezifischer Mechanismus beschrieben wurde, hat die Entdeckung von speziellen Proteinadaptoren gezeigt, dass Autophagie auch ein spezifischer Prozess sein kann [39]. p62 ist der erste beschriebene Rezeptor für selektive Autophagie ubiquitiniertes Proteinaggregate. p62 hat eine Ubiquitinbindungsdomäne (UBA) und eine LC3 Interaktionsregion (LIR), welche ihm ermöglichen Ubiquitin-positive Proteinaggregate und Autophagie Membranen miteinander zu verbinden [44].

Histondeacetylase 6 (HDAC6) ist eine zytosolische Deacetylase welche die Deacetylierung von α -Tubulin vermittelt. Weiterhin spielt HDAC6 eine vorherrschende Rolle in PQK, da es verschiedene Funktionen innerhalb des Aggresome/Autophagie Systems innehat. Einerseits erkennt HDAC6 Ubiquitin-markierte Proteine durch seine BUZ Domäne (Ubiquitin-bindende Domäne), und ermöglicht deren Aggregation durch Dynein-vermittelten retrograden Transport entlang der Mikrotubuli in Richtung der

Mikrotubulus organisierenden Zentrums (MTOC) [66]. Andererseits rekrutiert HDAC6 ein Cortactin Netzwerk, welches für die Autophagosom-Lysosom-Fusion während der Autophagie von Proteinaggregaten benötigt wird, aber für Nährstoffentzug-induzierte Autohagie erlässlich ist [69]. In beiden Fällen wird die katalytische deacetylierende Aktivität von HDAC6 benötigt.

Proteasominhibitoren des 26S Proteasoms, wie z.B. Bortezomib, und katalytische Inhibitoren von HDAC6 können synergistisch Zelltod in Tumoren, wie z.B. Ovarialkarzinom [125] induzieren. Durch die simultane Inhibition von zwei Hauptsystemen der PQC entsteht erhöhter proteotoxischer Stress welcher letztendlich zur Induktion von Apoptose führt.

Rhabdomyosarkome (RMS), die häufigsten Weichgewebe Tumore bei Kindern, sind sensitiv gegenüber Bortezomib Behandlung [112]. Diese Arbeit beruht auf der Hypothese, dass die Inhibition des Aggresome/Autophagie Systems, durch einen HDAC6 spezifischen katalytischen Inhibitor ST80 [117], zusammen mit Bortezomib Behandlung den Zelltod in RMS verstärken kann.

Wie erwartet konnte durch die gleichzeitige Inhibition beider Systeme die DNA Fragmentierung in allen getesteten RMS Zelllinien erhöht werden. Allerdings konnte eine resistente Subpopulation identifiziert werden, welche die Behandlung überlebte und sich vergleichbar zu unbehandelten Zellen erholte.

Unser Ziel war es den molekularen Mechanismus, der dieser Resistenz zugrunde liegt, zu identifizieren. Hier konnten wir das Co-Chaperon BAG3 als Hauptmediator dieser Erholung nach der Bortezomib/ST80 Behandlung identifizieren. BAG3 vermittelt die Degradation von zytotoxischen Proteinaggregaten durch die Induktion von selektiver Autophagie.

Dieser Effekt konnte auf verschiedenen Ebenen bewiesen werden. Einerseits zeigen überlebende Zellen erhöhte BAG3 Spiegel, sowohl auf transkriptioneller als auch translationeller Ebene, beginnend 30 Stunden nach der Behandlung. Dieser Effekt wird bis zu drei Tagen während der Erholungsphase aufrechterhalten. Zudem werden die innerhalb dieser drei Tage durch die Doppelbehandlung entstandenen Ubiquitin-positiven zytotoxischen Aggregate nicht abgebaut falls BAG3 durch RNA-Interferenz depletiert wird. Weiterhin zeigen die BAG3-depletierten Zellen keine Anzeichen von Erholung nach der Entfernung der Behandlung, sondern sterben vermehrt apoptotisch und zeigen vermindertes klonogenes Überleben. BAG3 wurde bisher im Zusammenhang mit der Induktion von selektiver Autophagie durch verminderte

proteasomale Aktivität beschrieben [84]. BAG3 vermittelt die Erkennung und Aggregation falsch-gefalteter Proteine und ermöglicht deren autophagosomale Erkennung durch direkte Interaktion mit p62 [76]. Überlebende Zellen der Bortezomib/ST80 Behandlung zeigen erhöhte Spiegel an unlöslichen Proteinaggregaten welche mit p62 Spiegeln positiv korrelieren. Wir vermuteten, dass der BAG3-vermittelte Abbau der p62-Ubiquitin-positiven Proteinaggregate durch autophagosomale-lysosomale Degradierung vermittelt wird. Daher regulierten wir die Autophagieinduktion durch konditionelle RNAi-vermittelte Depletion des Autophagie-Schlüsselproteins ATG7 oder durch die Inhibition der Autophagosom-Lysosom Fusion, durch den Lysosomeninhibitor BafilomycinA1, bis zu drei Tage während der Erholungsphase. Diese Inhibition resultierte in einem vergleichbaren Phänotyp wie die permanente BAG3 Depletion: Die überlebenden Zellen waren nicht mehr in der Lage weiter zu proliferieren, starben vermehrt apoptotisch ab und wiesen Defekte im Abbau von Proteinaggregaten auf. Unsere Daten unterstützen die Annahme, dass die Induktion proteotoxischen Stress, welcher durch die Interferenz mit den konstitutiven PQQ Systemen entsteht, einen Überlebensmechanismus aktiviert der durch die transkriptionelle Regulation des Co-Chaperons BAG3 gekennzeichnet ist. BAG3 reaktiviert die Erkennung Ubiquitin-positiver Proteinaggregate durch die Autophagie-Maschinerie, gefolgt vom Abbau der Aggregate und anschließender Zellproliferation. Nivon und Kollegen zeigten [137], dass die BAG3 Hochregulation in einem HeLa Hitzeschock Modell NF- κ B vermittelt stattfindet. Um diese Möglichkeit auch in unserem System zu überprüfen, generierten wir NF- κ B defiziente Zellen, welche einen Defekt in BAG3 Regulation aufzeigten. NF- κ B Inhibition verhinderte die BAG3 Induktion vollständig in den ST80/Bortezomib Behandlung überlebenden Zellen. In zukünftigen Experimenten soll untersucht werden, wie NF- κ B während der pharmakologischen Inhibition des Proteasoms aktiviert werden kann. Weiterhin soll die Rolle dieser Familie von Transkriptionsfaktoren in der Reaktion auf proteotoxischen Stress untersucht werden.

Unsere Arbeit zeigt, dass nach der gleichzeitigen Inhibition des 26S Proteasoms und des HDAC6 vermittelten Aggresome/Autophagy Systems, die Induktion des Co-Chaperons BAG3 unerlässlich für die Erholung von RMS Zellen nach der Behandlung ist. Diese Erkenntnisse tragen maßgeblich zu einem verbesserten Verständnis der PQQ Regulation in Krebszellen bei: Bisher wurde gezeigt, dass die Inhibition einer der beiden konstitutiven PQQ Signalwege zur vermehrten Aktivierung des anderen Systems

führt um besser mit Stresssituationen umgehen zu können [113]. Dieser Mechanismus vermittelt Resistenz von Krebszellen gegenüber einer Einzelbehandlung und liefert die Rationale für die synergistische Wirkung einer Kombinationsbehandlung wie z.B. Bortezomib/ST80. In dieser Arbeit identifizieren wir einen zusätzlichen Überlebensmechanismus, durch welchen Krebszellen, in denen die konstitutiven PQKs inhibitiert sind, über die Induktion von BAG3-vermitteltem Abbau von Proteinaggregaten nicht nur ihr Überleben sichern, sondern auch deren Proliferation angeregt wird.

BAG3 wird in jungem gesundem [164] Gewebe sehr niedrig exprimiert. Rhabdomyosarkom ist ein pädiatrischer Tumor, der meistens zwischen dem 1 und 5 Lebensjahr auftritt. Die Identifikation von BAG3 als wichtige Komponente des Erholungsmechanismus nach Inhibition von konstitutiven PQK Systemen, eröffnet die Möglichkeit der Entwicklung eines selektiven BAG3 Inhibitors, welcher im jungen Gewebe der Patienten, welche nur niedrige BAG3 Spiegel exprimieren, weniger Toxizität aufweisen könnte.

Die Identifizierung von BAG3-vermittelter selektiver Autophagie als neuen Resistenz Mechanismus um simultane Inhibition von konstitutiven Degradierungssignalwegen zu kompensieren, könnte maßgeblich zu der Weiterentwicklung aktueller Behandlungsstrategien beitragen: So könnte, dass die Inhibition von konstitutiven zusammen mit induzierbaren PQKs, die Zelltodinduktion verstärken, die Erholung verhindern und dadurch neue Perspektiven für deren therapeutische Anwendung ermöglichen.

References

References

1. Kong, X., et al., *Emerging roles of DNA-PK besides DNA repair*. Cell Signal, 2011. **23**(8): p. 1273-80.
2. Dutta, D., et al., *Contribution of impaired mitochondrial autophagy to cardiac aging: mechanisms and therapeutic opportunities*. Circ Res, 2012. **110**(8): p. 1125-38.
3. Jana, N.R., *Protein homeostasis and aging: role of ubiquitin protein ligases*. Neurochem Int, 2012. **60**(5): p. 443-7.
4. Wang, S. and R.J. Kaufman, *The impact of the unfolded protein response on human disease*. J Cell Biol, 2012. **197**(7): p. 857-67.
5. Schonthal, A.H., *Pharmacological targeting of endoplasmic reticulum stress signaling in cancer*. Biochem Pharmacol, 2013. **85**(5): p. 653-66.
6. Verfaillie, T., et al., *Linking ER Stress to Autophagy: Potential Implications for Cancer Therapy*. Int J Cell Biol, 2010. **2010**: p. 930509.
7. Zheng, Q.Y., et al., *Ursolic acid induces ER stress response to activate ASK1-JNK signaling and induce apoptosis in human bladder cancer T24 cells*. Cell Signal, 2013. **25**(1): p. 206-13.
8. Penna, F., et al., *Caspase 2 activation and ER stress drive rapid Jurkat cell apoptosis by clofibrate*. PLoS One, 2012. **7**(9): p. e45327.
9. Kubota, H., *Quality control against misfolded proteins in the cytosol: a network for cell survival*. J Biochem, 2009. **146**(5): p. 609-16.
10. Driscoll JJ, C.R., *Molecular crosstalk between the proteasome, aggresomes and autophagy: translational potential and clinical implications*. Cancer Lett, 2012 Dec 28. **325**(2): p. 147-54.
11. Willis, M.S., et al., *Sent to destroy: the ubiquitin proteasome system regulates cell signaling and protein quality control in cardiovascular development and disease*. Circ Res, 2010. **106**(3): p. 463-78.
12. Su, H. and X. Wang, *The ubiquitin-proteasome system in cardiac proteinopathy: a quality control perspective*. Cardiovasc Res, 2010. **85**(2): p. 253-62.
13. Micel, L.N., et al., *Role of ubiquitin ligases and the proteasome in oncogenesis: novel targets for anticancer therapies*. J Clin Oncol, 2013. **31**(9): p. 1231-8.
14. Chen, P.C., C.H. Na, and J. Peng, *Quantitative proteomics to decipher ubiquitin signaling*. Amino Acids, 2012. **43**(3): p. 1049-60.

15. Hershko, A., A. Ciechanover, and A. Varshavsky, *Basic Medical Research Award. The ubiquitin system*. Nat Med, 2000. **6**(10): p. 1073-81.
16. Neutzner, M. and A. Neutzner, *Enzymes of ubiquitination and deubiquitination*. Essays Biochem, 2012. **52**: p. 37-50.
17. Zeinab, R.A., et al., *UBE4B: A Promising Regulatory Molecule in Neuronal Death and Survival*. Int J Mol Sci, 2012. **13**(12): p. 16865-79.
18. Jacobson, A.D., et al., *The lysine 48 and lysine 63 ubiquitin conjugates are processed differently by the 26 S proteasome*. J Biol Chem, 2009. **284**(51): p. 35485-94.
19. Tanaka, K., *The proteasome: from basic mechanisms to emerging roles*. Keio J Med, 2013. **62**(1): p. 1-12.
20. Isasa, M., A. Zuin, and B. Crosas, *Integration of multiple ubiquitin signals in proteasome regulation*. Methods Mol Biol, 2012. **910**: p. 337-70.
21. Radhakrishnan, S.K., et al., *Transcription factor Nrfl mediates the proteasome recovery pathway after proteasome inhibition in mammalian cells*. Mol Cell, 2010. **38**(1): p. 17-28.
22. Das, G., B.V. Shrivage, and E.H. Baehrecke, *Regulation and function of autophagy during cell survival and cell death*. Cold Spring Harb Perspect Biol, 2012. **4**(6).
23. Li, W.W., J. Li, and J.K. Bao, *Microautophagy: lesser-known self-eating*. Cell Mol Life Sci, 2012. **69**(7): p. 1125-36.
24. Kaushik, S. and A.M. Cuervo, *Chaperone-mediated autophagy: a unique way to enter the lysosome world*. Trends Cell Biol, 2012. **22**(8): p. 407-17.
25. Nakatogawa, H., et al., *Dynamics and diversity in autophagy mechanisms: lessons from yeast*. Nat Rev Mol Cell Biol, 2009. **10**(7): p. 458-67.
26. Wu, L., et al., *Rapamycin Upregulates Autophagy by Inhibiting the mTOR-ULK1 Pathway, Resulting in Reduced Podocyte Injury*. PLoS One, 2013. **8**(5): p. e63799.
27. Wilz, L., W. Fan, and Q. Zhong, *Membrane curvature response in autophagy*. Autophagy, 2011. **7**(10): p. 1249-50.
28. Hamasaki M, F.N., Matsuda A, Nezu A, Yamamoto A, Fujita N, Oomori H, Noda T, Haraguchi T, Hiraoka Y, Amano A, Yoshimori T, *Autophagosomes form at ER-mitochondria contact sites*. Nature, 2013. **495**(7441): p. 389-93.
29. Geng, J. and D.J. Klionsky, *The Atg8 and Atg12 ubiquitin-like conjugation systems in macroautophagy. 'Protein modifications: beyond the usual suspects' review series*. EMBO Rep, 2008. **9**(9): p. 859-64.
30. Sou YS, W.S., Iwata J, Ueno T, Fujimura T, Hara T, Sawada N, Yamada A, Mizushima N, Uchiyama Y, Kominami E, Tanaka K, Komatsu M, *The Atg8 conjugation system is indispensable for proper development of autophagic isolation membranes in mice*. Mol Biol Cell, 2008. **19**(11): p. 4762-75.

31. Barth, S., D. Glick, and K.F. Macleod, *Autophagy: assays and artifacts*. J Pathol, 2010. **221**(2): p. 117-24.
32. Noda, N.N., Y. Ohsumi, and F. Inagaki, *Atg8-family interacting motif crucial for selective autophagy*. FEBS Lett, 2010. **584**(7): p. 1379-85.
33. Fader, C.M., et al., *Induction of autophagy promotes fusion of multivesicular bodies with autophagic vacuoles in k562 cells*. Traffic, 2008. **9**(2): p. 230-50.
34. Hyttinen, J.M., et al., *Maturation of autophagosomes and endosomes: a key role for Rab7*. Biochim Biophys Acta, 2013. **1833**(3): p. 503-10.
35. Klionsky DJ, E.Z., Seglen PO, Rubinsztein DC., *Does bafilomycin A1 block the fusion of autophagosomes with lysosomes?* autophagy, 2008. **4**(7): p. 849-950.
36. Rabinowitz, J.D. and E. White, *Autophagy and metabolism*. Science, 2010. **330**(6009): p. 1344-8.
37. Komatsu M, I.Y., *Selective autophagy regulates various cellular functions*. Genes Cells, 2010. **15**(9): p. 923-33.
38. Lynch-Day, M.A. and D.J. Klionsky, *The Cvt pathway as a model for selective autophagy*. FEBS Lett, 2010. **584**(7): p. 1359-66.
39. Johansen, T. and T. Lamark, *Selective autophagy mediated by autophagic adapter proteins*. Autophagy, 2011. **7**(3): p. 279-96.
40. Youle, R.J. and D.P. Narendra, *Mechanisms of mitophagy*. Nat Rev Mol Cell Biol, 2011. **12**(1): p. 9-14.
41. von Muhlinen, N., et al., *NDP52, a novel autophagy receptor for ubiquitin-decorated cytosolic bacteria*. Autophagy, 2010. **6**(2): p. 288-9.
42. Kirkin, V., et al., *A role for ubiquitin in selective autophagy*. Mol Cell, 2009. **34**(3): p. 259-69.
43. Gal, J., et al., *Sequestosome 1/p62 links familial ALS mutant SOD1 to LC3 via an ubiquitin-independent mechanism*. J Neurochem, 2009. **111**(4): p. 1062-73.
44. Lin X, L.S., Zhao Y, Ma X, Zhang K, He X, Wang Z., *Interaction Domains of p62: A Bridge Between p62 and Selective Autophagy*. DNA Cell Biol, 2013. **32**(5): p. 220-7.
45. Lim, J., et al., *Binding preference of p62 towards LC3-II during dopaminergic neurotoxin-induced impairment of autophagic flux*. Autophagy, 2011. **7**(1): p. 51-60.
46. Pankiv, S., et al., *p62/SQSTM1 binds directly to Atg8/LC3 to facilitate degradation of ubiquitinated protein aggregates by autophagy*. J Biol Chem, 2007. **282**(33): p. 24131-45.
47. Klucken, J., et al., *Alpha-synuclein aggregation involves a bafilomycin A 1-sensitive autophagy pathway*. Autophagy, 2012. **8**(5): p. 754-66.
48. Wong, E., et al., *Molecular determinants of selective clearance of protein inclusions by autophagy*. Nat Commun, 2012. **3**: p. 1240.

49. Schreiber, A. and M. Peter, *Substrate recognition in selective autophagy and the ubiquitin-proteasome system*. *Biochim Biophys Acta*, 2013. **4889**(13): p. 120-1.
50. Olzmann, J.A. and L.S. Chin, *Parkin-mediated K63-linked polyubiquitination: a signal for targeting misfolded proteins to the aggresome-autophagy pathway*. *Autophagy*, 2008. **4**(1): p. 85-7.
51. Matsumoto, G., et al., *Serine 403 phosphorylation of p62/SQSTM1 regulates selective autophagic clearance of ubiquitinated proteins*. *Mol Cell*, 2011. **44**(2): p. 279-89.
52. Ishii, T., et al., *Low micromolar levels of hydrogen peroxide and proteasome inhibitors induce the 60-kDa A170 stress protein in murine peritoneal macrophages*. *Biochem Biophys Res Commun*, 1997. **232**(1): p. 33-7.
53. Lau, A., et al., *A noncanonical mechanism of Nrf2 activation by autophagy deficiency: direct interaction between Keap1 and p62*. *Mol Cell Biol*, 2010. **30**(13): p. 3275-85.
54. Isakson, P., P. Holland, and A. Simonsen, *The role of ALFY in selective autophagy*. *Cell Death Differ*, 2013. **20**(1): p. 12-20.
55. Simonsen, A., R.C. Cumming, and K.D. Finley, *Linking lysosomal trafficking defects with changes in aging and stress response in Drosophila*. *Autophagy*, 2007. **3**(5): p. 499-501.
56. New, M., H. Olzscha, and N.B. La Thangue, *HDAC inhibitor-based therapies: can we interpret the code?* *Mol Oncol*, 2012. **6**(6): p. 637-56.
57. Gu, B. and W.G. Zhu, *Surf the post-translational modification network of p53 regulation*. *Int J Biol Sci*, 2012. **8**(5): p. 672-84.
58. de Ruijter, A.J., et al., *Histone deacetylases (HDACs): characterization of the classical HDAC family*. *Biochem J*, 2003. **370**(Pt 3): p. 737-49.
59. Yuan, H. and R. Marmorstein, *Structural basis for sirtuin activity and inhibition*. *J Biol Chem*, 2012. **287**(51): p. 42428-35.
60. Finnin, M.S., et al., *Structures of a histone deacetylase homologue bound to the TSA and SAHA inhibitors*. *Nature*, 1999. **401**(6749): p. 188-93.
61. Yang, X.J. and E. Seto, *The Rpd3/Hda1 family of lysine deacetylases: from bacteria and yeast to mice and men*. *Nat Rev Mol Cell Biol*, 2008. **9**(3): p. 206-18.
62. Verdin, E., F. Dequiedt, and H.G. Kasler, *Class II histone deacetylases: versatile regulators*. *Trends Genet*, 2003. **19**(5): p. 286-93.
63. Li Y, S.D., Kwon SH., *Histone deacetylase 6 plays a role as a distinct regulator of diverse cellular processes*. *FEBS J*, 2013 **280**(3): p. 775-93.
64. Lian, Z.R., et al., *Suppression of histone deacetylase 11 promotes expression of IL-10 in Kupffer cells and induces tolerance following orthotopic liver transplantation in rats*. *J Surg Res*, 2012. **174**(2): p. 359-68.

65. Pai, M.T., et al., *Solution structure of the Ubp-M BUZ domain, a highly specific protein module that recognizes the C-terminal tail of free ubiquitin*. J Mol Biol, 2007. **370**(2): p. 290-302.
66. Kawaguchi, Y., et al., *The deacetylase HDAC6 regulates aggresome formation and cell viability in response to misfolded protein stress*. Cell, 2003. **115**(6): p. 727-38.
67. Su, M., et al., *HDAC6 regulates aggresome-autophagy degradation pathway of alpha-synuclein in response to MPP+-induced stress*. J Neurochem, 2011. **117**(1): p. 112-20.
68. Tsai, Y.C., et al., *The Guanine nucleotide exchange factor kalirin-7 is a novel synphilin-1 interacting protein and modifies synphilin-1 aggregate transport and formation*. PLoS One, 2012. **7**(12): p. e51999.
69. Lee, J.Y., et al., *HDAC6 controls autophagosome maturation essential for ubiquitin-selective quality-control autophagy*. EMBO J, 2010. **29**(5): p. 969-80.
70. Lamark, T. and T. Johansen, *Aggrephagy: selective disposal of protein aggregates by macroautophagy*. Int J Cell Biol, 2012. **2012**: p. 736905.
71. Behl, C., *BAG3 and friends: co-chaperones in selective autophagy during aging and disease*. Autophagy, 2011. **7**(7): p. 795-8.
72. Takayama, S., Z. Xie, and J.C. Reed, *An evolutionarily conserved family of Hsp70/Hsc70 molecular chaperone regulators*. J Biol Chem, 1999. **274**(2): p. 781-6.
73. Doong, H., et al., *CAIR-1/BAG-3 abrogates heat shock protein-70 chaperone complex-mediated protein degradation: accumulation of poly-ubiquitinated Hsp90 client proteins*. J Biol Chem, 2003. **278**(31): p. 28490-500.
74. Carra, S., et al., *HspB8 chaperone activity toward poly(Q)-containing proteins depends on its association with Bag3, a stimulator of macroautophagy*. J Biol Chem, 2008. **283**(3): p. 1437-44.
75. Carra, S., et al., *HspB8 participates in protein quality control by a non-chaperone-like mechanism that requires eIF2{alpha} phosphorylation*. J Biol Chem, 2009. **284**(9): p. 5523-32.
76. Gamerding, M., et al., *BAG3 mediates chaperone-based aggresome-targeting and selective autophagy of misfolded proteins*. EMBO Rep, 2011. **12**(2): p. 149-56.
77. Gamerding, M., et al., *Protein quality control during aging involves recruitment of the macroautophagy pathway by BAG3*. EMBO J, 2009. **28**(7): p. 889-901.
78. Fontanella, B., et al., *The co-chaperone BAG3 interacts with the cytosolic chaperonin CCT: new hints for actin folding*. Int J Biochem Cell Biol, 2010. **42**(5): p. 641-50.
79. Voellmy, R. and F. Boellmann, *Chaperone regulation of the heat shock protein response*. Adv Exp Med Biol, 2007. **594**: p. 89-99.
80. Gentilella, A. and K. Khalili, *BAG3 expression is sustained by FGF2 in neural progenitor cells and impacts cell proliferation*. Cell Cycle, 2010. **9**(20): p. 4245-7.

81. Li, N., et al., *PKCdelta-mediated phosphorylation of BAG3 at Ser187 site induces epithelial-mesenchymal transition and enhances invasiveness in thyroid cancer FRO cells*. *Oncogene*, 2012: p. Epub ahead of print.
82. Zhang, Y., et al., *Bag3 promotes resistance to apoptosis through Bcl-2 family members in non-small cell lung cancer*. *Oncol Rep*, 2012. **27**(1): p. 109-13.
83. Suh, D.H., et al., *Unfolded protein response to autophagy as a promising druggable target for anticancer therapy*. *Ann N Y Acad Sci*, 2012. **1271**: p. 20-32.
84. Du, Z.X., et al., *Proteasome inhibitor MG132 induces BAG3 expression through activation of heat shock factor 1*. *J Cell Physiol*, 2009. **218**(3): p. 631-7.
85. Boyault, C., et al., *HDAC6 controls major cell response pathways to cytotoxic accumulation of protein aggregates*. *Genes Dev*, 2007. **21**(17): p. 2172-81.
86. Su, H. and X. Wang, *p62 Stages an interplay between the ubiquitin-proteasome system and autophagy in the heart of defense against proteotoxic stress*. *Trends Cardiovasc Med*, 2011. **21**(8): p. 224-8.
87. Watanabe, Y., et al., *p62/SQSTM1-dependent autophagy of Lewy body-like alpha-synuclein inclusions*. *PLoS One*, 2012. **7**(12): p. e52868.
88. Jemal, A., et al., *Global cancer statistics*. *CA Cancer J Clin*, 2011. **61**(2): p. 69-90.
89. Shen H, L.P., *Interplay between the cancer genome and epigenome*. *Cell*, 2013. **153**(1): p. 38-55.
90. Muller, P.A. and K.H. Vousden, *p53 mutations in cancer*. *Nat Cell Biol*, 2013. **15**(1): p. 2-8.
91. Decock, A., et al., *Neuroblastoma epigenetics: from candidate gene approaches to genome-wide screenings*. *Epigenetics*, 2011. **6**(8): p. 962-70.
92. Lynch, T.J., et al., *Activating mutations in the epidermal growth factor receptor underlying responsiveness of non-small-cell lung cancer to gefitinib*. *N Engl J Med*, 2004. **350**(21): p. 2129-39.
93. Colombino M, C.M., Lissia A, Cossu A, Rubino C, De Giorgi V, Massi D, Fonsatti E, Staibano S, Nappi O, Pagani E, Casula M, Manca A, Sini M, Franco R, Botti G, Caracò C, Mozzillo N, Ascierto PA, Palmieri G., *BRAF/NRAS mutation frequencies among primary tumors and metastases in patients with melanoma*. *J Clin Oncol*, 2012. **30**(20): p. 2522-9.
94. Li, X., K. Zhang, and Z. Li, *Unfolded protein response in cancer: the physician's perspective*. *J Hematol Oncol*, 2011. **4**: p. 8.
95. Madonna G, U.C., Gentilcore G, Palmieri G, Ascierto PA, *NF- κ B as potential target in the treatment of melanoma*. *J Transl Med.*, 2012. **10**(53).
96. Hayden, M.S. and S. Ghosh, *Shared principles in NF-kappaB signaling*. *Cell*, 2008. **132**(3): p. 344-62.

97. Jennewein, C., et al., *Identification of a novel pro-apoptotic role of NF-kappaB in the regulation of TRAIL- and CD95-mediated apoptosis of glioblastoma cells.* *Oncogene*, 2012. **31**(11): p. 1468-74.
98. Charge, S.B. and M.A. Rudnicki, *Cellular and molecular regulation of muscle regeneration.* *Physiol Rev*, 2004. **84**(1): p. 209-38.
99. Tonin, P.N., et al., *Muscle-specific gene expression in rhabdomyosarcomas and stages of human fetal skeletal muscle development.* *Cancer Res*, 1991. **51**(19): p. 5100-6.
100. Graadt van Roggen, J.F. and P.C. Hogendoorn, *[New insights in the classification of soft tissue tumors].* *Ned Tijdschr Geneesk*, 2002. **146**(43): p. 2022-6.
101. Barr, F.G., *Gene fusions involving PAX and FOX family members in alveolar rhabdomyosarcoma.* *Oncogene*, 2001. **20**(40): p. 5736-46.
102. Guo, J.Y., et al., *Activated Ras requires autophagy to maintain oxidative metabolism and tumorigenesis.* *Genes Dev*, 2011. **25**(5): p. 460-70.
103. Chardin, P., et al., *N-ras gene activation in the RD human rhabdomyosarcoma cell line.* *Int J Cancer*, 1985. **35**(5): p. 647-52.
104. Herrero Martin, D., A. Boro, and B.W. Schafer, *Cell-based small-molecule compound screen identifies fenretinide as potential therapeutic for translocation-positive rhabdomyosarcoma.* *PLoS One*, 2013. **8**(1): p. e55072.
105. Gosiengfiao Y, R.J., Walterhouse D., *What is new in rhabdomyosarcoma management in children?* *Paediatr Drugs*, 2012. **14**(6): p. 389-400.
106. Zanola, A., et al., *Rhabdomyosarcomas: an overview on the experimental animal models.* *J Cell Mol Med*, 2012. **16**(7): p. 1377-91.
107. Tostar, U., et al., *Reduction of human embryonal rhabdomyosarcoma tumor growth by inhibition of the hedgehog signaling pathway.* *Genes Cancer*, 2010. **1**(9): p. 941-51.
108. Guenther M, G.U., Fulda S., *Synthetic lethal interaction between PI3K/Akt/mTOR and Ras/MEK/ERK pathway inhibition in rhabdomyosarcoma.* *Cancer Lett.*, 2013.
109. Wu, W.K., et al., *Macroautophagy modulates cellular response to proteasome inhibitors in cancer therapy.* *Drug Resist Updat*, 2010. **13**(3): p. 87-92.
110. Lawasut, P., et al., *New proteasome inhibitors in myeloma.* *Curr Hematol Malig Rep*, 2012. **7**(4): p. 258-66.
111. McConkey, D.J., M. White, and W. Yan, *HDAC inhibitor modulation of proteotoxicity as a therapeutic approach in cancer.* *Adv Cancer Res*, 2012. **116**: p. 131-63.
112. Bersani, F., et al., *Bortezomib-mediated proteasome inhibition as a potential strategy for the treatment of rhabdomyosarcoma.* *Eur J Cancer*, 2008. **44**(6): p. 876-84.
113. Selimovic D, P.B., El-Khattouti A, Badura HE, Ahmad M, Ghanjati F, Santourlidis S, Haikel Y, Hassan M., *Bortezomib/proteasome inhibitor triggers both apoptosis*

- and autophagy-dependent pathways in melanoma cells.* Cell Signal, 2013. **25**(1): p. 308-18.
114. Barneda-Zahonero, B. and M. Parra, *Histone deacetylases and cancer.* Mol Oncol, 2012. **6**(6): p. 579-89.
 115. Dallavalle, S., C. Pisano, and F. Zunino, *Development and therapeutic impact of HDAC6-selective inhibitors.* Biochem Pharmacol, 2012. **84**(6): p. 756-65.
 116. Haakenson, J. and X. Zhang, *HDAC6 and Ovarian Cancer.* Int J Mol Sci, 2013. **14**(5): p. 9514-35.
 117. Scott, G.K., et al., *Destabilization of ERBB2 transcripts by targeting 3' untranslated region messenger RNA associated HuR and histone deacetylase-6.* Mol Cancer Res, 2008. **6**(7): p. 1250-8.
 118. Jia, L., et al., *Blocking autophagy prevents bortezomib-induced NF-kappaB activation by reducing I-kappaBalpha degradation in lymphoma cells.* PLoS One, 2012. **7**(2): p. e32584.
 119. Bastian, L., et al., *Synergistic activity of bortezomib and HDACi in preclinical models of B-cell precursor acute lymphoblastic leukemia via modulation of p53, PI3K/AKT, and NF-kappaB.* Clin Cancer Res, 2013. **19**(6): p. 1445-57.
 120. Rosati, A., et al., *Role of BAG3 protein in leukemia cell survival and response to therapy.* Biochim Biophys Acta, 2012. **1826**(2): p. 365-9.
 121. Festa, M., et al., *BAG3 protein is overexpressed in human glioblastoma and is a potential target for therapy.* Am J Pathol, 2011. **178**(6): p. 2504-12.
 122. Yunoki, T., et al., *The combination of silencing BAG3 and inhibition of the JNK pathway enhances hyperthermia sensitivity in human oral squamous cell carcinoma cells.* Cancer Lett, 2013. **335**(1): p. 52-7.
 123. Dolloff, N.G. and G. Talamo, *Targeted therapy of multiple myeloma.* Adv Exp Med Biol, 2013. **779**: p. 197-221.
 124. Perego, P., et al., *Sensitization of tumor cells by targeting histone deacetylases.* Biochem Pharmacol, 2012. **83**(8): p. 987-94.
 125. Bazzaro, M., et al., *Ubiquitin proteasome system stress underlies synergistic killing of ovarian cancer cells by bortezomib and a novel HDAC6 inhibitor.* Clin Cancer Res, 2008. **14**(22): p. 7340-7.
 126. Buglio, D., et al., *The class-I HDAC inhibitor MGCD0103 induces apoptosis in Hodgkin lymphoma cell lines and synergizes with proteasome inhibitors by an HDAC6-independent mechanism.* Br J Haematol, 2010. **151**(4): p. 387-96.
 127. Denk, A., et al., *Activation of NF-kappa B via the Ikappa B kinase complex is both essential and sufficient for proinflammatory gene expression in primary endothelial cells.* J Biol Chem, 2001. **276**(30): p. 28451-8.
 128. Gonzalez, P., et al., *Impairment of lysosomal integrity by B10, a glycosylated derivative of betulinic acid, leads to lysosomal cell death and converts autophagy into a detrimental process.* Cell Death Differ, 2012. **19**(8): p. 1337-46.

129. Fulda, S., et al., *The CD95 (APO-1/Fas) system mediates drug-induced apoptosis in neuroblastoma cells*. *Cancer Res*, 1997. **57**(17): p. 3823-9.
130. Garcia-Mata, R., et al., *Characterization and dynamics of aggresome formation by a cytosolic GFP-chimera*. *J Cell Biol*, 1999. **146**(6): p. 1239-54.
131. Wanker, E.E., et al., *Membrane filter assay for detection of amyloid-like polyglutamine-containing protein aggregates*. *Methods Enzymol*, 1999. **309**: p. 375-86.
132. Cvek, B. and Z. Dvorak, *The ubiquitin-proteasome system (UPS) and the mechanism of action of bortezomib*. *Curr Pharm Des*, 2011. **17**(15): p. 1483-99.
133. Klionsky, D.J., et al., *Guidelines for the use and interpretation of assays for monitoring autophagy*. *Autophagy*, 2012. **8**(4): p. 445-544.
134. Tsukahara, F. and Y. Maru, *Bag1 directly routes immature BCR-ABL for proteasomal degradation*. *Blood*, 2010. **116**(18): p. 3582-92.
135. Basit, F., R. Humphreys, and S. Fulda, *RIP1 protein-dependent assembly of a cytosolic cell death complex is required for inhibitor of apoptosis (IAP) inhibitor-mediated sensitization to lexatumumab-induced apoptosis*. *J Biol Chem*, 2012. **287**(46): p. 38767-77.
136. Ni Chonghaile, T. and A. Letai, *Mimicking the BH3 domain to kill cancer cells*. *Oncogene*, 2008. **27 Suppl 1**: p. S149-57.
137. Nivon, M., et al., *NF-kappaB regulates protein quality control after heat stress through modulation of the BAG3-HspB8 complex*. *J Cell Sci*, 2012. **125**(Pt 5): p. 1141-51.
138. Azoitei, N., T. Wirth, and B. Baumann, *Activation of the IkappaB kinase complex is sufficient for neuronal differentiation of PC12 cells*. *J Neurochem*, 2005. **93**(6): p. 1487-501.
139. Gamberdinger, M., S. Carra, and C. Behl, *Emerging roles of molecular chaperones and co-chaperones in selective autophagy: focus on BAG proteins*. *J Mol Med (Berl)*, 2011. **89**(12): p. 1175-82.
140. Mathew, R. and E. White, *Autophagy in tumorigenesis and energy metabolism: friend by day, foe by night*. *Curr Opin Genet Dev*, 2011. **21**(1): p. 113-9.
141. Milani, M., et al., *The role of ATF4 stabilization and autophagy in resistance of breast cancer cells treated with Bortezomib*. *Cancer Res*, 2009. **69**(10): p. 4415-23.
142. Stessman, H.A., et al., *Profiling bortezomib resistance identifies secondary therapies in a mouse myeloma model*. *Mol Cancer Ther*, 2013. **12**(6): p. 1140-50.
143. Hui, B., et al., *Proteasome inhibitor interacts synergistically with autophagy inhibitor to suppress proliferation and induce apoptosis in hepatocellular carcinoma*. *Cancer*, 2012. **118**(22): p. 5560-71.
144. Zhang, H.Y., et al., *Beclin 1 enhances proteasome inhibition-mediated cytotoxicity of thyroid cancer cells in macroautophagy-independent manner*. *J Clin Endocrinol Metab*, 2013. **98**(2): p. E217-26.

145. Ouyang, H., et al., *Protein aggregates are recruited to aggresome by histone deacetylase 6 via unanchored ubiquitin C termini*. J Biol Chem, 2012. **287**(4): p. 2317-27.
146. Carew, J.S., et al., *Autophagy inhibition enhances vorinostat-induced apoptosis via ubiquitinated protein accumulation*. J Cell Mol Med, 2010. **14**(10): p. 2448-59.
147. Krug, S. and P. Michl, *New developments in pancreatic cancer treatment*. Minerva Gastroenterol Dietol, 2012. **58**(4): p. 427-43.
148. Baumann, K.H., U. Wagner, and A. du Bois, *The changing landscape of therapeutic strategies for recurrent ovarian cancer*. Future Oncol, 2012. **8**(9): p. 1135-47.
149. Haar, C.P., et al., *Drug resistance in glioblastoma: a mini review*. Neurochem Res, 2012. **37**(6): p. 1192-200.
150. Ammirante, M., et al., *IKK γ protein is a target of BAG3 regulatory activity in human tumor growth*. Proc Natl Acad Sci U S A, 2010. **107**(16): p. 7497-502.
151. Boiani, M., et al., *The stress protein BAG3 stabilizes Mcl-1 protein and promotes survival of cancer cells and resistance to antagonist ABT-737*. J Biol Chem, 2013. **288**(10): p. 6980-90.
152. Ulbricht, A., et al., *Cellular mechanotransduction relies on tension-induced and chaperone-assisted autophagy*. Curr Biol, 2013. **23**(5): p. 430-5.
153. Seidel, K., et al., *The HSPB8-BAG3 chaperone complex is upregulated in astrocytes in the human brain affected by protein aggregation diseases*. Neuropathol Appl Neurobiol, 2012. **38**(1): p. 39-53.
154. Wang, H.Q., et al., *Transcriptional upregulation of BAG3 upon proteasome inhibition*. Biochem Biophys Res Commun, 2008. **365**(2): p. 381-5.
155. Du, Z.X., et al., *Caspase-dependent cleavage of BAG3 in proteasome inhibitors-induced apoptosis in thyroid cancer cells*. Biochem Biophys Res Commun, 2008. **369**(3): p. 894-8.
156. Santonocito, M., et al., *The apoptotic transcriptome of the human MII oocyte: characterization and age-related changes*. Apoptosis, 2013. **18**(2): p. 201-11.
157. Nivon, M., et al., *Autophagy activation by NF κ B is essential for cell survival after heat shock*. Autophagy, 2009. **5**(6): p. 766-83.
158. Gentilella, A., et al., *Activation of BAG3 by Egr-1 in response to FGF-2 in neuroblastoma cells*. Oncogene, 2008. **27**(37): p. 5011-8.
159. Liao Q, O.F., Friess H, Zimmermann A, Takayama S, Reed JC, Kleeff J, Büchler MW., *The anti-apoptotic protein BAG-3 is overexpressed in pancreatic cancer and induced by heat stress in pancreatic cancer cell lines*. FEBS Lett., 2001 August 17. **503**(2-3): p. 151-7.
160. Jacobs, A.T. and L.J. Marnett, *HSF1-mediated BAG3 expression attenuates apoptosis in 4-hydroxynonenal-treated colon cancer cells via stabilization of anti-apoptotic Bcl-2 proteins*. J Biol Chem, 2009. **284**(14): p. 9176-83.

161. Franco, R., et al., *Expression of the anti-apoptotic protein BAG3 in human melanomas*. J Invest Dermatol, 2012. **132**(1): p. 252-4.
162. Rosati, A., et al., *Expression of the antiapoptotic protein BAG3 is a feature of pancreatic adenocarcinoma and its overexpression is associated with poorer survival*. Am J Pathol, 2012. **181**(5): p. 1524-9.
163. Suzuki, M., et al., *BAG3 (BCL2-associated athanogene 3) interacts with MMP-2 to positively regulate invasion by ovarian carcinoma cells*. Cancer Lett, 2011. **303**(1): p. 65-71.
164. Davenport, K.P., F.C. Blanco, and A.D. Sandler, *Pediatric malignancies: neuroblastoma, Wilm's tumor, hepatoblastoma, rhabdomyosarcoma, and sacroccygeal teratoma*. Surg Clin North Am, 2012. **92**(3): p. 745-67, x.
165. Shen HM, T.V., *NFkappaB signaling in carcinogenesis and as a potential molecular target for cancer therapy*. Apoptosis, 2009. **14**(4): p. 348-63.
166. Kwon, K.R., et al., *Disruption of bis leads to the deterioration of the vascular niche for hematopoietic stem cells*. Stem Cells, 2010. **28**(2): p. 268-78.

Acknowledgments

After three years of work there are many people I have to thank.

First, my boss and supervisor Dr. Prof. Fulda for have given me the opportunity to work in her lab.

Second, Dr. Prof. Marschalek for his advices and helpful observations on my work.

I have to thank the Institut für Experimentelle Tumorforschung in der Pädiatrie for the technical support and Christina Hugenberg for her multitasking help and support.

Then, I have to thank all my colleagues, in particular Silvia Cristofanon, Ivonne Naumann, Farhan Basit, Benhaz Ahangarian, Juliane Liese and Ines Eckhardt for being my very good friends and for making my staying in Frankfurt memorable.

Finally, I have to thank my family which has been always near me in the happy and not so happy moments of these three years. Obviously, my biggest thanks go to Gianluca with whom I have the pleasure to share my journey in this life.

Curriculum Vitae



Europass Curriculum Vitae

Personal information

First name / Surname **Francesca Rapino**
Address 43a, Hedderichstrasse 60594 Frankfurt am Main (Germany)
Mobile +4915238042747
E-mail(s) francesca.rapino@yahoo.it
Nationality Italian
Date of birth 02 June 1985
Gender Female

Work experience

Dates	December 2010 →
Occupation or position held	PhD position in the research group of Prof. Simone Fulda
Main activities and responsibilities	-Translational cancer research: mechanistically studies on efficacy and inducible resistance to proteasome and selective autophagy combined treatment - Autonomous planning and designing experimental work; writing scientific articles and grant application - Increase experience on transcriptional analysis (EMSA); FACS analysis; genetically modified cell lines; fractionation
Name and address of employer	Institute for Experimental Cancer Research in Pediatrics, J.W. Goethe University Hospital Frankfurt Komturstrasse 3a, 60528 Frankfurt am Main (Germany)
Type of business or sector	Scientific research
Dates	October 2008 – October 2010
Occupation or position held	Trainee in the research group of Prof. Mauro Piacentini
Main activities and responsibilities	-Study of the crosstalk between autophagy, apoptosis and ER stress - Use of the basic techniques of molecular biology: western blot, MTT, RNA interference, DNA cloning, real time PCR, immunofluorescence, etc. - Cell culture
Name and address of employer	Istituto Nazionale per le Malattie Infettive “Lazzaro Spallanzani” I.R.C.C.S. Via Portuense, 292, 00149 Rome (Italy)
Type of business or sector	Scientific research
Dates	January 2008 - July 2008
Occupation or position held	Management and accounting supervisor
Main activities and responsibilities	- Reorganization of the accounts of the “Associação Caritas Sao Francisco”: filing of all the historical data (accounts and cash flow of nearly 20 years of activity), formatting the incoming/outcoming files, improving the clarity of the outcoming - Teach the technical staff how to redact a budget and a balance sheet - Mediator activity among the Italian financial backers (“Gruppo Missionario Jandira onlus”) and the

Name and address of employer	Brazilian association (Associação Caritas Sao Francisco) "Associação Caritas Sao Francisco" Rua Paulino Longo, 03, Jardim Rosa Emília, Jandira- Sao Paolo (Brasil)
Type of business or sector	Social activity - Volunteering
Dates	January 2007 - May 2007
Occupation or position held	Trainee in the research group of Prof. Escrich
Main activities and responsibilities	- Assistance in the preparatory phases of the experiment: analytical production of the diet of the experimental animals; weight of the animals and measurement of the tumours developed in the mouse - Study of the previous experimental data and involvement in the reunions of improvement of the experimental strategy - Analysis of the vaginal fluid at the optic microscope - Sacrifice and dissection of the experimental animals
Name and address of employer	Prof. Eduard Escrich Campus de la UAB, Bellaterra (Cerdanyola del Vallès), 08193 Barcelona (Spain)
Type of business or sector	Scientific research
Dates	September 2004 – October 2010
Occupation or position held	Teaching (English, Literature, Math, Physics, History, Philosophy)
Main activities and responsibilities	- Development of an autonomous method of work - Improvement of the knowledge of basic Italian language and fundamental mathematics - Creation of interdisciplinary conceptual maps
Type of business or sector	Private lessons
Papers	
Authors	Rapino F; Jung M and Fulda S
Title	BAG3 induction is required to mitigate proteotoxicity via selective autophagy following inhibition of constitutive protein degradation pathways
Journal	Oncogene 6 May 2013; doi:10.1038/onc.2013.110
Authors	Rapino F; Naumann I and Fulda S
Title	Bortezomib antagonizes microtubule-interfering drug-induced apoptosis by inhibiting G2/M transition and MCL-1 degradation.
Journal	Cell Death and Disease (in revision)
Scholarship	
Dates	15 December 2011
Title of qualification awarded	Premio Rita e Sebastiano Raeli
Name and type of organisation providing education and training	Università degli Studi di Roma "Tor Vergata" (University) Via Orazio Raimondo, 18, 00173 Rome (Italy)
Dates	November 2011
Title of qualification awarded	UCT Scholarship for young researchers
Name and type of organisation	Universitären Centrum für Tumorerkrankungen

providing education and training Theodor-Stern-Kai 7, 60590 Frankfurt am Main (Germany)

Conferences

Dates 6 September 2012

Title of qualification awarded **UCT International Science Day**

Principal subjects / occupational skills covered - Poster presentation: BAG3 is critically required for cell recovery of rhabdomyosarcoma cells after proteotoxic stress due to simultaneous inhibition of proteasomal degradation and selective autophagy.

Name and type of organisation providing education and training Universitären Centrum für Tumorerkrankungen
Theodor-Stern-Kai 7, 60590 Frankfurt am Main (Germany)

Dates 26-28 January 2012

Title of qualification awarded **EACR conference "Cell death in Cancer"**

Principal subjects / occupational skills covered -Poster presentation: Targeting selective aggresome autophagy enhances Bortezomib- induced cell death in rhabdomyosarcoma.

Name and type of organisation providing education and training De Rode Hoed
Keizersgracht 102, 1015 CV Amsterdam (Netherlands)

Dates March 2007 - May 2007

Title of qualification awarded **Cycle of Conferences**

Principal subjects / occupational skills covered - "Aspectos generales y de investigación básica en cáncer de mama" (General aspects and basic investigation on breast cancer)

Name and type of organisation providing education and training Medicine Departement (Universitat Autonoma di Barcellona (UAB))
Campus de la UAB Bellaterra (Cerdanyola del Vallès), 08193 Barcelona (Spain)

Education and training

Dates October 2008 – October 2010

Title of qualification awarded **Master of Science in Cellular and Molecular Biology** ; graduated 110/110 et laude

Principal subjects / occupational skills covered - Chosen curriculum: Functional Genomics and Proteomics
- Study of the modern techniques of molecular biology in order to analyze prokaryotic and eukaryotic cells
- Approach to System biology: theoretical study of genomic and proteomic techniques
- Knowledge of analytical techniques of acquisition and analysis of data

Name and type of organisation providing education and training Università degli Studi di Roma "Tor Vergata" (University)
Via Orazio Raimondo, 18, 00173 Rome (Italy)

Dates September 2004 - October 2007

Title of qualification awarded **Bachelor in Biological Science** (classe 12), graduated with 110/110 et laude

Principal subjects / occupational skills covered - Select curriculum: Molecular and cellular biology
- Study of the molecular interaction in biological systems with particular stress on the genetic, biochemical and cellular level
- Study of the biochemical, microbiological and genetic techniques used in common research laboratories
- Theoretical and practical approach to biotechnologies

Name and type of organisation providing education and training

Università degli Studi di Pisa (University)
Lungarno Pacinotti, 43/44, 56100 Pisa (Italy)

Dates

September 1999 - July 2004

Title of qualification awarded

Graduation at the European High School (note: 100/100)

Principal subjects / occupational skills covered

- Experimental school characterized by a massive study of history and philosophy (7h per week)
- Improvement of linguistic and literary skills both in ancient (Greek and Latin) and modern (English and French) languages
- Study of two subjects in foreign languages: "law and economy" in English and "geography" in French
- Study of Math and Physics as in a scientific high school

Name and type of organisation providing education and training

Convitto Nazionale Vittorio Emanuele II "Liceo Classico Europeo" (European High School)
Piazza Monte Grappa, 5, 00195 Rome (Italy)

Personal skills and competences

Other language(s)

Self-assessment

European level ()*

English

French

Spanish/Castilian

Understanding				Speaking				Writing	
Listening		Reading		Spoken interaction		Spoken production			
C2	Proficient user	C2	Proficient user	C2	Proficient user	C1	Proficient user	C1	Proficient user
B1	Independent user	B2	Independent user	B1	Independent user	B1	Independent user	B1	Independent user
B2	Independent user	B2	Independent user	B1	Independent user	B1	Independent user	A2	Basic user

(*) [Common European Framework of Reference \(CEF\) level](#)

ERKLÄRUNG

Erklärung der Verfasserin.

Hiermit erkläre ich eidesstattlich, dass ich die vorliegende Arbeit selbständig und ohne Benutzung anderer als der angegebenen Hilfsmittel angefertigt, sowie die aus fremden Quellen direkt oder indirekt übernommenen Gedanken als solche kenntlich habe.

Die Arbeit wurde bisher in gleicher oder ähnlicher Form keiner anderen Prüfungsbehörde vorgelegt und auch noch veröffentlicht

Frankfurt am Main, 11.07.2013

Francesca Rapino